

Cover Page



Universiteit Leiden



The handle <http://hdl.handle.net/1887/138734> holds various files of this Leiden University dissertation.

**Author:** Hajmohammadebrahimtehrani, K.

**Title:** Small-molecule inhibitors of bacterial metallo- $\beta$ -lactamases

**Issue Date:** 2020-12-16



The printing of this thesis was financially supported by:

Universiteit Leiden

Shimadzu Benelux B. V.

Büchi Labortechnik GmbH

Sysmex Nederland B. V. – Sysmex Belgium N. V.

The cover is a kind gift painted by Emma van Groesen

Thesis was printed by Proefschriftmaken; [www.proefschriftmaken.nl](http://www.proefschriftmaken.nl)

ISBN: 978-94-6423-047-5

# Small-molecule inhibitors of bacterial metallo- $\beta$ -lactamases

Proefschrift

ter verkrijging van  
de graad van Doctor aan de Universiteit Leiden,  
op gezag van Rector Magnificus prof.mr. C.J.J.M. Stolker,  
volgens besluit van het College voor Promoties  
te verdedigen op woensdag 16 december 2020  
klokke 13:45 uur

door

Kamaleddin Hajmohammadebrahimtehrani

geboren te Teheran, Iran

30 juli 1987

Promotor:

Prof. dr. N.I. Martin

Promotiecommissie:

Prof. dr. G.P. van Wezel

Prof. dr. M. Ubbink

Prof. dr. G.J. Poelarends

Dr. L.H. Heitman

Dr. M.H. Weingarh

*Don't take refuge in the false security of consensus.*

*Christopher Hitchens*

# Table of Contents

<b>Chapter 1</b>	1
Introduction	
<b>Chapter 2</b>	43
Small-molecule aminocarboxylic acids as metallo- $\beta$ -lactamase inhibitors; Part I	
<b>Chapter 3</b>	63
Small-molecule aminocarboxylic acids as metallo- $\beta$ -lactamase inhibitors; Part II	
<b>Chapter 4</b>	81
Thiol-containing metallo- $\beta$ -lactamase inhibitors: synergy, zinc-binding affinity and stability evaluation	
<b>Chapter 5</b>	103
Cephalosporin conjugates of the thiol inhibitors of metallo- $\beta$ -lactamases are potent inhibitors of IMP enzymes	
<b>Chapter 6</b>	124
Biochemical evaluation of FLC-1, a novel carbapenemase encoded by an <i>Enterobacter cloacae</i> complex isolated from food products	
<b>Addendum</b>	133
Summary	
Samenvatting	
List of publications	
<i>Curriculum vitae</i>	
Afterword	

# Chapter 1

## Introduction: $\beta$ -lactam resistance and $\beta$ -lactamase inhibitors

Parts of this chapter have been published in:

Tehrani, K. H. M. E., and Martin, N. I. (2018)  $\beta$ -lactam/ $\beta$ -lactamase inhibitor combinations: an update. *Medchemcomm* **9**, 1439–1456.



## 1. Introduction

There is an urgent need to develop new therapeutic options to combat the increasing number of pathogens that have become resistant to  $\beta$ -lactam antibiotics by gaining the ability to express  $\beta$ -lactamase enzymes. The  $\beta$ -lactamases are classified by both structural approaches (Ambler)<sup>1</sup> and functional approaches (Bush-Jacoby-Medeiros).<sup>2</sup> Throughout this chapter, the Ambler classification will be used to describe the  $\beta$ -lactamases. Class A is represented by the classic  $\beta$ -lactamases such as the TEM (named after a patient) and SHV (name derived from sulfhydryl reagent variable) families which inactivate penicillins and narrow-spectrum cephalosporins. Some members of the TEM and SHV families, along with the CTX-M (active against cefotaxime, isolated in Munich) class, are also able to inactivate extended-spectrum  $\beta$ -lactams and are therefore referred to as extended-spectrum  $\beta$ -lactamases (ESBLs). There are also carbapenemases among class A enzymes which include KPC (*K. pneumoniae* carbapenemase), IMI (imipenem-hydrolyzing  $\beta$ -lactamase) and SME (*S. marcescens* enzyme).<sup>3,4</sup> Unlike members of class A/C/D families which hydrolyze  $\beta$ -lactams by action of a serine nucleophile, class B  $\beta$ -lactamases are metalloenzymes that contain zinc ion in their active site. In these so-called metallo- $\beta$ -lactamases a water molecule, activated via coordination to zinc, serves as a nucleophile and hydrolyzes the  $\beta$ -lactam ring rendering the antibiotic inactive (figure 1). With the exception of monobactams, class B metallo- $\beta$ -lactamases (MBLs) are able to hydrolyze all classes of  $\beta$ -lactams. The rapidly emerging NDM (New-Delhi metallo- $\beta$ -lactamase) along with VIM (Verona integron-encoded metallo- $\beta$ -lactamase) and IMP (imipenemase) are among the most clinically important MBLs which possess carbapenemase activity.<sup>5-8</sup> Class C is represented by CMY (cephamycinase), ACT (AmpC type) and DHA (discovered in Dhahran hospital). Gram-negative bacteria producing this class of enzymes are often resistant to penicillins and some cephalosporins. Class D contains OXA (oxacillinase) family the members of which are able to metabolize penicillins, cephalosporins, and carbapenems. In this regard, the emergence of OXA-producing *Pseudomonas aeruginosa* and *Acinetobacter baumannii* is of particular concern.<sup>9</sup>

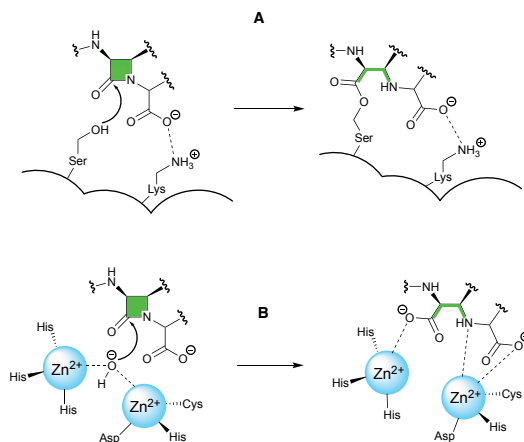


**Figure 1. A.**  $\beta$ -lactam inactivation mediated by serine  $\beta$ -lactamases (Ambler class A, C and D) is facilitated by the attack of a nucleophilic serine. **B.** MBL (class B)-mediated inactivation of  $\beta$ -lactams involves a nucleophilic attack by an activated water molecule coordinated to zinc ions.

For the purpose of clarity, figure 2 provides an overview of the various antibiotics **1-13** that have been tested in combination with the  $\beta$ -lactamase inhibitors covered in this chapter. The first generation of  $\beta$ -lactamase inhibitors including clavulanic acid **14**, sulbactam **15**, and tazobactam **16** (figure 3) were granted FDA-approval between 1984 and 1993. They were formulated with penicillins and include amoxicillin **1**-clavulanic acid, ticarcillin **2**-clavulanic acid, ampicillin **3**-sulbactam, and piperacillin **4**-tazobactam combinations.<sup>10</sup> However, the spectrum of activity of these inhibitor/ $\beta$ -lactam combinations covers primarily the  $\beta$ -lactamases of class A (with the exception of KPC). In addition, the emergence of inhibitor-resistant TEM variants with lowered susceptibility to clavulanic acid, sulbactam, and tazobactam has been documented.<sup>11</sup>

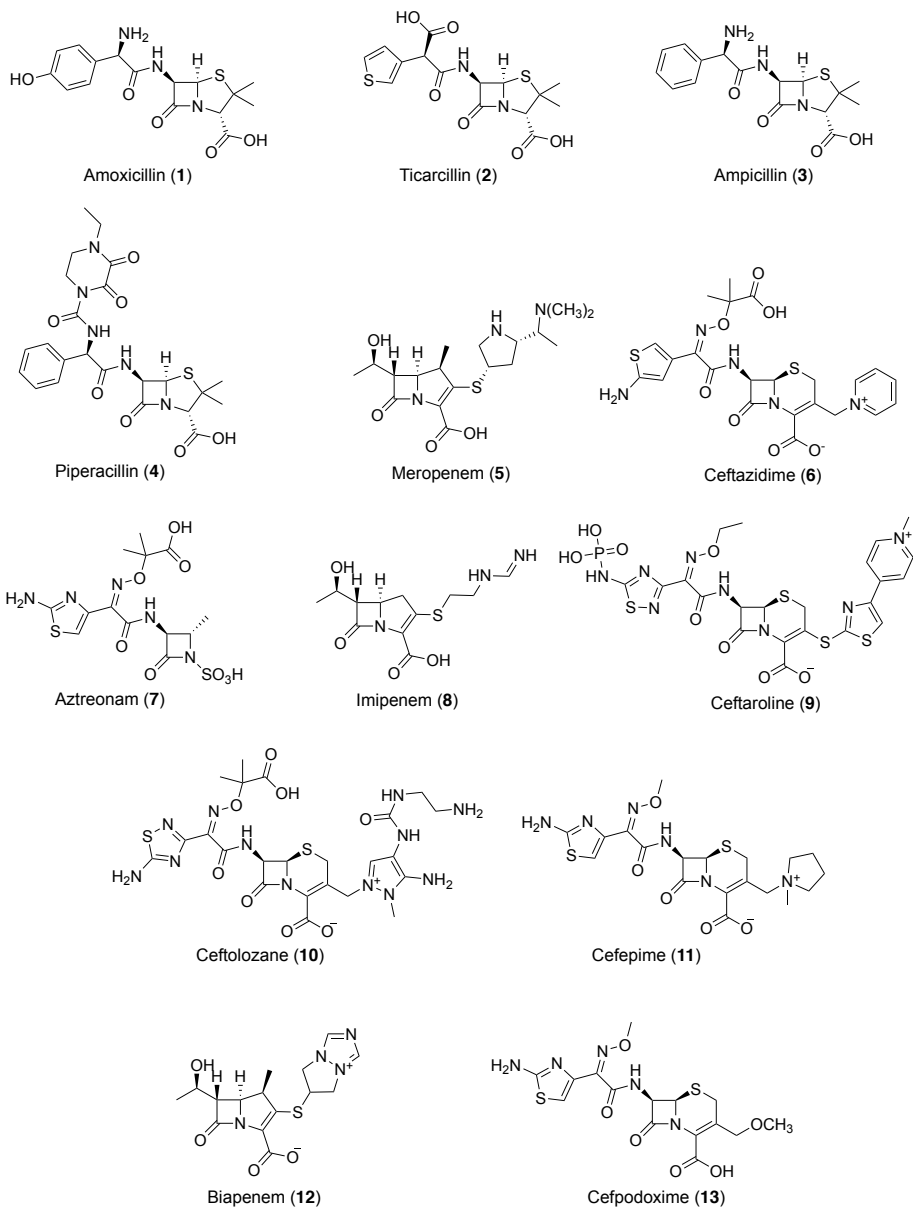


**Figure 2.**  $\beta$ -lactam antibiotics evaluated in combination with  $\beta$ -lactamase inhibitors.

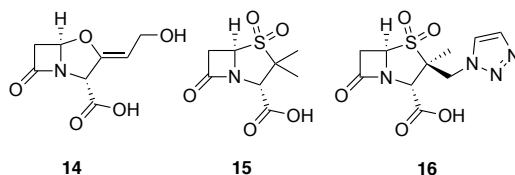


**Figure 3.** First generation of  $\beta$ -lactamase inhibitors; clavulanic acid **14**, sulbactam **15** and tazobactam **16**.

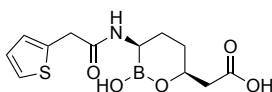
In response to the increasing risk of drug-resistant bacterial infections, new generations of  $\beta$ -lactamase inhibitors including avibactam and vaborbactam have been added to our arsenal in recent years. Despite these advances, carbapenem-resistant *Enterobacteriaceae*<sup>12–15</sup> and difficult to treat microorganisms such as *P. aeruginosa* and *A. baumannii* produce a variety of  $\beta$ -lactamases and exhibit other resistance mechanisms that continue to challenge existing antibiotic treatments.<sup>9,16,17</sup> In this chapter we first review the  $\beta$ -lactam/ $\beta$ -lactamase inhibitor (BL/BLI) combinations being marketed or under clinical development. We then continue by an overview of the research articles and patents published on the topic of small-molecule inhibitors of  $\beta$ -lactamases with particular attention paid to progress made in the past decade.

## 2. Recent FDA-approved BL/BLI combinations

### 2.1 Vabomere® (meropenem + vaborbactam)

Vaborbactam **17** (formerly known as RPX7009, figure 4) is the first FDA-approved  $\beta$ -lactamase inhibitor containing a cyclic boronate pharmacophore.<sup>18–21</sup> The design of vaborbactam is the result of medicinal chemistry efforts to develop a cyclic boronate analog with selectivity towards bacterial  $\beta$ -lactamases over mammalian serine hydrolases. X-ray crystallography studies confirmed that vaborbactam forms a covalent adduct with the catalytic serine residue of CTX-M-15 and AmpC. In addition, vaborbactam inhibited various Class A/C  $\beta$ -lactamases with sub- $\mu$ M  $IC_{50}$  values.<sup>22</sup> The combination of vaborbactam and meropenem **5** was tested against more than 300 *Enterobacteriaceae* clinical isolates, the majority of which carried KPC genes. A fixed vaborbactam concentration of 8  $\mu$ g/mL potentiated the activity of meropenem **5** by at least 64-fold leading to  $MIC_{50}$  and  $MIC_{90}$  values of  $\leq 0.06$  and 1  $\mu$ g/mL respectively.<sup>23</sup> A follow-up study on a larger number of non-fastidious gram-negative bacteria collected worldwide confirmed the potent activity of meropenem-vaborbactam against KPC-producing *Enterobacteriaceae* ( $MIC_{50}$  and  $MIC_{90}$  values of 0.12 and 0.5  $\mu$ g/mL respectively), however vaborbactam did not reduce the MIC of meropenem **5** against bacterial strains expressing MBLs

(Ambler class B) or OXA-48 (Ambler class D).<sup>24</sup> In a complimentary study, Lomovskaya and co-workers used a panel of engineered *E. coli* strains producing  $\beta$ -lactamases of all four Ambler classes to assess the ability of vaborbactam to potentiate a number of antibiotics.<sup>25</sup> Since most of the strains producing  $\beta$ -lactamases of Ambler class A and C are already susceptible to meropenem **5**, adding ceftazidime **6** and aztreonam **7** to their panel allowed them to fully characterize the inhibition spectrum of combinations with vaborbactam. Their findings reveal a broad spectrum synergistic effect against *E. coli* strains producing  $\beta$ -lactamases of Ambler class A (KPC, SME, NMC, SHV, TEM, CTX) and class C (DHA, MIR, FOX, AmpC-ECL, CMY) when 4  $\mu\text{g/mL}$  vaborbactam is added to meropenem **5**, ceftazidime **6**, or aztreonam **7**. In line with studies employing clinical isolates, vaborbactam did not decrease the MIC of  $\beta$ -lactams against engineered *E. coli* strains producing MBLs including class B (NDM-1, VIM-1) or class D (OXA) enzymes.<sup>25</sup> In addition to strong *in vitro* activity, meropenem-vaborbactam exhibited promising results in clinical trials which indicated the safety, tolerability, and efficacy of the combination.<sup>26,27</sup> In a randomized clinical trial meropenem-vaborbactam along with its comparator drug combination (piperacillin-tazobactam) were evaluated for the treatment of complicated urinary tract infection. Meropenem-vaborbactam was well tolerated by patients and proved to be non-inferior to the comparator therapy.<sup>27</sup> Vaborbactam in combination with meropenem (Vabomere®) was approved by FDA in 2017 for treating complicated urinary tract infections and is marketed by Melinta therapeutics as an injectable solution with each vial containing 1 g of meropenem and 1 g of vaborbactam.<sup>28,29</sup> At present other vaborbactam-antibiotic combinations are under clinical evaluation.



17

**Figure 4.** Vaborbactam **17**.

## 2.2 Avycaz® (ceftazidime + avibactam)

The avibactam/ceftazidime combination marketed as Avycaz was granted FDA-approval in 2015 for the treatment of complicated intra-abdominal infection (cIAI) and complicated urinary tract infection (cUTI). Structurally, avibactam **18** (formerly NXL104, figure 5) is a first-in-class SBL inhibitor with a cyclic urea replacing the  $\beta$ -lactam pharmacophore present in the older generation of  $\beta$ -lactamase inhibitors.<sup>30</sup> Using a variety of biophysical techniques including UV spectroscopy, MS, and NMR, Ehmann and co-workers<sup>31</sup> found that avibactam employs a mechanism based on covalent inhibition of TEM-1 with slow regeneration of the inhibitor. This covalent acylation with reversible deacylation through recyclization is unique to avibactam among  $\beta$ -lactamase inhibitors. When avibactam was tested against a larger panel of  $\beta$ -lactamases including TEM-1, CTX-M-15, KPC-2 (class A), *Enterobacter cloacae* P99 AmpC, *P. aeruginosa* PAO1 AmpC (class C), OXA-10 and OXA-48 (class D), it was confirmed that acylation of enzymes followed by slow release of inhibitor through cyclization could be considered as a general mechanism of inhibition by avibactam.<sup>32</sup> In the case of KPC-2 inhibition however, it was found that recyclization competes with desulfation of avibactam followed by further degradation steps.<sup>32</sup> Studies of avibactam in complex with class A and class C  $\beta$ -lactamases using X-ray crystallography suggest the stability of carbamate bond upon avibactam addition and the substrate-like conformation of the enzyme-bound avibactam as the explanations for the favorability of recyclization over hydrolytic cleavage.<sup>33–35</sup> There are multiple reports on the *in vitro* activity of avibactam combined with cephalosporins, carbapenems, and monobactams against both gram-negative and gram-positive bacterial pathogens. When tested against 126 *P. aeruginosa* clinical isolates, avibactam at 4  $\mu\text{g}/\text{mL}$  reduced the  $\text{MIC}_{90}$  of ceftazidime **6** from 64 to 8  $\mu\text{g}/\text{mL}$ , superior to the effect of clavulanic acid **14** and tazobactam which led to no change and two-fold reduction of  $\text{MIC}_{90}$  respectively. Avibactam also potentiated imipenem **8** with an  $\text{MIC}_{90}$  reduction of 16 to 2  $\mu\text{g}/\text{mL}$ .<sup>36</sup> The combination of avibactam with

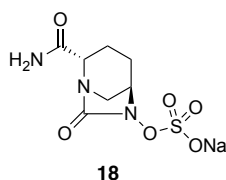


**Figure 5.** Avibactam **18**.

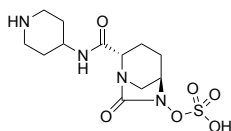
1

ceftaroline **9** inhibited *Enterobacteriaceae* strains containing multiple  $\beta$ -lactamases of class A and C. In addition, avibactam did not appear to adversely affect the activity of ceftaroline **9** against methicillin-resistant *Staphylococcus aureus* (MRSA) strains. The avibactam/ceftaroline **9** combination however showed little activity against *Acinetobacter* spp and *P. aeruginosa* strains containing OXA (class D) enzymes or MBL-producing strains.<sup>37</sup> Another study found the same trend of limited potency of ceftazidime-avibactam combination against *A. baumannii* strains producing PER-1, OXA-51 and OXA-58, while promising activity was observed against *Klebsiella pneumoniae* strains producing CTX-M-15 or OXA-48 and *E. coli* strains producing CTX-M-15.<sup>38</sup> Susceptibility screening of 701 *Enterobacteriaceae* isolates with positive ESBL-phenotype collected from U.S. hospitals showed potent activity of ceftazidime-avibactam as well as tigecycline.<sup>39</sup> Another published screening of 8,640 *Enterobacteriaceae* collected from U.S. medical centers found the similar results with ceftazidime-avibactam, although the combination showed limited activity against *Acinetobacter* spp. isolates and MBL-producers.<sup>40</sup> Avibactam restored the activity of ceftazidime **6** against isolates producing KPC, CTX-M-15-like, CTX-M-14-like and SHV ESBLs and CMY-2-like enzymes ( $\text{MIC}_{90} \leq 2 \mu\text{g}/\text{mL}$  in all the cases).<sup>39</sup> Wang and co-workers performed a series of *in vitro* assays with avibactam combined with ceftazidime **6** or aztreonam **7** revealing similar trends.<sup>41</sup> The same study also found that avibactam resensitized *Enterobacteriaceae* isolates producing Ambler class A and C to ceftazidime **6** and aztreonam **7**.<sup>41</sup> Combining avibactam with aztreonam **7** appears to be an appealing strategy to extend the activity to MBL-producers, since aztreonam **7** is a poor substrate for MBLs.<sup>3,42,43</sup> Wang and co-workers found that unlike ceftazidime-avibactam, aztreonam-avibactam did retain potency against the isolates co-producing IMP or NDM.<sup>41</sup> Based on these findings and further *in vitro* susceptibility screenings<sup>44–46</sup> it can be concluded that avibactam greatly potentiates ceftazidime **6** against bacterial pathogens producing class A, C, and some class D  $\beta$ -lactamases and outperforms older generation  $\beta$ -lactamase inhibitors such as clavulanic acid **14** and tazobactam. The ceftazidime-avibactam combination does however exhibit a higher range of MICs against *P. aeruginosa* strains and poor activity against *Acinetobacter* spp and MBL-producer strains.<sup>37,38,40,47</sup> Overproduction of efflux pumps and reduced outer membrane permeability has been suggested to be responsible for ceftazidime-avibactam resistance in *P. aeruginosa* isolates.<sup>48</sup> Ceftazidime-avibactam has also been evaluated in a number of clinical trials for the treatment of complicated urinary tract infections (cUTI) and complicated intra-abdominal infections (cIAI). The published data indicate that overall the combination is well-tolerated by patients and noninferiority to its comparator drugs such as imipenem-cilastatin,

meropenem **5** and doripenem was achieved.<sup>49–52</sup> Avycaz® is manufactured and marketed by Allergan as a powder for injection containing a 4:1 ratio of ceftazidime **6** to avibactam based on dry weight.<sup>53</sup> Clinical trials are ongoing to evaluate the efficacy of avibactam in combination with other  $\beta$ -lactam partners including ceftaroline **9** and aztreonam **7** for a number of other indications (ClinicalTrials.gov identifiers: NCT01624246, NCT01281462, NCT01689207 and NCT03329092).

### 2.3 Recarbrio® (imipenem + cilastatin + relebactam)

As recently summarized by Zhanel and co-workers,<sup>54</sup> the diazabicyclooctane (DBO) analog relebactam **19** (figure 6) has a spectrum of  $\beta$ -lactamase inhibition similar to that of the preeminent DBO-based SBL inhibitor avibactam. Relebactam is active against  $\beta$ -lactamases of Ambler class A including KPC carbapenemase and class C. Again as observed with avibactam, metallo- $\beta$ -lactamases of class B and OXA-type enzymes of class D are not affected by relebactam.<sup>54</sup> This inhibition spectrum is well reflected in the results of susceptibility screenings using a combination of relebactam and imipenem **8**. Used at 4  $\mu\text{g}/\text{mL}$ , relebactam potentiated imipenem **8** against gram-negative clinical isolates.<sup>55</sup> While  $\text{MIC}_{50/90}$  against *E. coli* strains were retained at 0.25/0.25  $\mu\text{g}/\text{mL}$  upon addition of relebactam, the combination was effectively synergistic against *K. pneumoniae*, *Enterobacter* spp., and *P. aeruginosa* isolates with  $\text{MIC}_{90/50}$  reduced to 0.25/0.25  $\mu\text{g}/\text{mL}$ , 0.25/0.5  $\mu\text{g}/\text{mL}$ , and 0.5/2  $\mu\text{g}/\text{mL}$  respectively. Relebactam also successfully reduced the  $\text{MIC}_{90/50}$  of KPC-producing *K. pneumoniae* and imipenem-resistant *P. aeruginosa* isolates from 16/>16  $\mu\text{g}/\text{mL}$  and 8/>16  $\mu\text{g}/\text{mL}$  to 0.25/1  $\mu\text{g}/\text{mL}$  and 1/2  $\mu\text{g}/\text{mL}$  respectively. However, the combination was not active against *A. baumannii* strains producing OXA-23.<sup>55</sup> Further screenings of gram-negative pathogens collected in U.S. and European hospitals confirmed that *A. baumannii*, along with other organisms that produce MBLs or OXA-type enzymes are likely to present a challenge in the use of imipenem-relebactam.<sup>56,57</sup> The *in vitro* performance of imipenem-relebactam was also evaluated against anaerobic gram-negatives of



**19**

**Figure 6.** Relebactam **19**.



**Bacteroides** group. Among the tested panel of antibiotics, imipenem **8** was found to be most potent with an MIC<sub>90</sub> of ≤1 µg/mL against all the *Bacteroides* species. However, addition of relebactam did not lead to a further improvement in the activity of imipenem **8**.<sup>58</sup> Similarly, the combination showed excellent activity against gram-positive anaerobes although overall it did not outperform imipenem **8** alone.<sup>59</sup> Phase II studies were conducted in which imipenem-cilastatin plus relebactam or placebo were administered to patients with cIAI<sup>60</sup> and cUTI.<sup>61</sup> Both studies proved non-inferiority of relebactam combination with similar adverse effects profile to the placebo group. Recently, relebactam also completed a Phase III clinical evaluation in combination with imipenem-cilastatin to treat patients with cIAI and cUTI (ClinicalTrials.gov identifier: NCT03293485). Following success in these trials, the combination Recarbrio® (imipenem + cilastatin + relebactam) was granted FDA-approval in 2019 for treating cUTI and cIAI and is currently manufactured and marketed by Merck.

#### 2.4 Zerbaxa® (ceftolozane + tazobactam)

Zerbaxa® received FDA approval in 2014 for the treatment of cIAI and cUTI. The drug consists of the novel fifth-generation cephalosporin antibiotic ceftolozane **10** (figure 2) and the established β-lactamase inhibitor tazobactam. Considering that this BL/BLI combination has been the focus of a number of detailed reviews,<sup>62–68</sup> here only the structural features of ceftolozane **10** as well as an overview of the antibacterial spectrum of its combination with tazobactam, including key outcomes of clinical trials, is covered. Ceftolozane **10** was evolved as the result of a medicinal chemistry efforts aimed at developing a cephalosporin with improved potency against AmpC-producing *P. aeruginosa* strains.<sup>69–71</sup> This was achieved by a series of structural modifications of the substituents at C3 and C7 position of the cephalosporin core. On C-7 position, in addition to the thiadiazole ring and oximino moiety, which are believed to be responsible for the extended spectrum of anti-gram-negative activity and resistance to some β-lactamases,<sup>72</sup> ceftolozane **10** also contains a dimethylacetic acid moiety which increases affinity to some PBPs, especially PBP3. After evaluating a number of protomolecules, it was eventually established that placement of a pyrazolium ring containing a basic side chain improves permeability, stability against Pseudomonas AmpC, and minimizes off target effects associated with the positively charged moiety.<sup>69,70</sup> To determine to what extent the activity of ceftolozane **10**, then known as FR264205, was affected by major resistance mechanisms of *P. aeruginosa*, it was assayed against variants producing AmpC, overexpressing efflux pumps, and lacking OprD. These studies revealed that ceftolozane **10** showed superior performance to ceftazidime **6** against

all the resistant mutants and its activity was not affected by efflux pump overexpression and OprD loss.<sup>71</sup> The inhibitory activity of tazobactam on the other hand, is highest against class A  $\beta$ -lactamases such as TEM, SHV, CTX-M enzymes.<sup>3</sup> In doing so this inhibitor extends the activity spectrum of ceftolozane **10** against ESBL-producing gram-negative bacteria. Indeed, when tazobactam was combined with ceftolozane **10**, it strongly enhanced the activity of ceftolozane **10** against ESBL-producer and AmpC-hyperproducing gram-negative bacteria in a concentration-dependent manner. Notably, strains producing KPC were not susceptible to the combination.<sup>73</sup> Farrel and co-workers reported the screening results of 7071 *Enterobacteriaceae* strains isolated from U.S. hospitals. Overall, ceftolozane-tazobactam (TOL-TAZ) showed potent activity with an MIC<sub>90</sub> of 1  $\mu\text{g}/\text{mL}$  making it equipotent to cefepime and tigecycline. Also noteworthy was the performance of the ceftolozane-tazobactam combination against *E. coli* isolates with an ESBL phenotype (MIC<sub>90</sub> = 4  $\mu\text{g}/\text{mL}$ ) as well as 1971 tested *P. aeruginosa* isolates (MIC<sub>90</sub> = 2  $\mu\text{g}/\text{mL}$ ) showing it to be superior to combinations of ceftazidime **6** or piperacillin **4** with tazobactam (MIC<sub>90</sub> = 32 and >64  $\mu\text{g}/\text{mL}$  respectively).<sup>20</sup> These findings were in agreement with the screening results against 2435 *P. aeruginosa* strains isolated from patients in Canadian hospitals.<sup>74</sup> The MIC<sub>90</sub> of 1  $\mu\text{g}/\text{mL}$  for TOL-TAZ was found to be superior to those of colistin (MIC<sub>90</sub> = 2  $\mu\text{g}/\text{mL}$ ) and meropenem (MIC<sub>90</sub> = 8  $\mu\text{g}/\text{mL}$ ) among the panel of tested antibiotics.<sup>74</sup> Tazobactam also potentiates the activity of ceftolozane **10** against anaerobes. Using a collection of 605 gram-negative and gram-positive anaerobic isolates, Snyderman and co-workers observed high activity for TOL-TAZ against *Bacteroides* spp specially *Bacteroides fragilis* (MIC<sub>90</sub> = 4  $\mu\text{g}/\text{mL}$ ) and excellent activity against gram-negative anaerobes *Prevotella* spp and *Fusobacterium* spp (MIC<sub>90</sub>  $\leq$  0.125  $\mu\text{g}/\text{mL}$ ).<sup>75</sup> The same study also revealed that ceftolozane-tazobactam has very little activity against *Clostridium* spp. Based on the results described above, TOL-TAZ can be viewed as a new carbapenem-sparing therapeutic option when facing clinically important pathogens such as ESBL-producing *Enterobacteriaceae* and *P. aeruginosa* including AmpC-hyperproducers. However, the antibiotic activity of the combination is expected to be compromised by pathogens expressing highly active carbapenemases and/or MBLs. In this regard a recent phase III clinical trial named ASPECT-cIAI evaluated TOL-TAZ plus metronidazole in patients with complicated intra-abdominal infections (cIAI).<sup>76</sup> The combination showed efficacy against infections with *Enterobacteriaceae* producing CTX-M-type ESBLs and proved to be non-inferior to meropenem **5** as the comparator drug. For the treatment of cUTI including pyelonephritis, another phase III clinical trial known as ASPECT-cUTI was conducted to compare the efficacy of TOL-TAZ with that of levofloxacin. Overall, TOL-TAZ

proved to be non-inferior to levofloxacin and adverse events were moderate.<sup>77</sup> Zerbaxa® is manufactured by Merck as powder for injection comprised of a 2:1 (by weight) mixture of ceftolozane **10** and tazobactam.<sup>78</sup>

### 3. SBL inhibitors: Recent and ongoing developments

Summarized in table 1 are the drug candidates currently being evaluated in clinical trials spanning the past 10 years. These SBLIs can be structurally classified into  $\beta$ -lactams and non- $\beta$ -lactams. BLIs with  $\beta$ -lactam structure are represented by the classic inhibitors such as clavulanic acid **14**, sulbactam **15**, and tazobactam. Recently, a structurally similar analog of tazobactam known as AAI101 successfully completed a phase II clinical trial (EudraCT Number in EU clinical trials register: 2016-005161-31). Efforts to discover BLIs among novel scaffolds have also resulted in two important new classes of SBLIs including the diazabicyclooctanes (represented by avibactam) and cyclic boronates (represented by vaborbactam). The following section covers these new SBLIs classes and their current state of clinical development.

#### 3.1. $\beta$ -lactams

As far as can be gleaned from published reports, AAI101 (**20**, figure 7) is being evaluated in clinical trials as a combination with the fourth-generation cephalosporin cefepime (EudraCT Number in EU clinical trials register: 2016-005161-31). The results of MIC screening using cefepime **11** and various concentrations of AAI101 showed a concentration-dependent

**Table 1.** BLIs currently in the clinical development stage.

Name/Code	Chemical class	Clinical development phase
Nacubactam	diazabicyclooctane	Phase I in combination with meropenem
Zidebactam	diazabicyclooctane	Phase I in combination with cefepime
ETX2514	diazabicyclooctane	Phase III in combination with sulbactam
Avibactam	diazabicyclooctane	Approved in combination with ceftazidime Phase II in combination with ceftaroline fosamil Phase I in combination with aztreonam
Vaborbactam	cyclic boronate	Approved in combination with meropenem Phase I in combination with biapenem
Taniborbactam	cyclic boronate	Phase III in combination with cefepime
AAI101	penam sulfone	Phase III in combination with cefepime

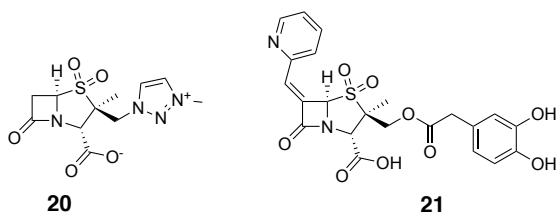


**Figure 7.** SBL inhibitor penam sulfones AAI101 (**20**) and LN-1-255 (**21**).

synergistic effect against *K. pneumoniae* and *E. coli* strains with carbapenem-resistance phenotypes.<sup>79</sup> Another study found high activity for the combination particularly against ESBL-producing *Enterobacteriaceae* ( $\text{MIC}_{50/90} = 0.125/0.5 \mu\text{g/mL}$ ).<sup>80</sup>

LN-1-255 (**21**, figure 7) is a penicillin sulfone inhibitor which has been reported to inhibit multiple class of SBLs.<sup>81</sup> Pattanaik and co-workers reported strong inhibition of SHV-1 and SHV-2 (class A) by LN-1-255 and potentiation of ceftazidime **6** against strains producing TEM, SHV, CTX-M and Sme-1 enzymes.<sup>82</sup> Crystallographic data obtained for SHV-1 suggests that LN-1-255 acylates the enzyme followed by rearrangement to a bicyclic indolizine adduct.<sup>82</sup> Also interesting was the potent activity of this inhibitor against multiple enzymes of OXA family and its ability to reduce the MIC of carbapenems against OXA-producing *E. coli*, *K. pneumoniae* and *A. baumannii* strains.<sup>83–85</sup>

### 3.2. Diazabicyclooctanes

**Zidebactam.** The acyl hydrazide DBO analog of the DBO family, zidebactam **22** (figure 8) belongs to the newest generation of DBO-based SBLs with potent PBP inhibitory activity. Although not an inhibitor of class D  $\beta$ -lactamases,<sup>86</sup> zidebactam selectively inhibited *P. aeruginosa* PAO1 PBP2 enzyme. A combination of zidebactam and cefepime **11** effectively inhibited growth of the *P. aeruginosa* PAO1 strain and its knock-outs with defective porins.<sup>87</sup> Also interesting was the increased activity of the combination of zidebactam with selected  $\beta$ -lactams against VIM-1/VIM-2-producing *P. aeruginosa* clones. The most potent activities were observed when the monobactam agent aztreonam **7** was used as  $\beta$ -lactam partner.<sup>87</sup> Likewise, an enzymatic study focusing on *A. baumannii* showed strong and selective inhibition of *A. baumannii* PBP2 by zidebactam, while no inhibition was observed against OXA-23. Interestingly, in antibacterial assays,  $8 \mu\text{g/mL}$  of zidebactam was found to reduce the MIC of cefepime **11** and sulbactam **15** against OXA-23 producing *A. baumannii* to  $16 \mu\text{g/mL}$  (4-fold reduction) and  $2 \mu\text{g/mL}$  (8-fold reduction) respectively. The enhancing effect in this case could

be attributed to the contribution of zidebactam to PBP (and not  $\beta$ -lactamase) inhibition.<sup>88</sup> Zidebactam in combination with cefepime **11** showed excellent *in vitro* inhibition when evaluated against 7876 gram-negative clinical isolate collected worldwide.<sup>89</sup> Overall, the 1:1 combination effectively inhibited *Enterobacteriaceae* isolates with an MIC<sub>90</sub> of 0.12  $\mu\text{g}/\text{mL}$  compared with 16  $\mu\text{g}/\text{mL}$  when cefepime **11** was tested alone. The combination also largely enhanced the potency of cefepime **11** by at least 16-fold against clinically important sub-classes including carbapenem-resistant *Enterobacteriaceae*, ESBL phenotype *E. coli*, and ESBL phenotype *Klebsiella* spp. Zidebactam reduced the MIC<sub>90</sub> of cefepime **11** from 32 to 4  $\mu\text{g}/\text{mL}$  against *P. aeruginosa* and from >64 to 32  $\mu\text{g}/\text{mL}$  against *Acinetobacter* spp.<sup>89</sup> Another study demonstrated the strong antibacterial activity of a 1:1 mixture of cefepime-zidebactam against a number of *Enterobacteriaceae* expressing various  $\beta$ -lactamases including: CTX-M-15 (MIC<sub>90</sub> = 1  $\mu\text{g}/\text{mL}$ ), SHV (MIC<sub>90</sub> = 0.25  $\mu\text{g}/\text{mL}$ ), ESBLs (MIC<sub>90</sub> = 1  $\mu\text{g}/\text{mL}$ ), plasmid AmpC (MIC<sub>90</sub>  $\leq$  0.06  $\mu\text{g}/\text{mL}$ ), derepressed AmpC (MIC<sub>90</sub> = 0.5  $\mu\text{g}/\text{mL}$ ), KPC (MIC<sub>90</sub> = 1  $\mu\text{g}/\text{mL}$ ) and MBLs (MIC<sub>90</sub> = 8  $\mu\text{g}/\text{mL}$ ). The inhibitory activity of the same combination had only moderate activity against *P. aeruginosa* and *A. baumannii* isolates.<sup>90</sup> Currently, two phase I clinical trials evaluating the safety, tolerability, and pharmacokinetics of zidebactam have been completed with a third study currently recruiting patients (ClinicalTrials.gov identifiers: NCT02674347, NCT02707107 and NCT02942810).

**Nacubactam.** Also known as OP0595, nacubactam **23** (figure 8) is an aminoethoxy-substituted analog of avibactam which inhibits class A/C  $\beta$ -lactamase and PBP2. Nitrocefin-based enzyme assays showed inhibition of TEM, CTX-M, KPC-2 (class A), AmpC and CMY-2 (class C) by nacubactam with sub- $\mu\text{M}$  IC<sub>50</sub> values. This inhibitor showed relatively weak activity against OXA enzymes and none against IMP-1. Similar to zidebactam, nacubactam selectively inhibited PBP2 (IC<sub>50</sub> = 0.12  $\mu\text{g}/\text{mL}$ ) and upon incubation with *E. coli*, it induced the formation of spherical cells which is an expected result of PBP2 inhibition.<sup>91</sup> Interestingly, nacubactam has been reported to possess antibacterial activity when tested alone.<sup>92–94</sup> A recent study found that when administered at  $\leq$  4  $\mu\text{g}/\text{mL}$ , nacubactam inhibited most of the *E. coli*, *Enterobacter* spp., *Citrobacter* spp., and *Klebsiella* spp. strains tested, although it had a poor performance against *Serratia* spp, *P. aeruginosa* and *A. baumannii*.<sup>94</sup> Against those strains with an MIC >4  $\mu\text{g}/\text{mL}$ , nacubactam strongly enhanced the activity of aztreonam **7**, cefepime **11**, biapenem **12** and piperacillin **4** in a concentration-dependent manner. In addition, the activity of nacubactam combined with the above-mentioned antibiotics against *Enterobacteriaceae* producing

carbapenemases (KPC, OXA-48 and MBLs) was significant and superior to that of ceftazidime-avibactam. However, nacubactam did not potentiate the same antibiotics when tested against *A. baumannii* strains and MBL-producing *P. aeruginosa*.<sup>94</sup> Since *in vitro* studies of  $\beta$ -lactamase inhibition by nacubactam is complicated due to its inherent antibacterial activity, Livermore and co-workers<sup>95</sup> prepared nacubactam-resistant *Enterobacteriaceae* mutants with elevated MIC values of 8 to >32  $\mu\text{g/mL}$ . When nacubactam was tested against these mutants producing ESBLs, KPC, and OXA enzymes, use of 2  $\mu\text{g/mL}$  of nacubactam, greatly enhanced the activity of piperacillin **4**, cefepime **11**, and aztreonam **7** leading to mean MIC values of <1  $\mu\text{g/mL}$  for these three  $\beta$ -lactamase families. A similar reduction of mean MIC (From 8.43  $\mu\text{g/mL}$  to <1  $\mu\text{g/mL}$ ) was observed when nacubactam was combined with meropenem **5** and assayed against KPC-producing mutants. Also interesting was the finding that nacubactam at 1  $\mu\text{g/mL}$  reduced the mean MIC of aztreonam **7** against MBL-producing mutants from 4.68 to 0.072  $\mu\text{g/mL}$ . Taken together the study suggests that the synergy observed by nacubactam is not limited to its PBP2 inhibition but also its inhibition of class A/C  $\beta$ -lactamase. In addition, nacubactam in combination with aztreonam **7** might provide a viable therapeutic option against MBL-producing gram-negative pathogens.<sup>95</sup> To date, two clinical trials evaluating safety, pharmacokinetics, and intrapulmonary lung penetration of nacubactam have been completed (ClinicalTrials.gov identifiers: NCT02134834 and NCT03182504).

**ETX2514.** Another recently described DBO-based  $\beta$ -lactamase inhibitor known as ETX2514 (**24**, figure 8) has demonstrated a very broad spectrum of activity including inhibition of class A/C/D  $\beta$ -lactamases and PBP2.<sup>96,97</sup> In preparing ETX2514 Durand-Réville and co-workers<sup>96</sup> modified avibactam with the aim of introducing activity against a broader panel of OXA enzymes known to complicate the treatment of resistant *A. baumannii* isolates. Introduction of an endocyclic double bond was implemented to increase chemical reactivity of the ring, and

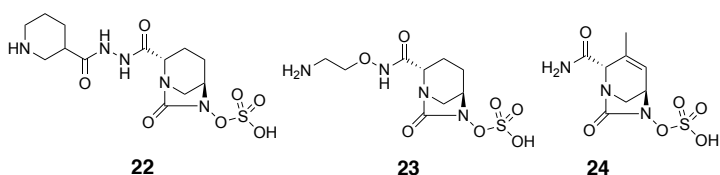


**Figure 8.** Diazabicyclooctanes in clinical development: zidebactam **22**, nacubactam **23**, ETX2514 **24**.

1

addition of a methyl group at C-3 (figure 8) led to ETX2514 which displayed a potent inhibitory activity against OXA-24 ( $IC_{50} = 0.19 \mu\text{M}$ ) along with enhanced biochemical and antibacterial activity. This finding was supported by X-ray crystallography data and molecular modeling of ETX2514 and avibactam which revealed the mode of binding to OXA-24.<sup>96</sup> Another interesting finding was the inhibitory activity of ETX2514 against PBPs with preference to PBP2 of *E. coli* and *A. baumannii*. Use of  $4 \mu\text{g/mL}$  of this inhibitor, decreases the  $MIC_{90}$  of imipenem **8** by 8-fold to  $2 \mu\text{g/mL}$ , while its combination with sulbactam **15** most effectively inhibited growth of *A. baumannii* reducing the  $MIC_{90}$  of sulbactam **15** from  $64 \mu\text{g/mL}$  to  $4 \mu\text{g/mL}$ . The intrinsic activity of sulbactam **15** against PBP3 plus the dual BL/PBP inhibition by ETX2514 may explain the excellent activity of their combination against *A. baumannii* a challenging nosocomial pathogen that is often multi-drug resistant.<sup>96</sup> A follow-up study showed that similar to avibactam, ETX2514 acylates  $\beta$ -lactamases of class A, C and D.<sup>98</sup> Mass-spectrometry analysis of the resulting enzyme-inhibitor complexes suggested that ETX2514 can recyclize and is released in intact form when incubated with AmpC, CTX-M-15, P99, SHV-5 and TEM-1. On the other hand, interaction with KPC-2, OXA-10, OXA-23, OXA-24 and OXA-48 was accompanied by desulfation and irreversible degradation of the inhibitor. A combination of ETX2514 with imipenem **8** and piperacillin **4** was highly active against isogenic *P. aeruginosa* producing class A, C and D  $\beta$ -lactamases. Compared to avibactam, ETX2514 displayed superior and broader spectrum of activity specially against OXA family of enzymes.<sup>98</sup> Additionally, Iyer and co-workers demonstrated that ETX2514 uses the outer membrane porin OmpA<sub>Ab</sub> to permeate the *A. baumannii* membrane and synergize with sulbactam **15**.<sup>99</sup> A phase III clinical trial of ETX2514 in combination with sulbactam **15** is currently recruiting participants (ClinicalTrials.gov identifier: NCT03894046).

Review of the recent patent literature reveals a number of other functionalized DBO analogs with SBL inhibitory activity (figure 9). Chang and co-workers reported isoxazoline analogs **25** and specially **26** reduced the MIC of meropenem **5** against *K. pneumoniae* strains producing class A/C/D enzymes by up to 1024-fold.<sup>100</sup> Gu and co-workers reported another group of oxadiazole-substituted analogs **27** as SBL inhibitors.<sup>101</sup> Hydroxamate and hydrazide analogs **28-30** were reported by Maiti and co-workers, as exhibiting potent inhibition of class A and C enzymes with  $<19 \text{ nM}$   $IC_{50}$  values. Of note, compound **30** not only demonstrated high intrinsic antibacterial activity but also when combined with meropenem **5** inhibited *E. coli* and *K. pneumoniae* strains expressing several  $\beta$ -lactamases of class A, B and C.<sup>102</sup> Also noteworthy is

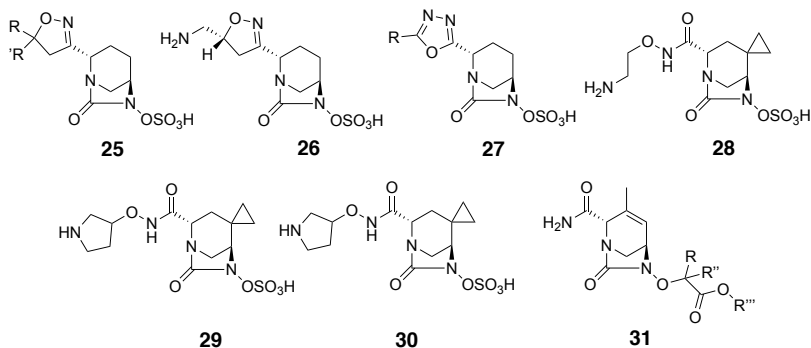


**Figure 9.** DBO analogs as  $\beta$ -lactamase inhibitors reported in the recent patents.

the report by Comita-prevoir and co-workers of a large library of DBO analogs closely related to ETX2514 wherein the sulfate moiety is replaced by functionalized glycolates.<sup>103</sup> Several compounds with the general structure of **31** demonstrated potent inhibition of TEM-1, AmpC, and OXA-48. These analogs also synergized with cefpodoxime **13** against *Citrobacter freundii*, *E. coli*, and *K. pneumoniae* strains producing multiple  $\beta$ -lactamases of class A, C, and D, and showed *in vivo* efficacy in mouse models of infection.<sup>103</sup>

### 3.3. Boronates

Boronate-based  $\beta$ -lactamase inhibitors have long been of interest given their resemblance to the tetrahedral intermediate formed upon  $\beta$ -lactam ring attacked by the nucleophilic serine of  $\beta$ -lactamases.<sup>104</sup> For this reason these BLIs are sometimes referred to as boronic acid transition-state inhibitors (BATSI).<sup>105</sup> Figure 10 shows the chemical structures of a number of such boronates that have been investigated for SBL inhibition including acyclic boronic acids (represented by **32-34**)<sup>106-108</sup> or cyclic boronate analogs (represented by **35, 37** and **38**).<sup>109-111</sup> Of particular note are recent studies aiming at developing cyclic boronates as pan- $\beta$ -lactamase inhibitors, the rationale being that both MBL- and SBL-mediated hydrolysis of  $\beta$ -lactams involve a tetrahedral transition state that precedes ring opening. Therefore, structures mimicking the transition state have the potential to exert cross-class  $\beta$ -lactamase inhibition (figure 11). Validation of this idea is found in the structural diversity of boronates contained in a number of patent applications claiming both SBL and MBL inhibition. Of note are the acyclic boronic acids represented by **36** which show inhibition of some SBLs and VIM-2 enzyme of class B<sup>112</sup> as well as the cyclic boronates **37**<sup>113,114</sup> and **38**<sup>115-118</sup> (figure 10) which display sub- $\mu\text{M}$  IC<sub>50</sub>



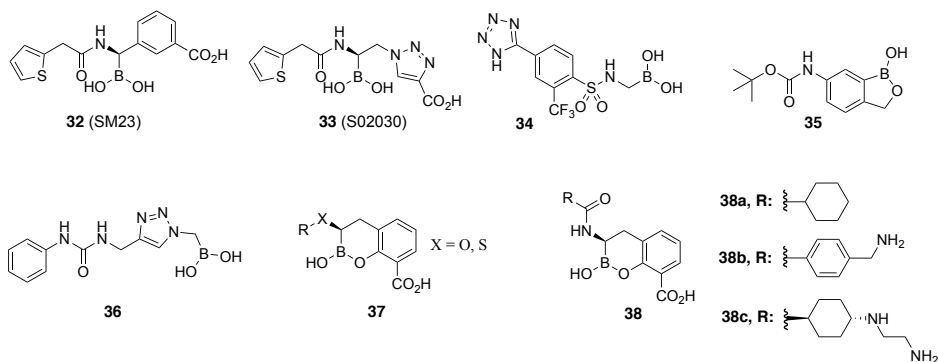


**Figure 10.** Representative boronic acids as  $\beta$ -lactamase inhibitors

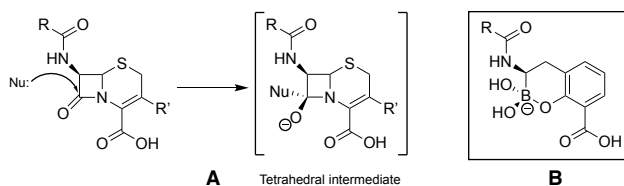


**Figure 11. A.** Tetrahedral intermediate formed by nucleophilic attack of SBLs (Nu: = serine-OH) and MBLs (Nu: is zinc-coordinated OH) on  $\beta$ -lactam ring. **B.** Cyclic boronates mimicking the tetrahedral transition state of  $\beta$ -lactam hydrolysis.<sup>110,111</sup>

values for both SBLs and MBLs. By screening a series of cyclic boronates, Brem and co-workers identified a series of SBL-inhibitor analogs with potent activity against MBLs, specifically VIM-2 and NDM-1.<sup>110</sup> Interestingly, **38b** was found to exert potent inhibition of PBP-5. X-ray crystallography studies with **38b** on BcII, VIM-2, OXA-10, and PBP-5 confirmed that the cyclic boronate structure interacts with the crucial  $\beta$ -lactamase residues (and coordinates with  $Zn^{2+}$  of MBLs) in the way that mimics the high energy transition state intermediates formed in each case. In addition, **38b** largely enhanced the activity of meropenem **5** towards *Enterobacteriaceae* expressing multiple  $\beta$ -lactamases.<sup>110</sup> A follow-up study confirmed nM range  $IC_{50}$ s for the activity of cyclic boronate analogs against TEM-1, CTX-M-15, and AmpC. Compound **38b** exhibited a synergistic relationship with carbapenems against *Enterobacteriaceae* producing multiple  $\beta$ -lactamases including KPC-2, OXA-181 (meropenem only), VIM-1, and VIM-4. However, carbapenemase-producing *P. aeruginosa* and *A. baumannii* strains remained resistant to all combinations.<sup>111</sup> Further structural optimizations with the aim of improving MBL-inhibition and

accumulation in gram-negative bacteria led to the development of taniborbactam (formerly VNRX-5133, **38c**).<sup>119–121</sup> Kinetic experiments using CTX-M-15, KPC-2 and P99 ApmC showed that this compound is a competitive inhibitor of these clinically important  $\beta$ -lactamases.<sup>121</sup> When tested against a large panel of  $\beta$ -lactamases, taniborbactam showed promising biochemical inhibition of enzymes of all 4 Ambler classes. It should, however, be mentioned that taniborbactam did not perform well against the class B enzyme IMP-1 in contrast with its potent inhibition of NDM-1 and VIM-types MBLs.<sup>119</sup> Notably, taniborbactam was found to be a selective  $\beta$ -lactamase inhibitor with no activity against human serine-hydrolases, showed little toxicity toward mammalian cell lines, and its pharmacokinetic parameters are compatible with that of cefepime, a fourth-generation broad-spectrum cephalosporin. In combination with cefepime, taniborbactam significantly reduced the bacterial count in mouse models for lung infection and ascending urinary tract infection.<sup>119</sup> A phase III clinical trial of cefepime/taniborbactam is currently in progress (ClinicalTrials.gov Identifier: NCT03840148).

#### 4. Recent advances in the development of MBL inhibitors

Based on their catalytic activities,  $\beta$ -lactamases are classified as serine  $\beta$ -lactamases (SBLs, Ambler class A, C and D) and metallo- $\beta$ -lactamases (MBLs, Ambler class B). The latter contains zinc ion(s) in the active site which is stabilized by histidine, cysteine and aspartate residues and is also bound to an active water molecule responsible for hydrolyzing  $\beta$ -lactams. MBLs in turn are divided into subclasses B1, B2, and B3. While enzymes of class B1 and B3 contain two zinc ions, B2 functions with only one.<sup>5,122</sup> The most clinically relevant MBLs include NDM, VIM, and IMP enzymes of class B1 which inactivate a broad range of  $\beta$ -lactams but have a low affinity for monobactams.<sup>123</sup> Due to their carbapenemase activity and rapid dissemination, MBLs pose a serious challenge to the antibiotic treatment of infections caused by gram-negative bacteria. The design and development of broad-spectrum MBL inhibitors is challenged by the high active site heterogeneity of the different enzymes of this family.<sup>3,8,124,125</sup> As a result, to date, there are no effective MBL inhibitors currently in clinical use.

Compounds classes with the potential to inhibit MBLs have been the subject of several detailed reviews.<sup>5,123–128</sup> Therefore, the rest of this chapter focuses on new developments in the field of MBL inhibitors over the past decade.

Traditionally, sulfur-containing compounds have been one of the most studied classes of small molecules in the search for MBL-inhibitors. Compounds containing a variety of free thiols, thioethers, thioesters, thioketones, and thioureas have been recently reported to possess inhibitory activity against different class of MBLs.<sup>124</sup> Also of note are thiol-containing drugs that while approved for other indications have shown some capacity to inhibit MBLs. In this regard Klingler and co-workers found that thiorphan (**39**, figure 12), the active metabolite of the antidiarrheal racecadotril, inhibits NDM-1, IMP-7, and VIM-1 with low- $\mu\text{M}$   $\text{IC}_{50}$  values and also markedly enhances the activity of imipenem **8** against MBL-producing strains.<sup>129</sup> In addition, captopril **40** an FDA-approved drug used for the treatment of hypertension, has also received some attention for its ability to inhibit NDM-1 ( $\text{IC}_{50} = 7.9 \mu\text{M}$ ).<sup>130</sup> Building upon these findings, efforts have been made to replace the prolyl residue of captopril with various other functional groups,<sup>130–133</sup> as well as modification of the thiolated acyl residue, and/or ring size.<sup>132–134</sup> Brem and co-workers also found the MBL inhibition of D-captopril to be superior to that of its other stereoisomers when evaluated against BCII, IMP-1, VIM-2, NDM-1, and SPM-1.<sup>135</sup> These findings were further supported and could be rationalized by X-ray crystallography studies reported in the same paper.<sup>135</sup>

It has long been known that mercaptoacetic acid and its related structural analogs are among the potent MBL-inhibitors.<sup>124</sup> Recent reports have described the development of aminoacid thioesters of mercaptoacetic acid as inhibitors of L1, an MBL of the B3 class.<sup>136,137</sup> Substituted amide derivatives of mercaptoacetic acid (mercaptoacetamides, **41**) are also prominent in a number of recent studies: Arjomandi and co-workers reported a series of amino acid conjugates of mercaptoacetamide and some longer chain homologs (mercaptpropionamide and mercaptobutyramide) which display IMP-1 inhibition.<sup>138</sup> Other studies employed mercaptoacetamide thioethers containing acetate<sup>139</sup> and azolyl ring<sup>140–143</sup> substituents. The diverse library of thiol-containing MBL-inhibitors also include thiomethylbenzoic acids,<sup>144</sup> bisthiazolidines,<sup>145,146</sup> rhodanines and its related thioenolates,<sup>147–150</sup> cysteine-containing oligopeptides,<sup>151,152</sup> mercaptopyridine *N*-oxides,<sup>153,154</sup> phosphonate and tetrazole bioisosteres of

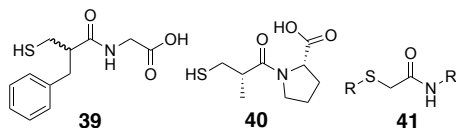


**Figure 12.** Thiol-containing MBL inhibitors, thiorphan **39**, captopril **40** and substituted mercaptoacetamides **41**.

mercaptoacids<sup>155</sup>, and thiones.<sup>156–158</sup> Finally, it should be added that although thiols are among the most potent and broad-spectrum inhibitors of MBLs, their tendency to rapidly oxidize to disulfides poses a serious challenge to further clinical developments. This is important since studies suggest that upon disulfide formation zinc-binding affinity is greatly reduced leading to a loss of MBL-inhibition and *in vitro* synergistic activity.<sup>159,160</sup> Creative chemical modifications to enhance the biological stability of thiol-based inhibitors may be the key to develop such compounds as clinically viable drug candidates.

Picolinic acid derivatives are another well-known class of zinc chelators and act via the same metal-sequestration mechanism as EDTA to inhibit MBLs.<sup>161</sup> In fact pyridine-2,6-dicarboxylic acid also known as dipicolinic acid or DPA (**42**, figure 13) is a commonly used reagent for the phenotypic detection of MBL-producing pathogens.<sup>162–165</sup> By evaluating a series of DPA analogs– represented by compound **43** – Chen and co-workers identified compounds with enhanced NDM-1 inhibition that retained MBL-selectivity over other zinc-dependent metalloenzymes.<sup>166</sup> Compound **43** inhibited NDM-1, VIM-2, and IMP-1 with IC<sub>50</sub> values of 0.080, 0.21 and 0.24  $\mu$ M respectively and demonstrated synergistic relationship with imipenem **8** when tested *in vitro* against NDM-1-producing *E. coli* and *K. pneumoniae* isolates. Also of note are the results of various experiments including NMR and equilibrium dialysis suggesting that compound **43** engages in a ternary complex with zinc and NDM-1 unlike its parent compound DPA and EDTA.<sup>166</sup> This was followed up by an isosteric replacement study of DPA (**42**) where the same group found **44** to be a potent inhibitor of NDM-1 (IC<sub>50</sub> = 0.13  $\mu$ M). The inhibitory

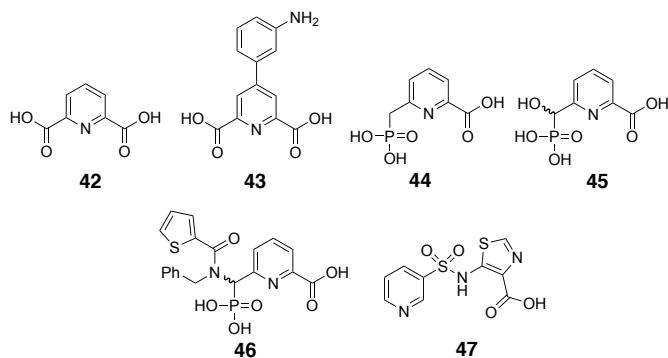


**Figure 13.** Pyridine derivatives as MBL-inhibitors.

mechanism of **44** studied by membrane dialysis assay and UV/VIS spectroscopy suggested that this compound removes a  $Zn^{2+}$  ion from the NDM-1 active site.<sup>167</sup> In a complimentary study, Hinchliffe and co-workers investigated the potential of phosphonate analogs of 2-picolinic acid to inhibit MBLs of B1 and B3 sub-class. They found potent and broad-spectrum inhibition of NDM-1, VIM-2, IMP-1, and L1 by compounds **44-46**. Compound **44** reduced the MIC of meropenem **5** down to 8 to  $<0.125$   $\mu\text{g}/\text{mL}$  against both recombinant and clinically isolated gram-negative strains producing the earlier mentioned MBLs.<sup>168</sup>

Recently, Antabio Inc. reported the discovery of the sulfonamide small molecule ANT431 (**47**) which was also evolved from 2-picolinic acid.<sup>169</sup> After demonstrating strong inhibition of NDM-1 ( $K_i = 0.29$   $\mu\text{M}$ ) and VIM-2 ( $K_i = 0.19$   $\mu\text{M}$ ) and the potentiation of meropenem **5** against the BL21 *E. coli* producing the mentioned enzymes, ANT431 was tested against 94 MBL-producing clinical isolates of *Enterobacteriaceae* family. When used at 30  $\mu\text{g}/\text{mL}$ , this compound resensitized 72% of the isolates to meropenem **5**. X-ray crystallography studies showed that the thiazole nitrogen as well as carboxylate of ANT431 interact with  $Zn^{2+}$  of VIM-2 enzyme.<sup>170</sup> ANT431 also demonstrated *in vivo* efficacy in a mouse model of infection with NDM-1 producing *E. coli* and is currently being considered as a suitable starting point for further lead optimization.<sup>169</sup>

There are multiple reports on the MBL inhibitory activity of dicarboxylic acids.<sup>124</sup> Guided by an X-ray crystallography study of compound **48** (figure 14) in complex with IMP-1, Hiraiwa and co-workers designed and synthesized di-substituted phthalic acids among which the bis(4-hydroxypiperidine) derivative **49** showed strongest inhibition towards IMP-1 ( $IC_{50} =$

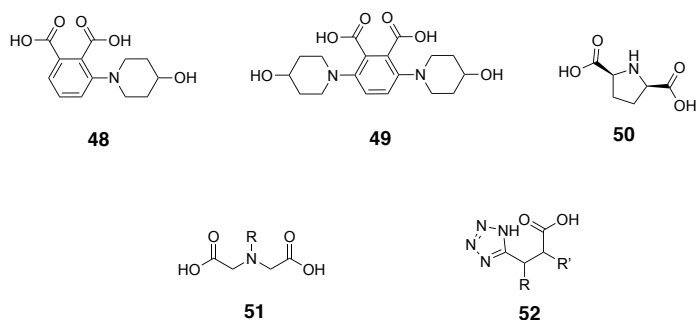


**Figure 14.** dicarboxylic acid analogs as MBL-inhibitors.

0.270  $\mu\text{M}$ ) and reduced the MIC of biapenem **12** against IMP-1 producing *P. aeruginosa* strains by at least 128-fold to  $\leq 0.5$   $\mu\text{g}/\text{mL}$ .<sup>171</sup> Also recently described as MBL inhibitors are dicarboxylate substituted, five-membered heterocycles with 2,5-pyrrolidinedicarboxylic acid **50** identified as a potent competitive inhibitor of CcrA ( $K_i = 0.73$   $\mu\text{M}$ ) and L1 ( $K_i = 0.69$   $\mu\text{M}$ ).<sup>172</sup> Notably, compound **50** reduced the MIC of cefazolin against CcrA and L1 producing *E. coli* strains to  $< 1$   $\mu\text{g}/\text{mL}$  concentrations.<sup>172</sup> As the linear analog of **50**, iminodiacetic acid derivatives (**51**) have been investigated for their potential to inhibit MBLs. Through a series of analog syntheses, it was found that NDM-1 inhibition was best for furyl-substituted analogs, although  $\text{IC}_{50}$  values were moderate (8.6  $\mu\text{M}$  being the lowest).<sup>173</sup> Tetrazolylpropionic acids such as compound **52** have also been explored as bioisosteres of dicarboxylates and reported to possess potent MBL activity with sub- $\mu\text{M}$   $\text{IC}_{50}$  values against NDM-1, IMP-1, and VIM-1.<sup>174</sup>

As described above,  $\text{Zn}^{2+}$  plays a vital role in the catalytic activity of MBLs and a variety of chelating agents have been shown to inhibit this class of enzymes and resensitize MBL-producing pathogens to  $\beta$ -lactam antibiotics. The MBL-inhibitory activity of aspergillomarasmine A (AMA) – a fungal metabolite with strong zinc chelating ability – was recently reported by King and co-workers.<sup>175</sup> After screening a collection of fungal extracts using a phenotypic assay for synergy with meropenem **5**, they isolated and characterized the active component, AMA (**53**, figure 15) and identified it as an inhibitor of NDM-1 ( $\text{IC}_{50} = 4.0$   $\mu\text{M}$ ) and VIM-2 ( $\text{IC}_{50} = 9.6$   $\mu\text{M}$ ). AMA greatly reduced the MIC of meropenem **5** to  $\leq 2$   $\mu\text{g}/\text{mL}$  against gram-negative strains producing NDM and VIM enzymes and demonstrated promising *in vivo* results in a mouse model of infection with NDM-1 producing *K. pneumoniae*.<sup>175</sup> Soon after this report, multiple chemical<sup>176–179</sup> and chemoenzymatic<sup>180</sup> methodologies were developed to synthesize AMA and its closely related analogs. It was found that the diastereomers of AMA possessed similar activities against NDM-1 and VIM-2.<sup>177</sup> The work by Bergstrom and co-workers<sup>181</sup> shed light upon the action mechanism of AMA as it was shown by isothermal titration calorimetry that AMA strongly binds to  $\text{Zn}^{2+}$  ( $K_d = 200$  nM). In addition, membrane dialysis and NMR experiments demonstrated that AMA inhibits NDM-1, VIM-2, and IMP-7 by stripping zinc from these enzymes.<sup>181</sup>

The semicarbazide moiety is a well-known metal chelator and has been employed in the search for MBL inhibitors.<sup>182</sup> As an example, compound **54** found in the recent patent literature exhibits strong inhibition of NDM-1 ( $\text{IC}_{50} = 35$  nM).<sup>182</sup> Other well established metal-chelators such as 1,4,7-triazacyclononane-1,4,7-triacetic acid (NOTA, **55**) and 1,4,7,10-

tetraazacyclododecane-1,4,7,10-tetraacetic acid (DOTA, **56**) and their analogs have also been described as MBL inhibitors with the ability to potentiate carbapenems against gram-negative strains producing NDM, IMP or VIM enzymes.<sup>183,184</sup> Similarly, the well-known zinc binder *N,N,N',N'*-tetrakis-(2-Pyridylmethyl)ethylenediamine (TPEN, **57**) has also been shown to synergize with  $\beta$ -lactam antibiotics to kill strains expressing various MBLs.<sup>185</sup> While such chelating agents have been described as nonhemolytic and nontoxic to mammalian cells *in vitro*, their potential to be advanced to clinical application should be viewed with caution due to their presumed lack of target specificity. To address this problem, Yarlagadda and co-workers covalently linked the zinc binding motif dipicolylamine to vancomycin in an attempt to produce bacterial cell-specific hybrid. Given that vancomycin's inability to effectively kill gram-negative pathogens is generally ascribed to its inability to penetrate the gram-negative outer membrane, it is somewhat surprising that the vancomycin derivative **58** showed activity against strains expressing NDM-1 and restored the activity of meropenem **5** in both *in vitro* and *in vivo* experiments.<sup>186</sup>

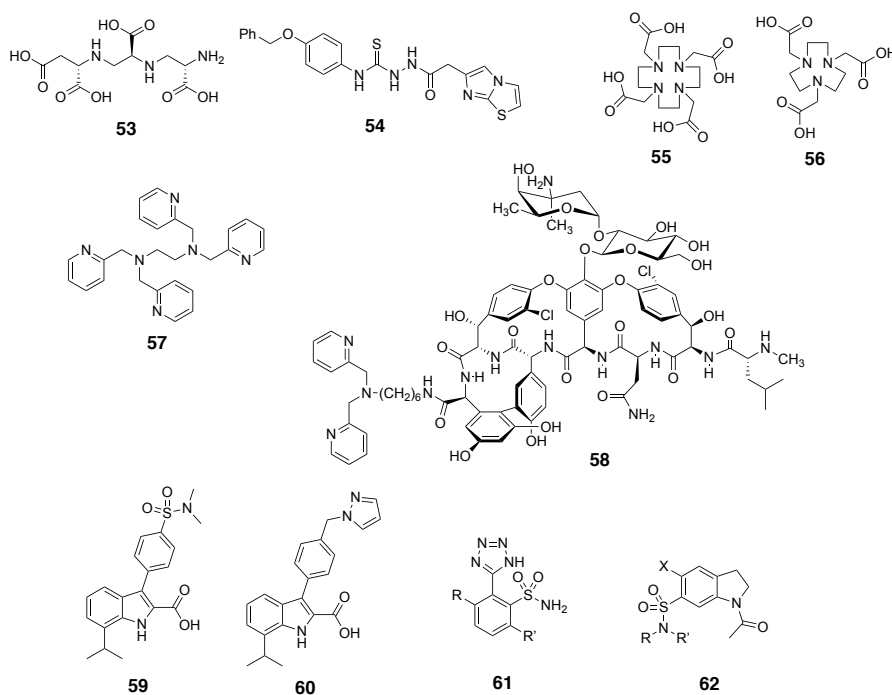


**Figure 15.** Zinc chelators **52-57** and other unique compounds with MBL inhibitory activity.

Another class of MBL inhibitors based on the 3,7-substituted-indole-2-carboxylic acid scaffold was recently reported in the patent literature by Berm and co-workers who screened a large library of analogs for activity against VIM-2, IMP-1, and NDM-1.<sup>187</sup> Several examples were found to possess sub- $\mu$ M activities among which compounds **59** and **60** were found to be most potent against NDM-1 (IC<sub>50</sub> values of 0.35 and 0.5 nM respectively). Researchers at Merck have also assessed numerous sulfonamides for MBL inhibitory activity and in a series of patents describe compounds such as 2-tetrazolylbenzenesulfonamides **61**<sup>188,189</sup> as potent inhibitors of IMP-1, VIM-1, and NDM-1. Using a related approach, Fast and co-workers also found indoline-7-sulfonamides such as compound **62** to possess single-digit  $\mu$ M IC<sub>50</sub> values against NDM-1.<sup>190</sup>

In addition to MBL inhibitors discovered by dedicated screening approaches, a range of other compounds have also been reported to possess anti-MBL activity including: the  $\beta$ -lactam antibiotic cefaclor,<sup>191</sup> 3-formylchromone,<sup>192</sup> ebselen,<sup>193</sup> as well as various hydrazones,<sup>194</sup> phosphonic acids,<sup>195</sup> oxoisindolines,<sup>196</sup> diphenylpyrroles,<sup>197</sup> and bismuth complexes.<sup>198</sup>

## 5. Conclusions

In summary, the new generation of SBL inhibitors including avibactam and vaborbactam were significant breakthroughs in that they were developed from non- $\beta$ -lactam structural backbones. While the activity spectrum of classic  $\beta$ -lactamase inhibitors was limited to non-carbapenemase enzymes of class A and some class C SBLs, avibactam and vaborbactam proved to be potent inhibitors of KPC carbapenemase as well as other class A/C enzymes. Building up the success of this compound class the advanced generation of DBO analogs has provided progress towards achieving broad spectrum SBL inhibitors with activity extending to the clinically important class D OXA enzymes and PBPs. In addition, the advent of cyclic boronate analogs could lead to the first pan- $\beta$ -lactamase inhibitors due to their structural resemblance to the common transition state formed upon both SBL- and MBL-mediated hydrolysis of  $\beta$ -lactams. For the various other compound classes recently described as MBL inhibitors, challenges including stability in physiological conditions (*i.e.* for thiol-based inhibitors) and site-specificity (as for metal chelators) must first be addressed before their clinical relevance can be properly assessed.



## 6. Outline

The theme of this thesis is tackling antibiotic resistance through the development of small molecules with the ability to inhibit metallo- $\beta$ -lactamase enzymes. To this end, we reasoned that molecules that act as zinc-binding ligands could be suitable candidates for preliminary screenings. This effort has been described in **chapter 2**, where a series of commonly-used buffer components previously known to possess metal-binding ability were screened for their inhibitory activity against clinically relevant metallo- $\beta$ -lactamases. In addition, further analyses on the 2 most potent compounds, including time- and zinc-dependency, zinc-binding affinity using isothermal titration calorimetry (ITC), and synergy assays are described.

The ability of the fungal metabolite AMA to inhibit NDM-1 and VIM-type enzymes was discovered in 2014 after which various groups reported the total synthesis of AMA. Following the success of the Poelarends' group in developing a chemoenzymatic route to synthesize AMA and its related aminocarboxylic acids, we evaluated these new AMA-like compounds for their inhibition of NDM-1, zinc-binding affinity, and ability to rescue meropenem against an NDM-1 producing clinical isolate of *E. coli*. These findings have been described in **chapter 3**.

Soon after the discovery of the MBLs, it was found that a number of thiol-containing molecules exhibit potent and broad-spectrum MBL inhibition. In **chapter 4**, we describe the results of our closer look at the ability of such thiol containing compounds to potentiate meropenem and cefoperazone in cell-based synergy assays. To this end, various concentrations of antibiotic-thiol combinations were tested against a panel of carbapenem-resistant gram-negative bacteria in a checkerboard format. In addition, we evaluated their zinc-binding ability and their chemical stability in culture media.

In **chapter 5** we describe our attempt to address the stability and selectivity problem associated with thiol-based MBL inhibitors using a prodrug approach. The concept applied is based on the hydrolysis pathway of some cephalosporins which leads to fragmentation of the molecule after  $\beta$ -lactam ring opening. This led us to design a prodrug system through which the MBL inhibitor might be released after being hydrolyzed by the MBL enzyme itself. The synthetic route to the novel cephalosporin-thiol conjugates as well as a detailed analysis of their enzyme mediated hydrolysis mechanism studied by  $^1\text{H-NMR}$  and LCMS are described. The most potent analogs were subjected to further kinetic experiment as well as structure-activity relationship studies.

**Chapter 6** describes our kinetic experiments on the bacterial lysate containing a newly identified class A carbapenemase. Previous DNA-sequencing and antimicrobial susceptibility assays performed at the Wageningen Bioveterinary Research centre hinted towards the preference of this new carbapenemase for carbapenems over third-generation cephalosporins. Our kinetic assays provided support for this pattern of substrate preference as well as the sensitivity of this enzyme to clavulanic acid.

**References**

- 1 R. P. Ambler, *Philos. Trans. R. Soc. Lond. B. Biol. Sci.*, 1980, **289**, 321–331.
- 2 K. Bush, G. A. Jacoby and A. A. Medeiros, *Antimicrob. Agents Chemother.*, 1995, **39**, 1211–1233.
- 3 S. M. Drawz and R. a. Bonomo, *Clin. Microbiol. Rev.*, 2010, **23**, 160–201.
- 4 K. Bush, *Antimicrob. Agents Chemother.*, 2018, **62**, e01076-18.
- 5 J.-F. Wang and K.-C. Chou, *Curr. Top. Med. Chem.*, 2013, **13**, 1242–1253.
- 6 S. Shakil, E. I. Azhar, S. Tabrez, M. A. Kamal, N. R. Jabir, A. M. Abuzenadah, G. A. Damanhoury and Q. Alam, *J. Chemother.*, 2011, **23**, 263–265.
- 7 A. P. Johnson and N. Woodford, *J. Med. Microbiol.*, 2013, **62**, 499–513.
- 8 Z. Wang, W. Fast, A. M. Valentine and S. J. Benkovic, *Curr. Opin. Chem. Biol.*, 1999, **3**, 614–622.
- 9 A. Potron, L. Poirel and P. Nordmann, *Int. J. Antimicrob. Agents*, 2015, **45**, 568–585.
- 10 D. de A. Viana Marques, S. E. F. Machado, V. Carvalho Santos Ebinuma, C. de A. L. Duarte, A. Converti and A. L. F. Porto, *Antibiotics*, 2018, **7**, 61.
- 11 E. B. Chaïbi, D. Sirot, G. Paul and R. Labia, *J. Antimicrob. Chemother.*, 1999, **43**, 447–458.
- 12 D. van Duin and Y. Doi, *Virulence*, 2017, **8**, 460–469.
- 13 R. A. Bonomo, E. M. Burd, J. Conly, B. M. Limbago, L. Poirel, J. A. Segre and L. F. Westblade, *Clin. Infect. Dis.*, 2017, **66**, 1290–1297.
- 14 R. R. Watkins and S. Deresinski, *Expert Rev. Anti. Infect. Ther.*, 2017, **15**, 893–895.
- 15 K. Bush, *ACS Infect. Dis.*, 2018, **4**, 84–87.
- 16 N. M. Clark, G. G. Zhanel and J. P. Lynch, *Curr. Opin. Crit. Care*, 2016, **22**, 491–499.
- 17 G. S. Tillotson and S. H. Zinner, *Expert Rev. Anti. Infect. Ther.*, 2017, **15**, 663–676.
- 18 Y. R. Lee and N. T. Baker, *Eur. J. Clin. Microbiol. Infect. Dis.*, 2018, **37**, 1411–1419.
- 19 S. C. J. Jorgensen and M. J. Rybak, *Pharmacotherapy*, 2018, **38**, 444–461.
- 20 D. J. Farrell, R. K. Flamm, H. S. Sader and R. N. Jones, *Antimicrob. Agents Chemother.*, 2013, **57**, 6305–6310.
- 21 J. C. Cho, M. T. Zmarlicka, K. M. Shaeer and J. Pardo, *Ann. Pharmacother.*, 2018, **52**, 769–779.
- 22 S. J. Hecker, K. R. Reddy, M. Totrov, G. C. Hirst, O. Lomovskaya, D. C. Griffith, P. King, R. Tsivkovski, D. Sun, M. Sabet, Z. Tarazi, M. C. Clifton, K. Atkins, A. Raymond, K. T. Potts, J. Abendroth, S. H. Boyer, J. S. Loutit, E. E. Morgan, S. Durso and M. N. Dudley,

- J. Med. Chem.*, 2015, **58**, 3682–3692.
- 23 M. Castanheira, P. R. Rhombert, R. K. Flamm and R. N. Jones, *Antimicrob. Agents Chemother.*, 2016, **60**, 5454–5458.
- 24 M. Castanheira, M. D. Huband, R. E. Mendes and R. K. Flamm, *Antimicrob. Agents Chemother.*, 2017, **61**, e00567-17.
- 25 O. Lomovskaya, D. Sun, D. Rubio-Aparicio, K. Nelson, R. Tsivkovski, D. C. Griffith and M. N. Dudley, *Antimicrob. Agents Chemother.*, 2017, **61**, e01443-17.
- 26 D. C. Griffith, J. S. Loutit, E. E. Morgan, S. Durso and M. N. Dudley, *Antimicrob. Agents Chemother.*, 2016, **60**, 6326–6332.
- 27 K. S. Kaye, T. Bhowmick, S. Metallidis, S. C. Bleasdale, O. S. Sagan, V. Stus, J. Vazquez, V. Zaitsev, M. Bidair, E. Chorvat, P. O. Dragoescu, E. Fedosiuk, J. P. Horcajada, C. Murta, Y. Sarychev, V. Stoev, E. Morgan, K. Fusaro, D. Griffith, O. Lomovskaya, E. L. Alexander, J. Loutit, M. N. Dudley and E. J. Giamarellos-Bourboulis, *JAMA - J. Am. Med. Assoc.*, 2018, **319**, 788–799.
- 28 Vabomere webpage, [www.vabomere.com](http://www.vabomere.com).
- 29 FDA label for Vabomere,  
[https://www.accessdata.fda.gov/drugsatfda\\_docs/label/2017/209776lbl.pdf](https://www.accessdata.fda.gov/drugsatfda_docs/label/2017/209776lbl.pdf).
- 30 M. Ball, A. Boyd, G. J. Ensor, M. Evans, M. Golden, S. R. Linke, D. Milne, R. Murphy, A. Telford, Y. Kalyan, G. R. Lawton, S. Racha, M. Ronsheim and S. H. Zhou, *Org. Process Res. Dev.*, 2016, **20**, 1799–1805.
- 31 D. E. Ehmann, H. Jahic, P. L. Ross, R.-F. Gu, J. Hu, G. Kern, G. K. Walkup and S. L. Fisher, *Proc. Natl. Acad. Sci.*, 2012, **109**, 11663–11668.
- 32 D. E. Ehmann, H. Jahić, P. L. Ross, R. F. Gu, J. Hu, T. F. Durand-Réville, S. Lahiri, J. Thresher, S. Livchak, N. Gao, T. Palmer, G. K. Walkup and S. L. Fisher, *J. Biol. Chem.*, 2013, **288**, 27960–27971.
- 33 S. D. Lahiri, M. R. Johnstone, P. L. Ross, R. E. McLaughlin, N. B. Olivier and R. A. Alm, *Antimicrob. Agents Chemother.*, 2014, **58**, 5704–5713.
- 34 S. D. Lahiri, S. Mangani, T. Durand-Reville, M. Benvenuti, F. De Luca, G. Sanyal and J. D. Docquier, *Antimicrob. Agents Chemother.*, 2013, **57**, 2496–2505.
- 35 C. Pozzi, F. Di Pisa, F. De Luca, M. Benvenuti, J. D. Docquier and S. Mangani, *ChemMedChem*, 2018, **13**, 1437–1446.
- 36 P. Levasseur, A. M. Girard, M. Claudon, H. Goossens, M. T. Black, K. Coleman and C. Miossec, *Antimicrob. Agents Chemother.*, 2012, **56**, 1606–1608.

- 1
- 37 M. Castanheira, H. S. Sader, D. J. Farrell, R. E. Mendes and R. N. Jones, *Antimicrob. Agents Chemother.*, 2012, **56**, 4779–4785.
- 38 Z. Aktaş, C. Kayacan and O. Oncul, *Int. J. Antimicrob. Agents*, 2012, **39**, 86–89.
- 39 M. Castanheira, S. E. Farrell, K. M. Krause, R. N. Jones and H. S. Sader, *Antimicrob. Agents Chemother.*, 2014, **58**, 833–838.
- 40 H. S. Sader, M. Castanheira, R. K. Flamm, D. J. Farrell and R. N. Jones, *Antimicrob. Agents Chemother.*, 2014, **58**, 1684–1692.
- 41 X. Wang, F. Zhang, C. Zhao, Z. Wang, W. W. Nichols, R. Testa, H. Li, H. Chen, W. He, Q. Wang and H. Wang, *Antimicrob. Agents Chemother.*, 2014, **58**, 1774–1778.
- 42 S. Marshall, A. M. Hujer, L. J. Rojas, K. M. Papp-Wallace, R. M. Humphries, B. Spellberg, K. M. Hujer, E. K. Marshall, S. D. Rudin, F. Perez, B. M. Wilson, R. B. Wasserman, L. Chikowski, D. L. Paterson, A. J. Vila, D. Van Duin, B. N. Kreiswirth, H. F. Chambers, V. G. Fowler, M. R. Jacobs, M. E. Pulse, W. J. Weiss and R. A. Bonomo, *Antimicrob. Agents Chemother.*, 2017, **61**, e02243-16.
- 43 R. Singh, A. Kim, M. A. Tanudra, J. J. Harris, R. E. McLaughlin, S. Patey, J. P. O'Donnell, P. A. Bradford and A. E. Eakin, *J. Antimicrob. Chemother.*, 2015, **70**, 2618–2626.
- 44 R. K. Flamm, D. J. Farrell, H. S. Sader and R. N. Jones, *J. Antimicrob. Chemother.*, 2014, **69**, 1589–1598.
- 45 M. Castanheira, J. C. Mills, S. E. Costello, R. N. Jones and H. S. Sader, *Antimicrob. Agents Chemother.*, 2015, **59**, 3509–3517.
- 46 H. Li, M. Estabrook, G. A. Jacoby, W. W. Nichols, R. T. Testa and K. Bush, *Antimicrob. Agents Chemother.*, 2015, **59**, 1789–1793.
- 47 N. Sherry and B. Howden, *Expert Rev. Anti. Infect. Ther.*, 2018, **16**, 289–306.
- 48 M. L. Winkler, K. M. Papp-Wallace, A. M. Hujer, T. N. Domitrovic, K. M. Hujer, K. N. Hurless, M. Tuohy, G. Hall and R. A. Bonomo, *Antimicrob. Agents Chemother.*, 2015, **59**, 1020–1029.
- 49 J. A. Vazquez, L. D. González Patzán, D. Stricklin, D. D. Duttaroy, Z. Kreidly, J. Lipka and C. Sable, *Curr. Med. Res. Opin.*, 2012, **28**, 1921–1931.
- 50 F. M. Wagenlehner, J. D. Sobel, P. Newell, J. Armstrong, X. Huang, G. G. Stone, K. Yates and L. B. Gasink, *Clin. Infect. Dis.*, 2016, **63**, 754–762.
- 51 J. E. Mazuski, L. B. Gasink, J. Armstrong, H. Broadhurst, G. G. Stone, D. Rank, L. Llorens, P. Newell and J. Pacht, *Clin. Infect. Dis.*, 2016, **62**, 1380–1389.

- 52 Y. Carmeli, J. Armstrong, P. J. Laud, P. Newell, G. Stone, A. Wardman and L. B. Gasink, *Lancet Infect. Dis.*, 2016, **16**, 661–673.
- 53 FDA label for Avycaz,  
[https://www.accessdata.fda.gov/drugsatfda\\_docs/label/2018/206494s004lbl.pdf](https://www.accessdata.fda.gov/drugsatfda_docs/label/2018/206494s004lbl.pdf).
- 54 G. G. Zhanel, C. K. Lawrence, H. Adam, F. Schweizer, S. Zelenitsky, M. Zhanel, P. R. S. Lagacé-Wiens, A. Walkty, A. Denisuik, A. Golden, A. S. Gin, D. J. Hoban, J. P. Lynch and J. A. Karlowisky, *Drugs*, 2018, **78**, 65–98.
- 55 A. Lapuebla, M. Abdallah, O. Olafisoye, C. Cortes, C. Urban, D. Landman and J. Quale, *Antimicrob. Agents Chemother.*, 2015, **59**, 5029–5031.
- 56 S. H. Lob, M. A. Hackel, K. M. Kazmierczak, K. Young, M. R. Motyl, J. A. Karlowisky and D. F. Sahn, *Antimicrob. Agents Chemother.*, 2017, **61**, e02209.
- 57 J. A. Karlowisky, S. H. Lob, K. M. Kazmierczak, S. P. Hawser, S. Magnet, K. Young, M. R. Motyl and D. F. Sahn, *J. Antimicrob. Chemother.*, 2018, **73**, 1872–1879.
- 58 D. R. Snyderman, N. V. Jacobus and L. A. McDermott, *Antimicrob. Agents Chemother.*, 2016, **60**, 6393–6397.
- 59 E. J. C. Goldstein, D. M. Citron, K. L. Tyrrell, E. Leoncio and C. V. Merriama, *Antimicrob. Agents Chemother.*, 2018, **62**, e01992.
- 60 C. Lucasti, L. Vasile, D. Sandesc, D. Venskutonis, P. McLeroth, M. Lala, M. L. Rizk, M. L. Brown, M. C. Losada, A. Pedley, N. A. Kartsonis and A. Paschke, *Antimicrob. Agents Chemother.*, 2016, **60**, 6234–6243.
- 61 M. Sims, V. Mariyanovski, P. McLeroth, W. Akers, Y.-C. Lee, M. L. Brown, J. Du, A. Pedley, N. A. Kartsonis and A. Paschke, *J. Antimicrob. Chemother.*, 2017, **72**, 2616–2626.
- 62 G. G. Zhanel, P. Chung, H. Adam, S. Zelenitsky, A. Denisuik, F. Schweizer, P. R. S. Lagacé-Wiens, E. Rubinstein, A. S. Gin, A. Walkty, D. J. Hoban, J. P. Lynch and J. A. Karlowisky, *Drugs*, 2014, **74**, 31–51.
- 63 A. J. Sucher, E. B. Chahine, P. Cogan and M. Fete, *Ann. Pharmacother.*, 2015, **49**, 1046–1056.
- 64 J. C. Cho, M. A. Fiorenza and S. J. Estrada, *Pharmacotherapy*, 2015, **35**, 701–715.
- 65 J. L. Liscio, M. V. Mahoney and E. B. Hirsch, *Int. J. Antimicrob. Agents*, 2015, **46**, 266–271.
- 66 L. J. Scott, *Drugs*, 2016, **76**, 231–242.
- 67 J. A. Jones, K. G. Virga, G. Gumina and K. E. Hevener, *Med. Chem. Commun.*, 2016, **7**,

- 1694–1715.
- 68 D. R. Giacobbe, M. Bassetti, F. G. De Rosa, V. Del Bono, P. A. Grossi, F. Menichetti, F. Pea, G. M. Rossolini, M. Tumbarello, P. Viale and C. Viscoli, *Expert Rev. Anti. Infect. Ther.*, 2018, **16**, 307–320.
- 69 A. Toda, H. Ohki, T. Yamanaka, K. Murano, S. Okuda, K. Kawabata, K. Hatano, K. Matsuda, K. Misumi, K. Itoh, K. Satoh and S. Inoue, *Bioorganic Med. Chem. Lett.*, 2008, **18**, 4849–4852.
- 70 K. Murano, T. Yamanaka, A. Toda, H. Ohki, S. Okuda, K. Kawabata, K. Hatano, S. Takeda, H. Akamatsu, K. Itoh, K. Misumi, S. Inoue and T. Takagi, *Bioorganic Med. Chem.*, 2008, **16**, 2261–2275.
- 71 S. Takeda, T. Nakai, Y. Wakai, F. Ikeda and K. Hatano, *Antimicrob. Agents Chemother.*, 2007, **51**, 826–830.
- 72 A. Bryskier, T. Procyk and M. T. Labro, *J. Antimicrob. Chemother.*, 1990, **26**, 1–8.
- 73 D. M. Livermore, S. Mushtaq and Y. Ge, *J. Antimicrob. Chemother.*, 2010, **65**, 1972–1974.
- 74 A. Walkty, J. A. Karlowsky, H. Adam, M. Baxter, P. Lagacé-Wiens, D. J. Hoban and G. G. Zhanel, *Antimicrob. Agents Chemother.*, 2013, **57**, 5707–5709.
- 75 D. R. Snyderman, L. A. McDermott and N. V. Jacobus, *Antimicrob. Agents Chemother.*, 2014, **58**, 1218–1223.
- 76 J. Solomkin, E. Hershberger, B. Miller, M. Popejoy, I. Friedland, J. Steenbergen, M. Yoon, S. Collins, G. Yuan, P. S. Barie and C. Eckmann, *Clin. Infect. Dis.*, 2015, **60**, 1462–1471.
- 77 F. M. Wagenlehner, O. Umeh, J. Steenbergen, G. Yuan and R. O. Darouiche, *Lancet*, 2015, **385**, 1949–1956.
- 78 FDA label for Zerbaxa,  
[https://www.accessdata.fda.gov/drugsatfda\\_docs/label/2014/206829lbl.pdf](https://www.accessdata.fda.gov/drugsatfda_docs/label/2014/206829lbl.pdf).
- 79 J. L. Crandon and D. P. Nicolau, *Antimicrob. Agents Chemother.*, 2015, **59**, 2688–2694.
- 80 J. L. Crandon and D. P. Nicolau, *Pathogens*, 2015, **4**, 620–625.
- 81 F. van den Akker and R. A. Bonomo, *Front. Microbiol.*, 2018, **9**, 622.
- 82 P. Pattanaik, C. R. Bethel, A. M. Hujer, K. M. Hujer, A. M. Distler, M. Taracila, V. E. Anderson, T. R. Fritsche, R. N. Jones, S. R. R. Pagadala, F. Van Den Akker, J. D. Buynak and R. A. Bonomo, *J. Biol. Chem.*, 2009, **284**, 945–953.

- 83 S. M. Drawz, C. R. Bethel, V. R. Doppalapudi, A. Sheri, S. R. R. Pagadala, A. M. Hujer, M. J. Skalweit, V. E. Anderson, S. G. Chen, J. D. Buynak and R. A. Bonomo, *Antimicrob. Agents Chemother.*, 2010, **54**, 1414–1424.
- 84 J. A. Vallejo, M. Martínez-Gutián, J. C. Vázquez-Ucha, C. González-Bello, M. Poza, J. D. Buynak, C. R. Bethel, R. A. Bonomo, G. Bou and A. Beceiro, *J. Antimicrob. Chemother.*, 2016, **71**, 2171–2180.
- 85 J. C. Vázquez-Ucha, M. Maneiro, M. Martínez-Gutián, J. Buynak, C. R. Bethel, R. A. Bonomo, G. Bou, M. Poza, C. González-Bello and A. Beceiro, *Antimicrob. Agents Chemother.*, 2017, **61**, e011172.
- 86 K. M. Papp-Wallace, N. Q. Nguyen, M. R. Jacobs, C. R. Bethel, M. D. Barnes, V. Kumar, S. Bajaksouzian, S. D. Rudin, P. N. Rather, S. Bhavsar, T. Ravikumar, P. K. Deshpande, V. Patil, R. Yeole, S. S. Bhagwat, M. V. Patel, F. Van Den Akker and R. A. Bonomo, *J. Med. Chem.*, 2018, **61**, 4067–4086.
- 87 B. Moya, I. M. Barcelo, S. Bhagwat, M. Patel, G. Bou, K. M. Papp-Wallace, R. A. Bonomo and A. Oliver, *Antimicrob. Agents Chemother.*, 2017, **61**, e02529-16.
- 88 B. Moya, I. M. Barcelo, S. Bhagwat, M. Patel, G. Bou, K. M. Papp-Wallace, R. A. Bonomo and B. Moya, *Antimicrob. Agents Chemother.*, 2017, **61**, e01238-17.
- 89 H. S. Sader, M. Castanheira, M. Huband, R. N. Jones and R. K. Flamm, *Antimicrob. Agents Chemother.*, 2017, **61**, e00072-17.
- 90 H. S. Sader, P. R. Rhomberg, R. K. Flamm, R. N. Jones and M. Castanheira, *J. Antimicrob. Chemother.*, 2017, **72**, 1696–1703.
- 91 A. Morinaka, Y. Tsutsumi, M. Yamada, K. Suzuki, T. Watanabe, T. Abe, T. Furuuchi, S. Inamura, Y. Sakamaki, N. Mitsuhashi, T. Ida and D. M. Livermore, *J. Antimicrob. Chemother.*, 2015, **70**, 2779–2786.
- 92 A. Morinaka, Y. Tsutsumi, K. Yamada, Y. Takayama, S. Sakakibara, T. Takata, T. Abe, T. Furuuchi, S. Inamura, Y. Sakamaki, N. Tsujii and T. Ida, *Antimicrob. Agents Chemother.*, 2016, **60**, 3001–3006.
- 93 A. Morinaka, Y. Tsutsumi, K. Yamada, Y. Takayama, S. Sakakibara, T. Takata, T. Abe, T. Furuuchi, S. Inamura, Y. Sakamaki, N. Tsujii and T. Ida, *J. Antibiot. (Tokyo)*, 2017, **70**, 246–250.
- 94 D. M. Livermore, S. Mushtaq, M. Warner and N. Woodford, *J. Antimicrob. Chemother.*, 2015, **70**, 3032–3041.
- 95 D. M. Livermore, M. Warner, S. Mushtaq and N. Woodford, *Antimicrob. Agents*



- Chemother.*, 2016, **60**, 554–560.
- 96 T. F. Durand-Réville, S. Guler, J. Comita-Prevoir, B. Chen, N. Bifulco, H. Huynh, S. Lahiri, A. B. Shapiro, S. M. McLeod, N. M. Carter, S. H. Moussa, C. Velez-Vega, N. B. Olivier, R. McLaughlin, N. Gao, J. Thresher, T. Palmer, B. Andrews, R. A. Giacobbe, J. V. Newman, D. E. Ehmann, B. De Jonge, J. O'Donnell, J. P. Mueller, R. A. Tommasi and A. A. Miller, *Nat. Microbiol.*, 2017, **2**, 17104.
- 97 R. Tommasi, R. Iyer and A. A. Miller, *ACS Infect. Dis.*, 2018, **4**, 686–695.
- 98 A. B. Shapiro, N. Gao, H. Jahić, N. M. Carter, A. Chen and A. A. Miller, *ACS Infect. Dis.*, 2017, **3**, 833–844.
- 99 R. Iyer, S. H. Moussa, T. F. Durand-Réville, R. Tommasi and A. Miller, *ACS Infect. Dis.*, 2018, **4**, 373–381.
- 100 H. K. Chang, S. Y. Baek, M. J. Kim, K. M. Oh, J. S. Choi, S. B. Ha, S. M. Kim, C.-W. Chung, D. H. Kang, H. J. Kwon, Y. L. Cho and Y. Z. Kim, US Pat., 20170096430A1, 2017.
- 101 Y. G. Gu, Y. He, N. Yin, D. C. Alexander, J. B. Cross and C. A. Metcalf III, US Pat., 20140315876A1, 2014.
- 102 S. N. Maiti, B. Ganguli, D. Q. Nguyen, J. Khan, R. Ling, C. M. Ha and V. Khlebnikov, WO Pat., 2014141132A1, 2014.
- 103 G. S. Basarab, B. Moss, J. Comita-Prevoir, T. F. Durand-Reville, Lise Gauthier, J. O'donnell, J. Romero, R. Tommasi, J. C. Verheijen, F. Wu, X. Wu and J. Zhang, WO Pat., 2018053215A1, 2018.
- 104 W. Ke, J. M. Sampson, C. Ori, F. Prati, S. M. Drawz, C. R. Bethel, R. A. Bonomo and F. Van Den Akker, *Antimicrob. Agents Chemother.*, 2011, **55**, 174–183.
- 105 P. C. Trippier and C. McGuigan, *Medchemcomm*, 2010, **1**, 183–198.
- 106 R. A. Powers, H. C. Swanson, M. A. Taracila, N. W. Florek, C. Romagnoli, E. Caselli, F. Prati, R. A. Bonomo and B. J. Wallar, *Biochemistry*, 2014, **53**, 7670–7679.
- 107 N. Q. Nguyen, N. P. Krishnan, L. J. Rojas, F. Prati, E. Caselli, C. Romagnoli, R. A. Bonomo and F. Van Den Akker, *Antimicrob. Agents Chemother.*, 2016, **60**, 1760–1766.
- 108 A. A. Bouza, H. C. Swanson, K. A. Smolen, A. L. Vandine, M. A. Taracila, C. Romagnoli, E. Caselli, F. Prati, R. A. Bonomo, R. A. Powers and B. J. Wallar, *ACS Infect. Dis.*, 2018, **4**, 325–336.
- 109 J. P. Werner, J. M. Mitchell, M. A. Taracila, R. A. Bonomo and R. A. Powers, *Protein Sci.*, 2017, **26**, 515–526.

- 110 J. Brem, R. Cain, S. Cahill, M. A. McDonough, I. J. Clifton, J. C. Jiménez-Castellanos, M. B. Avison, J. Spencer, C. W. G. Fishwick and C. J. Schofield, *Nat. Commun.*, 2016, **7**, 12406.
- 111 S. T. Cahill, R. Cain, D. Y. Wang, C. T. Lohans, D. W. Wareham, H. P. Oswin, J. Mohammed, J. Spencer, C. W. G. Fishwick, M. A. McDonough, C. J. Schofield and J. Brem, *Antimicrob. Agents Chemother.*, 2017, **61**, e02260-16.
- 112 R. Bonomo, F. Prati, E. Caselli and C. Romagnoli, US Pat., 20170065626A1, 2017.
- 113 R. K. Reddy, T. Glinka, M. Totrov, S. Hecker and O. Rodny, WO Pat., 2016003929A1, 2016.
- 114 R. Reddy, T. Glinka, M. Totrov and S. Hecker, WO Pat., 2014107536A1, 2014.
- 115 C. J. Burns, B. Liu, J. Yao, D. Daigle and S. A. Boyd, US Pat., 20170073360A1, 2017.
- 116 C. J. Burns, D. Daigle, B. Liu, D. McGarry, D. C. Pevear and R. E. Lee Trout, WO Pat., 2014151958A1, 2014.
- 117 C. J. Burns, D. Daigle, B. Liu, R. W. Jackson, J. Hamrick, D. McGarry, D. C. Pevear and R. E. Lee Trout, US Pat., 20160264598A1, 2016.
- 118 C. J. Burns, D. Daigle, B. Liu, D. McGarry, D. C. Pevear, R. E. Lee Trout and R. W. Jackson, US Pat., US20140194386A1, 2014.
- 119 B. Liu, R. E. L. Trout, G.-H. Chu, D. McGarry, R. W. Jackson, J. C. Hamrick, D. M. Daigle, S. M. Cusick, C. Pozzi, F. De Luca, M. Benvenuti, S. Mangani, J.-D. Docquier, W. J. Weiss, D. C. Pevear, L. Xerri and C. J. Burns, *J. Med. Chem.*, 2020, **63**, 2789–2801.
- 120 A. Krajnc, J. Brem, P. Hinchliffe, K. Calvopiña, T. D. Panduwawala, P. A. Lang, J. J. A. G. Kamps, J. M. Tyrrell, E. Widlake, B. G. Seward, T. R. Walsh, J. Spencer and C. J. Schofield, *J. Med. Chem.*, 2019, **62**, 8544–8556.
- 121 J. C. Hamrick, J. D. Docquier, T. Uehara, C. L. Myers, D. A. Six, C. L. Chatwin, K. J. John, S. F. Vernacchio, S. M. Cusick, R. E. L. Trout, C. Pozzi, F. De Luca, M. Benvenuti, S. Mangani, B. Liu, R. W. Jackson, G. Moeck, L. Xerri, C. J. Burns, D. C. Pevear and D. M. Daigle, *Antimicrob. Agents Chemother.*, 2020, **64**, e01963-19.
- 122 A. M. Somboro, J. Osei Sekyere, D. G. Amoako, S. Y. Essack and L. A. Bester, *Appl. Environ. Microbiol.*, 2018, AEM.00698-18.
- 123 D. T. King and N. C. J. Strynadka, *Future Med. Chem.*, 2013, **5**, 1243–1263.
- 124 W. Fast and L. D. Sutton, *Biochim. Biophys. Acta - Proteins Proteomics*, 2013, **1834**, 1648–1659.

- 125 L. C. Ju, Z. Cheng, W. Fast, R. A. Bonomo and M. W. Crowder, *Trends Pharmacol. Sci.*, 2018, **39**, 635–647.
- 126 P. W. Groundwater, S. Xu, F. Lai, L. Váradi, J. Tan, J. D. Perry and D. E. Hibbs, *Future Med. Chem.*, 2016, **8**, 993–1012.
- 127 C. M. Rotondo and G. D. Wright, *Curr. Opin. Microbiol.*, 2017, **39**, 96–105.
- 128 R. P. McGeary, D. T. Tan and G. Schenk, *Future Med. Chem.*, 2017, **9**, 673–691.
- 129 F. M. Klingler, T. A. Wichelhaus, D. Frank, J. Cuesta-Bernal, J. El-Delik, H. F. Müller, H. Sjuts, S. Göttig, A. Koenigs, K. M. Pos, D. Pogoryelov and E. Proschak, *J. Med. Chem.*, 2015, **58**, 3626–3630.
- 130 N. Li, Y. Xu, Q. Xia, C. Bai, T. Wang, L. Wang, D. He, N. Xie, L. Li, J. Wang, H. G. Zhou, F. Xu, C. Yang, Q. Zhang, Z. Yin, Y. Guo and Y. Chen, *Bioorganic Med. Chem. Lett.*, 2014, **24**, 386–389.
- 131 S. Liu, L. Jing, Z. J. Yu, C. Wu, Y. Zheng, E. Zhang, Q. Chen, Y. Yu, L. Guo, Y. Wu and G. B. Li, *Eur. J. Med. Chem.*, 2018, **145**, 649–660.
- 132 D. Büttner, J. S. Kramer, F. M. Klingler, S. K. Wittmann, M. R. Hartmann, C. G. Kurz, D. Kohnhäuser, L. Weizel, A. Brüggerhoff, D. Frank, D. Steinhilber, T. A. Wichelhaus, D. Pogoryelov and E. Proschak, *ACS Infect. Dis.*, 2018, **4**, 360–372.
- 133 G. B. Li, J. Brem, R. Lesniak, M. I. Abboud, C. T. Lohans, I. J. Clifton, S. Y. Yang, J. C. Jiménez-Castellanos, M. B. Avison, J. Spencer, M. A. McDonough and C. J. Schofield, *Chem. Commun.*, 2017, **53**, 5806–5809.
- 134 Y. Yusof, D. T. C. Tan, O. K. Arjomandi, G. Schenk and R. P. McGeary, *Bioorganic Med. Chem. Lett.*, 2016, **26**, 1589–1593.
- 135 J. Brem, S. S. Van Berkel, D. Zollman, S. Y. Lee, O. Gileadi, P. J. McHugh, T. R. Walsh, M. A. McDonough and C. J. Schofield, *Antimicrob. Agents Chemother.*, 2016, **60**, 142–150.
- 136 X. L. Liu, Y. Shi, J. S. Kang, P. Oelschlaeger and K. W. Yang, *ACS Med. Chem. Lett.*, 2015, **6**, 660–664.
- 137 X. L. Liu, K. W. Yang, Y. J. Zhang, Y. Ge, Y. Xiang, Y. N. Chang and P. Oelschlaeger, *Bioorganic Med. Chem. Lett.*, 2016, **26**, 4698–4701.
- 138 O. K. Arjomandi, W. M. Hussein, P. Vella, Y. Yusof, H. E. Sidjabat, G. Schenk and R. P. McGeary, *Eur. J. Med. Chem.*, 2016, **114**, 318–327.
- 139 Y. N. Chang, Y. Xiang, Y. J. Zhang, W. M. Wang, C. Chen, P. Oelschlaeger and K. W. Yang, *ACS Med. Chem. Lett.*, 2017, **8**, 527–532.

- 140 Y. L. Zhang, K. W. Yang, Y. J. Zhou, A. E. LaCuran, P. Oelschlaeger and M. W. Crowder, *ChemMedChem*, 2014, **9**, 2445–2448.
- 141 S.-K. Yang, J. S. Kang, P. Oelschlaeger and K.-W. Yang, *ACS Med. Chem. Lett.*, 2015, **6**, 455–460.
- 142 L. Zhai, Y. L. Zhang, J. S. Kang, P. Oelschlaeger, L. Xiao, S. S. Nie and K. W. Yang, *ACS Med. Chem. Lett.*, 2016, **7**, 413–417.
- 143 Y. Xiang, Y.-N. Chang, Y. Ge, J. S. Kang, Y.-L. Zhang, X.-L. Liu, P. Oelschlaeger and K.-W. Yang, *Bioorg. Med. Chem. Lett.*, 2017, **27**, 5225–5229.
- 144 R. Cain, J. Brem, D. Zollman, M. A. McDonough, R. M. Johnson, J. Spencer, A. Makena, M. I. Abboud, S. Cahill, S. Y. Lee, P. J. McHugh, C. J. Schofield and C. W. G. Fishwick, *J. Med. Chem.*, 2018, **61**, 1255–1260.
- 145 M. M. González, M. Kosmopoulou, M. F. Mojica, V. Castillo, P. Hinchliffe, I. Pettinati, J. Brem, C. J. Schofield, G. Mahler, R. A. Bonomo, L. I. Llarrull, J. Spencer and A. J. Vila, *ACS Infect. Dis.*, 2016, **1**, 544–554.
- 146 P. Hinchliffe, M. M. González, M. F. Mojica, J. M. González, V. Castillo and C. Saiz, *Proc. Natl. Acad. Sci. U. S. A.*, 2016, E3745–E3754.
- 147 J. Brem, S. S. Van Berkel, W. Aik, A. M. Rydzik, M. B. Avison, I. Pettinati, K. D. Umland, A. Kawamura, J. Spencer, T. D. W. Claridge, M. A. McDonough and C. J. Schofield, *Nat. Chem.*, 2014, **6**, 1084–1090.
- 148 Y. Xiang, C. Chen, W. M. Wang, L. W. Xu, K. W. Yang, P. Oelschlaeger and Y. He, *ACS Med. Chem. Lett.*, 2018, **9**, 359–364.
- 149 D. Zhang, M. S. Markoulides, D. Stepanovs, A. M. Rydzik, A. El-Hussein, C. Bon, J. J. A. G. Kamps, K. D. Umland, P. M. Collins, S. T. Cahill, D. Y. Wang, F. von Delft, J. Brem, M. A. McDonough and C. J. Schofield, *Bioorganic Med. Chem.*, 2018, **26**, 2928–2936.
- 150 J. W. Betts, L. M. Phee, M. H. F. Abdul Momin, K. D. Umland, J. Brem, C. J. Schofield and D. W. Wareham, *Medchemcomm*, 2016, **7**, 190–193.
- 151 J. Xiao, M. Fang, Y. Shi, H. Chen, B. Shen, J. Chen, X. Lao, H. Xu and H. Zheng, *Mol. Inform.*, 2015, **34**, 559–567.
- 152 B. Shen, C. Zhu, X. Gao, G. Liu, J. Song and Y. Yu, *PLoS One*, 2017, **12**, e0177293.
- 153 W. S. Shin, A. Bergstrom, R. A. Bonomo, M. W. Crowder, R. Muthyala and Y. Y. Sham, *ChemMedChem*, 2017, **12**, 845–849.
- 154 A. C. Jackson, J. M. Zaengle-Barone, E. A. Puccio and K. J. Franz, *ACS Infect. Dis.*,

- 2020, **6**, 1264–1272.
- 155 S. Skagseth, S. Akhter, M. H. Paulsen, Z. Muhammad, S. Lauksund, Ø. Samuelsen, H.-K. S. Leiros and A. Bayer, *Eur. J. Med. Chem.*, 2017, **135**, 159–173.
- 156 S. R. Schlesinger, B. Bruner, P. J. Farmer and S. K. Kim, *J. Enzyme Inhib. Med. Chem.*, 2013, **28**, 137–142.
- 157 L. Sevaille, L. Gavara, C. Bebrone, F. De Luca, L. Nauton, M. Achard, P. Mercuri, S. Tanfoni, L. Borgianni, C. Guyon, P. Lonjon, G. Turan-Zitouni, J. Dzieciolowski, K. Becker, L. Bénard, C. Condon, L. Maillard, J. Martinez, J. M. Frère, O. Dideberg, M. Galleni, J. D. Docquier and J. F. Hernandez, *ChemMedChem*, 2017, **12**, 972–985.
- 158 G. Q. Song, W. M. Wang, Z. S. Li, Y. Wang and J. G. Wang, *Chinese Chem. Lett.*, 2018, **29**, 899–902.
- 159 C. Mollard, C. Moali, C. Papamicael, C. Damblon, S. Vessilier, G. Amicosante, C. J. Schofield, M. Galleni, J. M. Frère and G. C. K. Roberts, *J. Biol. Chem.*, 2001, **276**, 45015–45023.
- 160 K. H. M. E. Tehrani and N. I. Martin, *ACS Infect. Dis.*, 2017, **3**, 711–717.
- 161 L. E. Horsfall, G. Garau, B. M. R. Liénard, O. Dideberg, C. J. Schofield, J. M. Frère and M. Galleni, *Antimicrob. Agents Chemother.*, 2007, **51**, 2136–2142.
- 162 K. S. Shin, B. R. Son, S. B. Hong and J. Kim, *Diagn. Microbiol. Infect. Dis.*, 2008, **62**, 102–105.
- 163 S. Kimura, Y. Ishii and K. Yamaguchi, *Diagn. Microbiol. Infect. Dis.*, 2005, **53**, 241–244.
- 164 F. Pasteran, O. Veliz, D. Faccione, L. Guerriero, M. Rapoport, T. Mendez and A. Corso, *Clin. Microbiol. Infect.*, 2011, **17**, 1438–1441.
- 165 D. Yong, Y. Lee, S. H. Jeong, K. Lee and Y. Chong, *J. Clin. Microbiol.*, 2012, **50**, 3227–3232.
- 166 A. Y. Chen, P. W. Thomas, A. C. Stewart, A. Bergstrom, Z. Cheng, C. Miller, C. R. Bethel, S. H. Marshall, C. V Credille, C. L. Riley, R. C. Page, R. A. Bonomo, M. W. Crowder, D. L. Tierney, W. Fast and S. M. Cohen, *J. Med. Chem.*, 2017, **60**, 7267–7283.
- 167 A. Y. Chen, P. W. Thomas, Z. Cheng, N. Y. Xu, D. L. Tierney, M. W. Crowder, W. Fast and S. M. Cohen, *ChemMedChem*, 2019, **14**, 1271–1282.
- 168 P. Hinchliffe, C. A. Tanner, A. P. Krismanich, G. Labbé, V. J. Goodfellow, L. Marrone, A. Y. Desoky, K. Calvopiña, E. E. Whittle, F. Zeng, M. B. Avison, N. C. Bols, S. Siemann, J. Spencer and G. I. Dmitrienko, *Biochemistry*, 2018, **57**, 1880–1892.
- 169 M. Everett, N. Sprynski, A. Coelho, J. Castandet, M. Bayet, J. Bougnon, C. Lozano, D.

- T. Davies, S. Leiris, M. Zalacain, I. Morrissey, S. Magnet, K. Holden, P. Warn, F. De Luca, J. D. Docquier and M. Lemonnier, *Antimicrob. Agents Chemother.*, 2018, **62**, e00074-18.
- 170 S. Leiris, A. Coelho, J. Castandet, M. Bayet, C. Lozano, J. Bougnon, J. Bousquet, M. Everett, M. Lemonnier, N. Sprynski, M. Zalacain, T. D. Pallin, M. C. Cramp, N. Jennings, G. Raphy, M. W. Jones, R. Pattipati, B. Shankar, R. Sivasubrahmanyam, A. K. Soodhagani, R. R. Juventhala, N. Pottabathini, S. Pothukanuri, M. Benvenuti, C. Pozzi, S. Mangani, F. De Luca, G. Cerboni, J.-D. Docquier and D. T. Davies, *ACS Infect. Dis.*, 2019, **5**, 131–140.
- 171 Y. Hiraiwa, J. Saito, T. Watanabe, M. Yamada, A. Morinaka, T. Fukushima and T. Kudo, *Bioorganic Med. Chem. Lett.*, 2014, **24**, 4891–4894.
- 172 L. Feng, K.-W. Yang, L.-S. Zhou, J.-M. Xiao, X. Yang, L. Zhai, Y.-L. Zhang and M. W. Crowder, *Bioorg. Med. Chem. Lett.*, 2012, **22**, 5185–5189.
- 173 A. Y. Chen, C. A. Thomas, P. W. Thomas, K. Yang, Z. Cheng, W. Fast, M. W. Crowder and S. M. Cohen, *ChemMedChem*, 2020, In Press.
- 174 H. Tang, S.-W. Yang, M. Mandal, J. Su, G. Li, W. Pan, H. Tang, R. DeJesus, J. Pan, W. Haggmann, F.-X. Ding, L. Xiao, A. Pasternak, Y. Huang, S. Dong and D. Yang, US Pat., 20170173035A1, 2017.
- 175 A. M. King, S. A. Reid-Yu, W. Wang, D. T. King, G. De Pascale, N. C. Strynadka, T. R. Walsh, B. K. Coombes and G. D. Wright, *Nature*, 2014, **510**, 503–506.
- 176 D. Liao, S. Yang, J. Wang, J. Zhang, B. Hong, F. Wu and X. Lei, *Angew. Chemie - Int. Ed.*, 2016, **55**, 4291–4295.
- 177 K. Koteva, A. M. King, A. Capretta and G. D. Wright, *Angew. Chemie - Int. Ed.*, 2016, **55**, 2210–2212.
- 178 S. A. Albu, K. Koteva, A. M. King, S. Al-Karmi, G. D. Wright and A. Capretta, *Angew. Chemie - Int. Ed.*, 2016, **55**, 13259–13262.
- 179 J. Zhang, S. Wang, Y. Bai, Q. Guo, J. Zhou and X. Lei, *J. Org. Chem.*, 2017, **82**, 13643–13648.
- 180 H. Fu, J. Zhang, M. Saifuddin, G. Cruiming, P. G. Tepper and G. J. Poelarends, *Nat. Catal.*, 2018, **1**, 186–191.
- 181 A. Bergstrom, A. Katko, Z. Adkins, J. Hill, Z. Cheng, M. Burnett, H. Yang, M. Aitha, M. R. Mehaffey, J. S. Brodbelt, K. H. M. E. Tehrani, N. I. Martin, R. A. Bonomo, R. C. Page, D. L. Tierney, W. Fast, G. D. Wright and M. W. Crowder, *ACS Infect. Dis.*, 2018, **4**,

- 135–145.
- 182 J. C. Sacchetti, J. A. Mire, C. C. Thurman, N. W. Zhou, A. Joachimiak, G. Babnigg and Kim Youngchang, WO Pat., 2015157618A1, 2015.
- 183 A. M. Somboro, D. Tiwari, L. A. Bester, R. Parboosing, L. Chonco, H. G. Kruger, P. I. Arvidsson, T. Govender, T. Naicker and S. Y. Essack, *J. Antimicrob. Chemother.*, 2015, **70**, 1594–1596.
- 184 E. Zhang, M. M. Wang, S. C. Huang, S. M. Xu, D. Y. Cui, Y. L. Bo, P. Y. Bai, Y. G. Hua, C. L. Xiao and S. Qin, *Bioorganic Med. Chem. Lett.*, 2018, **28**, 214–221.
- 185 R. Azumah, J. Dutta, A. M. Somboro, M. Ramtahal, L. Chonco, R. Parboosing, L. A. Bester, H. G. Kruger, T. Naicker, S. Y. Essack and T. Govender, *J. Appl. Microbiol.*, 2016, **120**, 860–867.
- 186 V. Yarlagadda, P. Sarkar, S. Samaddar, G. B. Manjunath, S. Das Mitra, K. Paramanandham, B. R. Shome and J. Haldar, *ACS Infect. Dis.*, 2018, **4**, 1093–1101.
- 187 J. Brem, A. M. Ryzdik, M. A. McDonough, C. J. Schofield, A. Morrison, J. Hewitt, A. Pannifer and P. Jones, WO Pat., 2017093727A1, 2017.
- 188 M. Mandal, H. Tang, L. Xiao, J. Su, G. Li, S.-W. Yang, W. Pan, H. Tang, R. DeJesus, J. Hicks, M. Lombardo, H. Chu, W. Hagemann, A. Pasternak, X. Gu, J. Jiang, S. Dong, F.-X. Ding, C. London, D. Biswas, K. Young, D. N. Hunter, Z. Zhao and D. Yang, US Pat., 20160333021A1, 2016.
- 189 F. Bennett, J. Jiang, A. Pasternak, S. Dong, X. Gu, J. D. Scott, H. Tang, Z. Zhao, Y. Huang, D. Hunter, D. Yang, Z. Zhang, J. Fu, Y. Bai, Z. Zheng, X. Zhang, K. Young and L. Xiao, WO Pat., 2016206101A1, 2016.
- 190 D. P. Becker, C. Reidl, M. Moore, T. K. Heath and W. Fast, WO pat., 2017011408A1, 2017.
- 191 P. W. Thomas, M. Cammarata, J. S. Brodbelt and W. Fast, *ChemBioChem*, 2014, **15**, 2541–2548.
- 192 T. Christopheit, A. Albert and H.-K. S. Leiros, *Bioorg. Med. Chem.*, 2016, **24**, 2947–2953.
- 193 J. Chiou, S. Wan, K. F. Chan, P. K. So, D. He, E. W. C. Chan, T. H. Chan, K. Y. Wong, J. Tao and S. Chen, *Chem. Commun.*, 2015, **51**, 9543–9546.
- 194 M. Brindisi, S. Brogi, S. Giovani, S. Gemma, S. Lamponi, F. De Luca, E. Novellino, G. Campiani, J. D. Docquier and S. Butini, *J. Enzyme Inhib. Med. Chem.*, 2016, **31**, 98–109.

- 195 Y. L. Zhang, Y. J. Zhang, W. M. Wang and K. W. Yang, *Phosphorus, Sulfur Silicon Relat. Elem.*, 2017, **192**, 14–18.
- 196 G.-B. Li, M. I. Abboud, J. Brem, H. Someya, C. T. Lohans, S.-Y. Yang, J. Spencer, D. W. Wareham, M. A. McDonough and C. J. Schofield, *Chem. Sci.*, 2017, **8**, 928–937.
- 197 R. P. McGearry, D. T. C. Tan, C. Selleck, M. Monteiro Pedroso, H. E. Sidjabat and G. Schenk, *Eur. J. Med. Chem.*, 2017, **137**, 351–364.
- 198 R. Wang, T. P. Lai, P. Gao, H. Zhang, P. L. Ho, P. C. Y. Woo, G. Ma, R. Y. T. Kao, H. Li and H. Sun, *Nat. Commun.*, 2018, **9**, 439.





## Chapter 2

### Small-molecule aminocarboxylic acids as metallo- $\beta$ -lactamase inhibitors; Part I.

Parts of this chapter have been published in:

Tehrani, K. H. M. E., Bröchle, N. C., Wade, N., Mashayekhi, V., Pesce, D., van Haren, M., and I. Martin, N. Small molecule carboxylates inhibit metallo- $\beta$ -lactamases and resensitize carbapenem-resistant bacteria to meropenem. *ACS Infect. Dis.* **6**, 1366–1371.

## 1. Introduction

Antibiotic resistance threatens to reduce the efficacy of currently available antibiotics and places a substantial burden on global health and the world economy.<sup>1,2</sup> Resistance to  $\beta$ -lactam antibiotics can be caused by a diverse group of enzymes known as  $\beta$ -lactamases. While based on sequence homology these enzymes are categorized in class A-D (known as Ambler classification),<sup>3</sup> mechanistically they are classified as serine- $\beta$ -lactamases (SBLs, Ambler class A, C, and D) or metallo- $\beta$ -lactamases (MBLs, Ambler class B).<sup>4</sup> SBLs inactivate  $\beta$ -lactams via the hydrolytic action of a nucleophilic serine in their active site. First-generation SBL inhibitors including clavulanic acid, sulbactam, and tazobactam as well as the more recently approved avibactam and vaborbactam, are available to rescue the antimicrobial activity of  $\beta$ -lactams in the presence of SBL-producing bacteria.<sup>5,6</sup> MBLs on the other hand are metallo-enzymes that hydrolyze  $\beta$ -lactams by action of a zinc-activated nucleophilic water molecule that is formed in the active site. To date there are no FDA-approved MBL inhibitors available. Of particular concern are the clinically important MBLs including the New Delhi metallo- $\beta$ -lactamase (NDM), Verona integron-encoded metallo- $\beta$ -lactamase (VIM), and imipenemase (IMP) families that possess carbapenemase activity,<sup>7</sup> adding further urgency to the development of MBL inhibitors to combat MBL-producing bacterial infections.

Small molecules with the ability to inhibit MBLs have been the topic of a number of comprehensive reviews.<sup>8-11</sup> The majority of known MBL inhibitors contain functional groups that can bind zinc. In this regard, the most common small molecules possessing anti-MBL activity are thiol-containing compounds,<sup>12-15</sup> sulfonylhydrazones,<sup>16</sup> bis-carboxylic acids,<sup>17,18</sup> picolinic acids,<sup>19,20</sup> and commonly used chelating agents<sup>21,22</sup> including their bacteria-targeting analogs.<sup>23,24</sup> As an example, the natural product aspergillomarasmine A (AMA), was recently identified by Wright and coworkers who screened fungal extracts for anti-MBL activity. AMA was shown to be a potent inhibitor of both NDM and VIM type enzymes and importantly displays *in vivo* efficacy.<sup>25</sup> Also of interest are the recently developed cyclic boronate SBL- and MBL-inhibitors which mimic the tetrahedral intermediate formed upon nucleophilic attack of a serine-hydroxyl group (SBLs) or zinc-bound water molecule (MBLs) at the  $\beta$ -lactam unit.<sup>26-30</sup> In addition, recent reports have also described compounds with alternative modes of MBL inhibition including covalent inhibitors<sup>31-33</sup> and DNA aptamers proposed to operate via allosteric mechanism of inhibition.<sup>34</sup>

In reviewing the literature we noted that sulfonic acid buffer components such as MES and PIPES have previously been reported to be weak MBL inhibitors.<sup>35</sup> This prompted us to investigate the possibility of identifying new MBL inhibitor candidates among other commonly used small molecule buffer components containing multiple carboxylic acid and/or phosphonate functionalities. Given that zinc binding is a key aspect of the mechanism of action for a majority of MBL inhibitors, we specifically focused our attention on common buffer reagents and structurally related small molecules reported to interact with metals (figure 1).

## 2. Results and discussion

The panel of small molecules shown in figure 1 were first screened for their inhibitory activity against purified MBLs including NDM-1, VIM-2, and IMP-28. The substrate used for the enzyme inhibition assay was a fluorescent cephalosporin derivative developed by Schofield and co-workers for assessing MBL activity.<sup>36</sup> As shown in table 1, nitrilotriacetic acid (NTA, **3**) and its bioisosteres (**4**, **5**) showed promising activity against NDM-1 and VIM-2 superior to that of dipicolinic acid (DPA), a well-studied MBL inhibitor.<sup>19,20</sup> Notably, the much weaker inhibitory activity of the disubstituted analogs **1** and **2** point to the necessity of three carboxyl(phosphoryl) substituents in order to achieve potent inhibition of NDM-1 and VIM-2, most probably by tightly chelating zinc ions. Interestingly, compounds **1-8** all exhibited little-to-no activity against IMP-28. This observation is in line with previous investigations that have found the IMP class of MBLs to be less sensitive to inhibition by zinc-binding agents.<sup>25,37</sup> To establish whether the inhibition measured was time-dependent, the IC<sub>50</sub> values of compounds **3**, **5**, and DPA for NDM-1 were

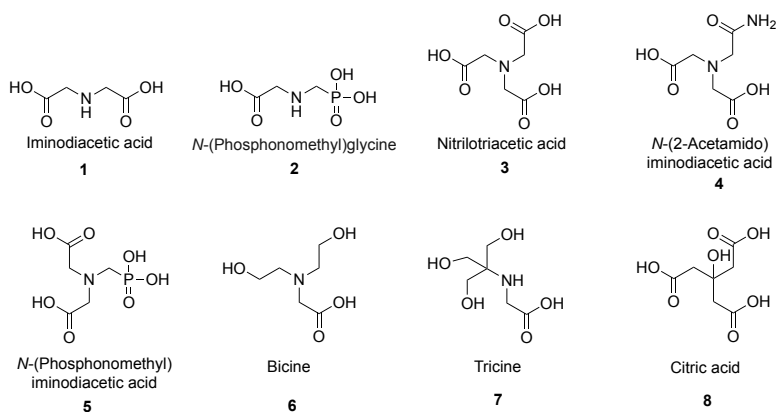


**Figure 1.** Small-molecule carboxylic acids as potential MBL inhibitors

also determined after pre-incubating the inhibitor and enzyme for various times including 0, 10, 20, 40, and 60 minutes as previously described for a different class of NDM-1 inhibitors.<sup>38</sup> As shown in figure 2A, pre-incubation time does not significantly affect the potency of the tested compounds under the assay conditions used.

The majority of MBL inhibitors fall into one of two groups: those that interact with zinc as part of their binding in the MBL active site forming a ternary complex, or those that actively strip zinc from the MBL active site driven by their strong chelating ability.<sup>39,40</sup> Captopril is an example of the former while known chelating agents such as EDTA and the fungal secondary metabolite AMA represent the latter.<sup>19,41</sup> In determining the IC<sub>50</sub> value of **5** against NDM-1 it was noted that in the presence of different concentrations of zinc sulfate (ranging from 0.1 μM to 20 μM), the IC<sub>50</sub> values measured also changed revealing a zinc-dependent effect similar to that for DPA. By comparison, and as expected, the inhibitory activity of captopril is not influenced by varying the concentration of exogenous zinc added to the assay media (figure 2B). These findings support a zinc-sequestration based mechanism of NDM-1 inhibition for compound **5**.

**Table 1.** IC<sub>50</sub> values determined against NDM-1, VIM-2, and IMP-28.

Compound	IC <sub>50</sub> (μM) <sup>a</sup>		
	NDM-1	VIM-2	IMP-28
<b>1</b>	>200	>200	>200
<b>2</b>	75 ± 2	41 ± 6	>200
<b>3</b>	1.3 ± 0.07	2.4 <sup>b</sup>	112 ± 3
<b>4</b>	2.3 ± 0.05	25 <sup>b</sup>	>200
<b>5</b>	0.91 ± 0.05	0.68 ± 0.02	39 ± 7
<b>6</b>	>200	>200	>200
<b>7</b>	>200	>200	>200
<b>8</b>	132 ± 15	102 ± 7	>200
<b>DPA</b>	3.8 ± 0.04	2.9 ± 0.5	17 ± 1

<sup>a</sup>Values reported as mean ± SD of at least 3 independent experiments.

<sup>b</sup>Due to the complex shape of the log[concentration]-activity plot, accurate fitting was not possible, the reported values are therefore an estimation.

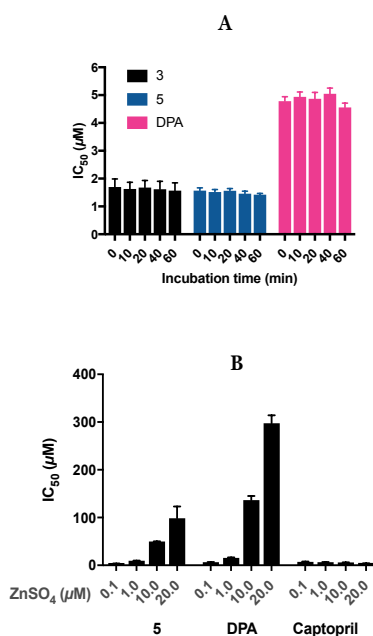


**Figure 2. A.** The inhibitory activity of compounds **3**, **5**, and DPA over the time-course of 0-60 min against NDM-1. **B.** The effect of zinc on the inhibitory activity of compound **5**, DPA, and captopril against NDM-1.

Further evidence for high affinity zinc binding by compound **5** was obtained by use of isothermal titration calorimetry (ITC). This technique allows for the direct determination of the dissociation constant ( $K_d$ ) as well as thermodynamic parameters including  $\Delta G$ ,  $\Delta H$ , and  $\Delta S$ . Among the small molecules tested as part of the current study, compounds **3-5** were found to be strong zinc-binders with  $K_d$  values of 121 nM, 231 nM, and 56 nM respectively (table 2). Interestingly, the affinity of compounds **3-5** for other biologically-relevant divalent cations like  $\text{Ca}^{2+}$  and  $\text{Mg}^{2+}$  was negligible by ITC with binding interactions too weak to allow for an accurate determination of thermodynamic parameters. Previous reports have also described potentiometric titration<sup>42-44</sup> and ITC based methods for studying the metal binding properties of related compounds.<sup>45-47</sup> It should be noted that in these earlier studies, the associated  $K_d$  values measured for the binding of  $\text{Ca}^{2+}$  and  $\text{Zn}^{2+}$  by DPA were somewhat lower than the values obtained in our investigations, an effect we ascribe to differences in the buffers used. Specifically, given the buffering capacity of the test compounds evaluated in our study, we chose to employ 100 mM Tris buffers to avoid any pH mismatch. Notably, our ITC data reveal a strong correlation between these compounds' capacity to inhibit MBL activity and their zinc binding ability (table 2).

The results of our investigations, as well as other recently published studies, indicate that incorporation of the phosphonic acid moiety is a promising approach in designing potent MBL inhibitors.<sup>48-50</sup> In line with our findings relating to the enhanced potency of compound **5** relative to compound **3** are recent studies showing that phosphonic acid analogs of picolinic acid demonstrate increased potency against NDM-1.<sup>20,49</sup> In addition, phosphonate analogs of the well-known mercapto-carboxylic acid MBL inhibitors (represented by thiomandelic acid) demonstrate enhanced inhibitory activity.<sup>48</sup> In light of our findings and the studies mentioned

**Table 2.** ITC based thermodynamic parameters for the binding of zinc by compounds **3-5**

Compound	$K_d$ (nM)	$\Delta H$ (kcal/mol)	$-T\Delta S$ (kcal/mol)	$\Delta G$ (kcal/mol)
<b>3</b> <sup>a</sup>	$\text{Zn}^{2+}$ 121 $\pm$ 8	-4.89 $\pm$ 0.22	-4.55 $\pm$ 0.25	-9.40 $\pm$ 0.04
<b>4</b> <sup>a</sup>	$\text{Zn}^{2+}$ 231 $\pm$ 10	-2.96 $\pm$ 0.07	-6.10 $\pm$ 0.08	-9.06 $\pm$ 0.03
<b>5</b> <sup>a</sup>	$\text{Zn}^{2+}$ 56 $\pm$ 15	-3.08 $\pm$ 0.11	-6.84 $\pm$ 0.28	-9.91 $\pm$ 0.16
<b>DPA</b> <sup>b</sup>	$\text{Zn}^{2+}$ 2373 $\pm$ 367	-2.46 $\pm$ 0.18	-5.21 $\pm$ 0.27	-7.68 $\pm$ 0.09
	$\text{Ca}^{2+}$ 34233 $\pm$ 525	-5.503 $\pm$ 0.05	-0.589 $\pm$ 0.05	-6.09 $\pm$ 0.01

<sup>a</sup>No appreciable binding to  $\text{Ca}^{2+}$  and  $\text{Mg}^{2+}$  was observed.

<sup>b</sup>No appreciable binding to  $\text{Mg}^{2+}$  was observed.

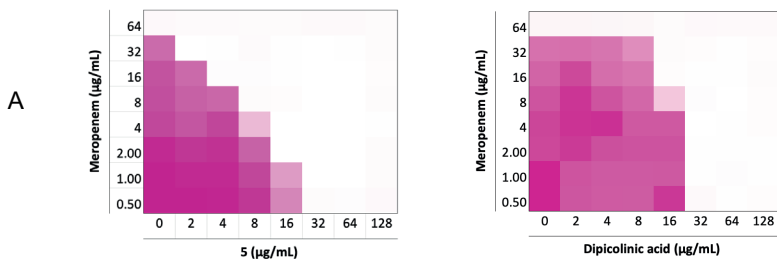
above, incorporation of a phosphonic acid moiety into the structures of other MBL inhibitors such as cyclic boronates (exemplified by VNRX-5133)<sup>30</sup> may also provide access to new classes of hybrid MBL inhibitors.

The ability of compounds **1-8** to restore the activity of meropenem, a last resort carbapenem, against a representative MBL-expressing strain was evaluated using a clinical NDM-1 positive isolate (coded *E. coli* RC0089). Using a checkerboard assay, multiple concentration combinations of MBL inhibitor + meropenem were tested allowing for calculation of the fractional inhibitory concentration (FIC) index according to the following expression (where an FIC index of <0.5 indicates a synergistic relationship):

$$\text{FICI} = \frac{\text{MIC of meropenem in combination}}{\text{MIC of meropenem alone}} + \frac{\text{MIC of MBL inhibitor in combination}}{\text{MIC of MBL inhibitor alone}}$$

Among the compounds tested, **3-5** showed a synergistic relationship with meropenem with compound **5** demonstrating the highest potency with the lowest FIC index of 0.047 (figure 3). Compounds **3** and **5** were both very effective in restoring the activity of meropenem against the NDM-1 producing *E. coli* strain used in the initial screen and were therefore also tested in combination with meropenem against a larger panel of 38 gram-negative clinical isolates displaying carbapenem resistance (table 3). While compounds **3** and **5** exhibited no antibacterial activity at the highest tested concentration of 256 µg/mL, both were found to effectively enhance the activity of meropenem against strains expressing NDM- and VIM-type enzymes. When administered at a concentration of 32 µg/mL both **3** and **5** reduced the MIC of meropenem by up to 128-fold against these strains, a synergism equivalent to or better than that observed for DPA. Overall, compound **5** reduced the MIC of meropenem to its clinically susceptible concentration (≤1 µg/mL) for 67% of the NDM- and VIM-type producing isolates tested while for compound **3** and DPA this ratio was 37% and 53% respectively. By comparison, when tested against strains expressing IMP-type enzymes, the synergistic activity of **3** and **5** was modest, leading to no more than a 4-fold reduction of MIC in most cases, a trend also mirrored for DPA. In addition, the complete lack of synergy observed against strains expressing serine-carbapenemases such as KPC-2 and OXA-48, further demonstrates the inhibitory activities of compounds **3** and **5** to be MBL-specific. Also, among the bacterial species screened, *P. aeruginosa* proved to be more resistant to the synergistic combinations tested. This is apparent when comparing the

antibacterial activities of the combinations against NDM-1 and VIM-2 producing *P. aeruginosa* isolates versus the corresponding *E. coli* and *K. pneumoniae* counterparts (see table 3).



**B**

Compound	1	2	3	4	5	6	7	8	DPA
Lowest FIC	>0.5	>0.5	0.078	0.266	0.047	>0.5	>0.5	>0.5	0.070

**Figure 3. A.** Checkerboard plots for compound **5** and DPA in combination with meropenem tested against an NDM-1 producing strain of *E. coli*. The optical density of the bacteria at 600 nm ( $OD_{600}$ ) has been shown as color gradient between white (no bacterial growth) and magenta (maximum growth); **B.** The lowest FIC values calculated for compounds **1-8**.



**Table 3.** MIC of meropenem alone or in combination with compound **3, 5**, and DPA against a panel of carbapenem-resistant clinical isolates of gram-negative bacteria.

Bacterial isolates	$\beta$ -lactamase	MIC ( $\mu\text{g/mL}$ )			
		Mer	Mer + 3 <sup>a</sup>	Mer + 5 <sup>a</sup>	Mer + DPA <sup>a</sup>
<i>E. coli</i> <sup>b</sup>	NDM-1	8	0.5 (16)	0.125 (64)	0.25 (32)
<i>E. coli</i> <sup>b</sup>	NDM-1	16	$\leq 0.125$ ( $\geq 128$ )	$\leq 0.125$ ( $\geq 128$ )	0.25 (64)
<i>E. coli</i> <sup>c</sup>	NDM-1	16	0.5 (32)	0.25 (64)	0.5 (32)
<i>E. coli</i> <sup>d</sup>	NDM-1	128	4 (32)	0.5 (256)	1 (128)
<i>K. pneumoniae</i> <sup>d</sup>	NDM-1	32	1 (32)	0.125 (256)	0.5 (64)
<i>K. pneumoniae</i> <sup>d</sup>	NDM-1	64	4 (16)	$\leq 0.5$ ( $\geq 128$ )	1 (64)
<i>K. pneumoniae</i> <sup>d</sup>	NDM-1	16	1 (16)	0.25 (64)	0.25 (64)
<i>P. aeruginosa</i> <sup>e</sup>	NDM-1	128	16 (8)	8 (16)	8 (16)
<i>P. stuartii</i> <sup>b</sup>	NDM-1	32	0.25 (128)	0.25 (128)	0.25 (128)
<i>A. baumannii</i> <sup>e</sup>	NDM-2	32	4 (8)	2 (16)	2 (16)
<i>E. coli</i> <sup>c</sup>	NDM-4	64	2 (32)	$\leq 0.5$ ( $\geq 128$ )	1 (64)
<i>E. coli</i> <sup>b</sup>	NDM-5	32	4 (8)	0.5 (64)	2 (16)
<i>E. coli</i> <sup>c</sup>	NDM-5	128	16 (8)	8 (16)	8 (16)
<i>E. coli</i> <sup>c</sup>	NDM-6	128	32 (4)	8 (16)	8 (16)
<i>E. coli</i> <sup>c</sup>	NDM-7	32	$\leq 0.5$ ( $\geq 64$ )	$\leq 0.5$ ( $\geq 64$ )	$\leq 0.5$ ( $\geq 64$ )
<i>E. coli</i> <sup>c</sup>	NDM-15	128	64 (2)	32 (4)	64 (2)
<i>E. aerogenes</i> <sup>d</sup>	VIM-1	16	1 (16)	$\leq 0.25$ ( $\geq 64$ )	0.5 (32)
<i>K. pneumoniae</i> <sup>b</sup>	VIM-1	256	16 (16)	$\leq 2$ ( $\geq 128$ )	4 (64)
<i>K. pneumoniae</i> <sup>d</sup>	VIM-1	32	2 (16)	$\leq 0.5$ ( $\geq 64$ )	$\leq 0.5$ ( $\geq 64$ )
<i>K. pneumoniae</i> <sup>d</sup>	VIM-1	256	8 (32)	$\leq 2$ ( $\geq 128$ )	4 (64)
<i>K. pneumoniae</i> <sup>d</sup>	VIM-1	64	$\leq 0.5$ ( $\geq 128$ )	$\leq 0.5$ ( $\geq 128$ )	$\leq 0.5$ ( $\geq 128$ )
<i>E. coli</i> <sup>b</sup>	VIM-2	8	0.25 (32)	0.125 (64)	0.125 (64)
<i>K. pneumoniae</i> <sup>e</sup>	VIM-2	8	0.5 (16)	0.25 (32)	0.25 (32)
<i>P. aeruginosa</i> <sup>b</sup>	VIM-2	32	8 (4)	4 (8)	4 (8)
<i>P. aeruginosa</i> <sup>b</sup>	VIM-2	16	4 (4)	1 (16)	2 (8)
<i>P. aeruginosa</i> <sup>b</sup>	VIM-2	32	2 (16)	2 (16)	4 (8)
<i>P. aeruginosa</i> <sup>d</sup>	VIM-2, <i>bla</i> <sub>PAO</sub>	16	2 (8)	1 (16)	2 (8)
<i>P. aeruginosa</i> <sup>b</sup>	VIM-2, OXA-50, <i>bla</i> <sub>PAO</sub>	16	2 (8)	1 (16)	2 (8)
<i>P. aeruginosa</i> <sup>c</sup>	VIM-11	16	2 (8)	1 (16)	1 (16)
<i>P. aeruginosa</i> <sup>c</sup>	VIM-28	>256	256 ( $\geq 2$ )	64 ( $\geq 8$ )	128 ( $\geq 4$ )
<i>P. aeruginosa</i> <sup>e</sup>	IMP-1	>256	256 ( $\geq 2$ )	256 ( $\geq 2$ )	256 ( $\geq 2$ )
<i>P. aeruginosa</i> <sup>c</sup>	IMP-7	64	16 (4)	16 (4)	16 (4)
<i>P. aeruginosa</i> <sup>c</sup>	IMP-13	64	32 (2)	16 (4)	16 (4)
<i>P. aeruginosa</i> <sup>d</sup>	IMP-13, IMP-37, <i>bla</i> <sub>PAO</sub>	64	32 (2)	16 (4)	16 (4)
<i>K. pneumoniae</i> <sup>d</sup>	IMP-28	4	0.5 (8)	0.5 (8)	2 (2)
<i>K. pneumoniae</i> <sup>d</sup>	KPC-2	256	256 (1)	256 (1)	256 (1)
<i>K. pneumoniae</i> <sup>d</sup>	OXA-48	32	32 (1)	32 (1)	32 (1)
<i>E. coli</i> <sup>f</sup>	-	$\leq 0.0625$	$\leq 0.0625$ ( $\geq 1$ )	$\leq 0.0625$ ( $\geq 1$ )	$\leq 0.0625$ ( $\geq 1$ )

<sup>a</sup>Each inhibitor was used at 32  $\mu\text{g/mL}$  in combination with meropenem. None of the inhibitors showed toxicity up to 256  $\mu\text{g/mL}$  against the tested strains. Fold reduction of MIC has been shown in brackets. <sup>b</sup>Source: Vrije Universiteit Medical center, The Netherlands. <sup>c</sup>Source: The Dutch national institute for public health and the environment. <sup>d</sup>Source: Utrecht university medical center, The Netherlands. <sup>e</sup>Source: National reference laboratory for multidrug-resistant gram-negative bacteria, Bochum, Germany. <sup>f</sup>ATCC 25922, this strain does not harbor any carbapenemase and was used as a negative control.

### 3. Conclusion

The most clinically relevant MBLs continue to be the NDM, VIM, and IMP classes and present a significant challenge to the efficacy of virtually all classes of  $\beta$ -lactam antibiotics including “last-line-of-defense” carbapenems such as meropenem. Despite this, no inhibitors are clinically available to combat resistant infections caused by gram-negative pathogens that express MBLs. The current study expands our understanding of the diversity of small molecule carboxylic acids that inhibit MBLs and synergize with carbapenems. By screening a series of available and commonly used small-molecule carboxylates, we found that nitrilotriacetic acid (**3**) and its phosphoric acid analog *N*-(phosphonomethyl)iminodiacetic acid (**5**) are both potent inhibitors of NDM- and VIM- type enzymes with sub- to low- $\mu$ M IC<sub>50</sub> values. Using ITC both **3** and **5** were shown to bind zinc with nanomolar affinity. When further tested against a broad panel of MBL-producing gram-negative pathogens, compounds **3** and **5** effectively reduced the MIC of meropenem against NDM- and VIM- type enzymes. As for the well-characterized DPA, the mechanism of MBL inhibition for **3** and **5** appears to be largely driven by zinc-sequestration. While such strong zinc-binding compounds are unlikely clinical candidates, they do represent readily available inhibitors for biochemical studies of MBLs. Furthermore, given their small size and structural simplicity, such compounds may serve as leads for further optimization. One approach may be to administer such compounds as prodrugs that are activated only upon entry to the bacterial cell. In the absence of clinically approved MBL-inhibitors, and with increasing rates of MBL-driven carbapenem resistance, it is important that many approaches, including unconventional avenues, be explored in the pursuit of an effective therapeutic response.

## 4. Experimental section

### *Enzyme production and purification*

For the production of VIM-2 and NDM-1, pOPINF NDM-1 and pTriEx-based pOPINF plasmids (ampicillin resistant) were used. The constructs were a generous gift from Prof. Christopher J. Schofield (Oxford university). In the case of IMP-28, the construct was designed in pET28b with a 6-His tag at the C-terminus. The plasmids of IMP-28, VIM-2, NDM-1 were transformed in BL21 competent *E. coli* using standard heat shock transformation method. The single colonies were grown overnight at 37 °C in LB medium containing 1% glucose and appropriate antibiotic (100 µg/mL ampicillin or 300 µg/mL amikacin). The cell suspension was diluted 100 times in YT2x supplemented with 0.1% glucose and antibiotic, shaking at 37 °C for about 4 h to reach OD<sub>600</sub> of 0.5-0.7. The expression of the enzymes was induced by addition of isopropyl β-D-1-thiogalactopyranoside (IPTG, final concentration 0.5 mM). The cells were incubated overnight at 25 °C with shaking and then harvested by centrifugation for 20 min at 6000 rpm. The pellet was resuspended in lysis buffer (PBS, 150 mM NaCl, 0.05% Triton X-100, protease inhibitor cocktail). After two freeze-thaw cycles the cell suspension was incubated with 1 mg/mL lysozyme for 30 min at 37 °C followed by 3 cycles of sonication (30-s pulse and 30-s rest each cycle). The cellular debris were removed by centrifugation at 12000 rpm for 20 min at 4 °C. Äkta Xpress chromatography system was used to purify the enzymes. Briefly, the supernatant was loaded on 1 mL HisTrap HP column and the enzymes were eluted with 300 mM imidazole. The fractions were then loaded on HiTrap desalting column to exchange the buffer. In case of IMP-28, the fractions were collected in 20 mM Tris, 150 mM NaCl, 10% glycerol, 20 µM ZnCl<sub>2</sub>. VIM-2 and NDM-1 fractions were buffer exchanged to 20 mM Tris, 200 mM NaCl. The purity of the fractions was determined on 15% SDS-PAGE gel (figure 4). The concentration of the enzymes was measured by Nanodrop at 280 nm. To remove the His tag at the N-termini of VIM-2 and NDM-1, the proteins were incubated overnight at 4 °C with HRV-3C protease (1:100

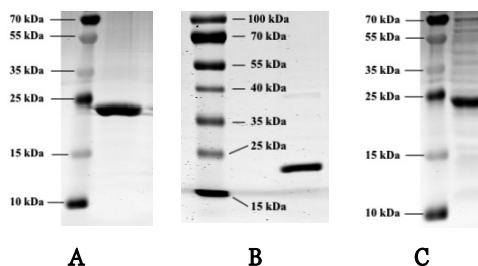


**Figure 4.** SDS-PAGE gels of purified NDM-1 (A), VIM-2 (B), and IMP-28 (C).

w/w). The digestion mixture was passed through a HisTrap column to separate cleaved from uncleaved enzymes. The cleavage of His tag was confirmed by western blot technique. Both enzymes were buffer exchanged to 50 mM Tris (pH 7.5) containing 500 mM NaCl

### *IC<sub>50</sub> and zinc dependency assay*

All the test compounds were dissolved and serially diluted in 50 mM HEPES pH 7.2, supplemented with 0.01% Triton X-100 and 1  $\mu$ M ZnSO<sub>4</sub>. The MBL enzymes (60 pM NDM-1, 100 pM VIM-2, and 60 pM IMP-28) were then added to the wells and incubated at 25 °C for 15 min. Next, the fluorescent cephalosporin substrate FC5<sup>36</sup> (0.5  $\mu$ M for NDM-1 and VIM-2, 16  $\mu$ M for IMP-28) was added to the wells and fluorescence was monitored immediately over 30-40 scanning cycles ( $\lambda_{\text{ex}}$  380 nm,  $\lambda_{\text{em}}$  460 nm) on a Tecan Spark plate reader. Using the initial velocity data plotted against inhibitor concentration, the half-maximal inhibitory concentrations were calculated by IC<sub>50</sub> curve-fitting model in GraphPad Prism 7 software (figure 5). 2,6-Dipicolinic acid was used as positive control. The IC<sub>50</sub> of captopril, dipicolinic acid, and **5** was also evaluated in the presence of different concentrations of zinc sulfate (0.1, 1, 10 and 20  $\mu$ M) against NDM-1 following the procedure described above.

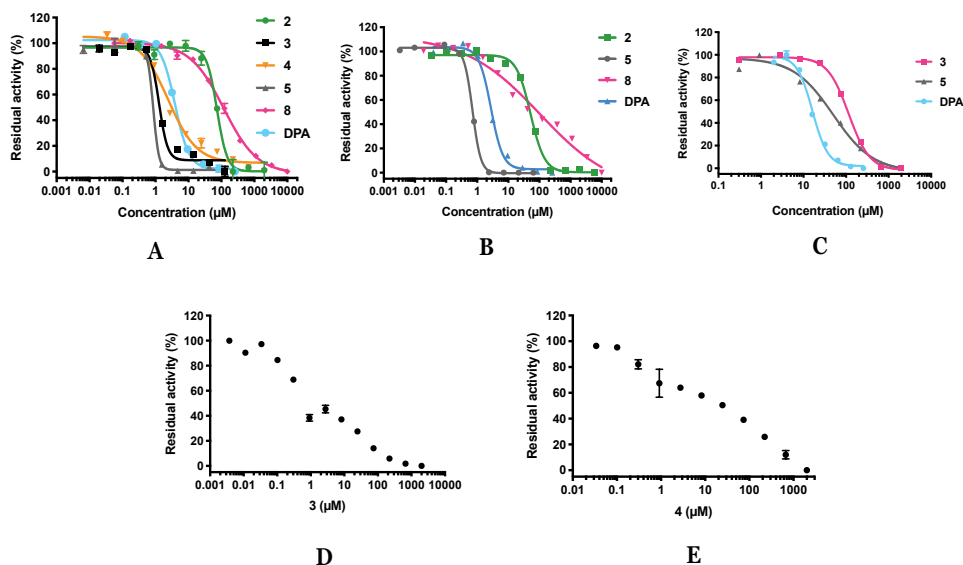


**Figure 5.** IC<sub>50</sub> curves of the test compounds against NDM-1 (A), VIM-2 (B), and IMP-28 (C). The activity plot of compounds **3** (D) and **4** (E) against VIM-2 did not have a sigmoidal shape.

### Isothermal Titration Calorimetry (ITC)

The test compounds were evaluated for their ability to bind zinc using an automated PEAQ-ITC calorimeter (Malvern). Zinc sulfate dissolved in 100 mM Tris (pH 7.0) was titrated into the test compounds dissolved in the same buffer over  $19 \times 2 \mu\text{L}$  aliquots (except for the first aliquot which was  $0.4 \mu\text{L}$ ). The titrations were performed at  $25^\circ\text{C}$  and reference power was set at  $10 \mu\text{cal}/\text{sec}$ . Peak integration and curve-fitting was done using the PEAQ-ITC data analysis software provided by the manufacturer. The blank titrations included buffer titrated in the test compounds, and zinc sulfate titrated in buffer all of which showed negligible signals attributed to heat of dilution (see figure 6 for the thermograms).

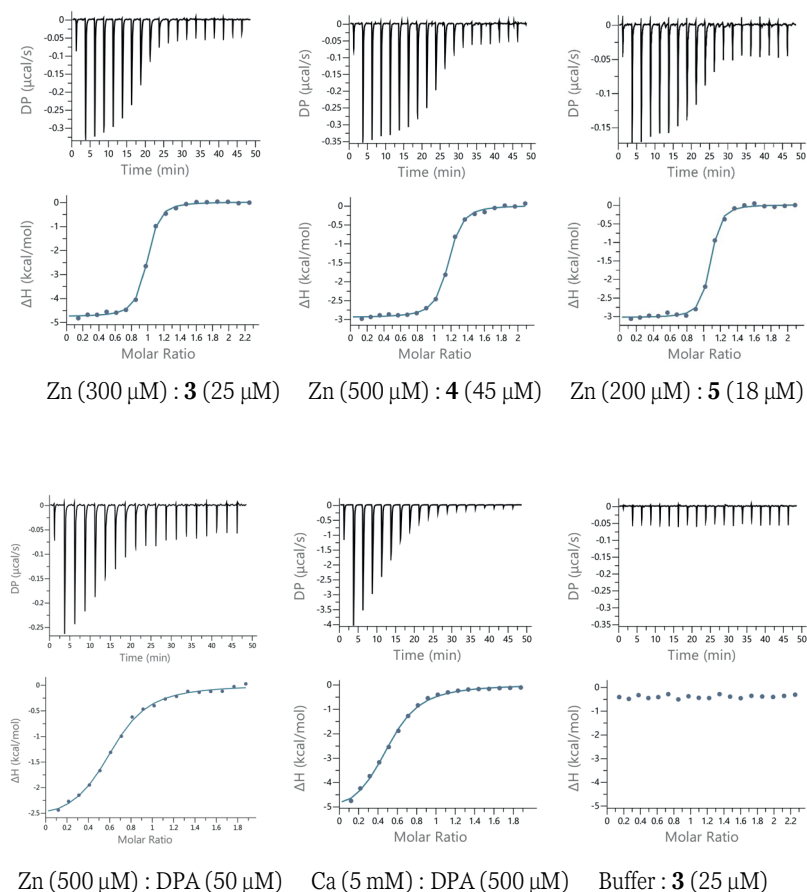


**Figure 6.** ITC thermograms

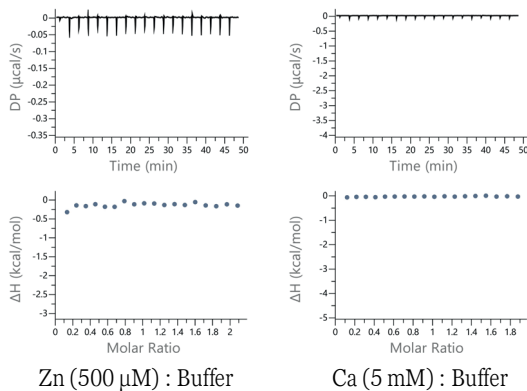
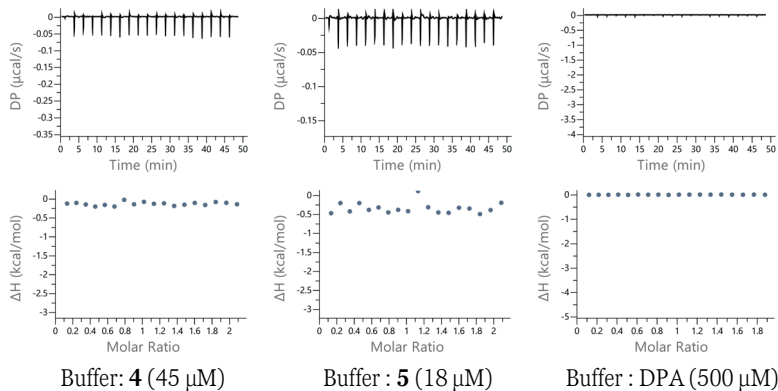


Figure 6. Continued

### ***Antibacterial assays***

All antibacterial assays were carried out following the guidelines published by the clinical and laboratory standards institute (CLSI). Bacterial strains and clinical isolates were cultured on blood agar and incubated overnight at 37 °C. Fresh colonies were suspended in tryptic soy broth (TSB) and incubated at 37 °C with shaking. Following growth to exponential phase ( $OD_{600} = 0.5$ ), the bacterial suspension was diluted to  $10^6$  CFU/mL in Mueller-Hinton broth (MHB) and added to the test compounds prepared as described for each assay:

*A. Single concentration synergy assay.* On a polypropylene microplate, meropenem was dissolved and serially diluted in MHB (25  $\mu$ L/well). Compounds **3**, **5**, and DPA with the final concentration of 32  $\mu$ g/mL (25  $\mu$ L/well) were then added to the wells. Following the addition of the diluted bacterial suspensions prepared as described above (50  $\mu$ L/well), the microplates were incubated at 37 °C with shaking and after 16-20 h, the plates were inspected for the bacterial growth. Minimum inhibitory concentration (MIC) values were reported as the lowest concentration of the antibiotic/test compounds that prevents the visible growth of bacteria. All the assays were performed in triplicate and the median values were used to report MICs.

*B.  $OD_{600}$  checkerboard assay.* Meropenem was dissolved and serially diluted on the polypropylene microplates in MHB (25  $\mu$ L/well). The test compounds dissolved and serially diluted to the final concentration ranging from 128  $\mu$ g/mL to 1  $\mu$ g/mL were then added to meropenem (25  $\mu$ L/well). *E. coli* RC0089, a clinical isolate producing NDM-1, grown to the exponential phase and diluted in MHB was added to the microplate (50  $\mu$ L/well) which was then incubated at 37 °C with shaking. After 16-20 h, the optical density of wells was scanned at 600 nm on a Tecan Spark plate reader (figure 7).

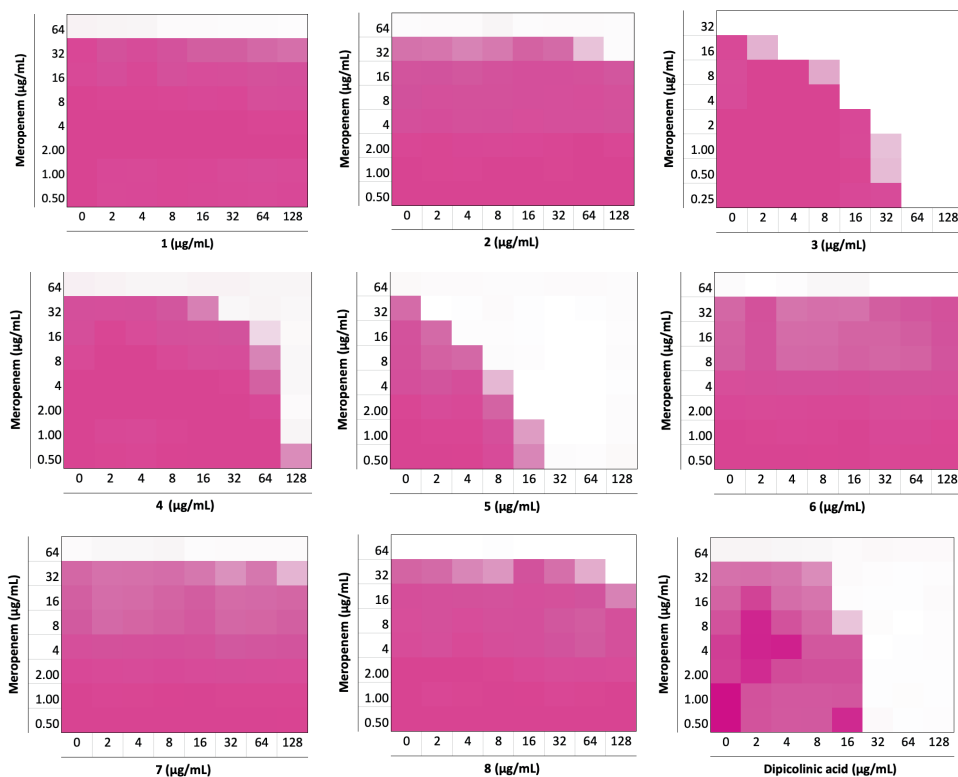


**Figure 7.** Checkerboard assays of the tested small molecules in combination with meropenem against an NDM-1 producing clinical isolate of *E. coli*. The optical density of the bacteria at 600 nm ( $OD_{600}$ ) has been shown as color gradient between white (no bacterial growth) and magenta (maximum growth).

## Acknowledgements

The enzyme experiments were made possible thanks to the contributions of Diego Pesce to design the plasmid construct of IMP-28, Vida Mashayekhi to express and purify NDM-1, VIM-2, and IMP-28, and Matthijs van Haren to synthesize the FC5 substrate.



## References

- 1 M. Ferri, E. Ranucci, P. Romagnoli and V. Giaccone, *Crit. Rev. Food Sci. Nutr.*, 2017, **57**, 2857–2876.
- 2 B. Aslam, W. Wang, M. I. Arshad, M. Khurshid, S. Muzammil, M. H. Rasool, M. A. Nisar, R. F. Alvi, M. A. Aslam, M. U. Qamar, M. K. F. Salamat and Z. Baloch, *Infect. Drug Resist.*, 2018, **2018**, 1645–1658.
- 3 R. P. Ambler, *Philos. Trans. R. Soc. Lond. B. Biol. Sci.*, 1980, **289**, 321–331.
- 4 S. M. Drawz and R. A. Bonomo, *Clin. Microbiol. Rev.*, 2010, **23**, 160–201.
- 5 K. H. M. E. Tehrani and N. I. Martin, *Medchemcomm*, 2018, **9**, 1439–1456.
- 6 K. Bush, *ACS Infect. Dis.*, 2018, **4**, 84–87.
- 7 M. F. Mojica and R. A. B. and W. Fast, *Curr. Drug Targets*, 2016, **17**, 1029–1050.
- 8 W. Fast and L. D. Sutton, *Biochim. Biophys. Acta - Proteins Proteomics*, 2013, **1834**, 1648–1659.
- 9 P. W. Groundwater, S. Xu, F. Lai, L. Váradi, J. Tan, J. D. Perry and D. E. Hibbs, *Future Med. Chem.*, 2016, **8**, 993–1012.
- 10 R. P. McGeary, D. T. Tan and G. Schenk, *Future Med. Chem.*, 2017, **9**, 673–691.
- 11 P. Linciano, L. Cendron, E. Gianquinto, F. Spyraakis and D. Tondi, *ACS Infect. Dis.*, 2019, **5**, 9–34.
- 12 C. Mollard, C. Moali, C. Papamicael, C. Damblon, S. Vessilier, G. Amicosante, C. J. Schofield, M. Galleni, J. M. Frère and G. C. K. Roberts, *J. Biol. Chem.*, 2001, **276**, 45015–45023.
- 13 K. H. M. E. Tehrani and N. I. Martin, *ACS Infect. Dis.*, 2017, **3**, 711–717.
- 14 D. Büttner, J. S. Kramer, F.-M. Klingler, S. K. Wittmann, M. R. Hartmann, C. G. Kurz, D. Kohnhäuser, L. Weizel, A. Brüggerhoff, D. Frank, D. Steinhilber, T. A. Wichelhaus, D. Pogoryelov and E. Proschak, *ACS Infect. Dis.*, 2018, **4**, 360–372.
- 15 Z. Meng, M.-L. Tang, L. Yu, Y. Liang, J. Han, C. Zhang, F. Hu, J.-M. Yu and X. Sun, *ACS Infect. Dis.*, 2019, **5**, 903–916.
- 16 S. Siemann, D. P. Evanoff, L. Marrone, A. J. Clarke, T. Viswanatha and G. I. Dmitrienko, *Antimicrob. Agents Chemother.*, 2002, **46**, 2450–2457.
- 17 L. Feng, K.-W. Yang, L.-S. Zhou, J.-M. Xiao, X. Yang, L. Zhai, Y.-L. Zhang and M. W. Crowder, *Bioorg. Med. Chem. Lett.*, 2012, **22**, 5185–5189.
- 18 Y. Hiraiwa, J. Saito, T. Watanabe, M. Yamada, A. Morinaka, T. Fukushima and T. Kudo, *Bioorg. Med. Chem. Lett.*, 2014, **24**, 4891–4894.

- 19 A. Y. Chen, P. W. Thomas, A. C. Stewart, A. Bergstrom, Z. Cheng, C. Miller, C. R. Bethel, S. H. Marshall, C. V Credille, C. L. Riley, R. C. Page, R. A. Bonomo, M. W. Crowder, D. L. Tierney, W. Fast and S. M. Cohen, *J. Med. Chem.*, 2017, **60**, 7267–7283.
- 20 A. Y. Chen, P. W. Thomas, Z. Cheng, N. Y. Xu, D. L. Tierney, M. W. Crowder, W. Fast and S. M. Cohen, *ChemMedChem*, 2019, **14**, 1271–1282.
- 21 A. M. Somboro, D. Tiwari, L. A. Bester, R. Parboosing, L. Chonco, H. G. Kruger, P. I. Arvidsson, T. Govender, T. Naicker and S. Y. Essack, *J. Antimicrob. Chemother.*, 2015, **70**, 1594–1596.
- 22 R. Azumah, J. Dutta, A. M. Somboro, M. Ramtahal, L. Chonco, R. Parboosing, L. A. Bester, H. G. Kruger, T. Naicker, S. Y. Essack and T. Govender, *J. Appl. Microbiol.*, 2016, **120**, 860–867.
- 23 V. Yarlagadda, P. Sarkar, S. Samaddar, G. B. Manjunath, S. Das Mitra, K. Paramanandham, B. R. Shome and J. Haldar, *ACS Infect. Dis.*, 2018, **4**, 1093–1101.
- 24 C. Schnaars, G. Kildahl-Andersen, A. Prandina, R. Popal, S. Radix, M. Le Borgne, T. Gjøen, A. M. S. Andresen, A. Heikal, O. A. Økstad, C. Fröhlich, Ø. Samuelsen, S. Lauksund, L. P. Jordheim, P. Rongved and O. A. H. Åstrand, *ACS Infect. Dis.*, 2018, **4**, 1407–1422.
- 25 A. M. King, S. A. Reid-Yu, W. Wang, D. T. King, G. De Pascale, N. C. Strynadka, T. R. Walsh, B. K. Coombes and G. D. Wright, *Nature*, 2014, **510**, 503–506.
- 26 A. Krajnc, P. A. Lang, T. D. Panduwawala, J. Brem and C. J. Schofield, *Curr. Opin. Chem. Biol.*, 2019, **50**, 101–110.
- 27 S. T. Cahill, J. M. Tyrrell, I. H. Navratilova, K. Calvopiña, S. W. Robinson, C. T. Lohans, M. A. McDonough, R. Cain, C. W. G. Fishwick, M. B. Avison, T. R. Walsh, C. J. Schofield and J. Brem, *Biochim. Biophys. Acta - Gen. Subj.*, 2019, **1863**, 742–748.
- 28 G. W. Langley, R. Cain, J. M. Tyrrell, P. Hinchliffe, K. Calvopiña, C. L. Tooke, E. Widlake, C. G. Dowson, J. Spencer, T. R. Walsh, C. J. Schofield and J. Brem, *Bioorg. Med. Chem. Lett.*, 2019, **29**, 1981–1984.
- 29 A. Krajnc, J. Brem, P. Hinchliffe, K. Calvopiña, T. D. Panduwawala, P. A. Lang, J. J. A. G. Kamps, J. M. Tyrrell, E. Widlake, B. G. Seward, T. R. Walsh, J. Spencer and C. J. Schofield, *J. Med. Chem.*, 2019, **62**, 8544–8556.
- 30 B. Liu, R. E. L. Trout, G.-H. Chu, D. McGarry, R. W. Jackson, J. C. Hamrick, D. M. Daigle, S. M. Cusick, C. Pozzi, F. De Luca, M. Benvenuti, S. Mangani, J.-D. Docquier, W. J. Weiss, D. C. Pevear, L. Xerri and C. J. Burns, *J. Med. Chem.*, 2020, **6**, 2789–2801.

- 31 P. W. Thomas, M. Cammarata, J. S. Brodbelt and W. Fast, *ChemBioChem*, 2014, **15**, 2541–2548.
- 32 J. Chiou, S. Wan, K.-F. Chan, P.-K. So, D. He, E. W. Chan, T. Chan, K. Wong, J. Tao and S. Chen, *Chem. Commun.*, 2015, **51**, 9543–9546.
- 33 T. Christopeit, A. Albert and H.-K. S. Leiros, *Bioorg. Med. Chem.*, 2016, **24**, 2947–2953.
- 34 N. H. Khan, A. A. Bui, Y. Xiao, R. B. Sutton, R. W. Shaw, B. J. Wylie and M. P. Latham, *PLoS One*, 2019, **14**, e0214440.
- 35 P. M. D. Fitzgerald, J. K. Wu and J. H. Toney, *Biochemistry*, 1998, **37**, 6791–6800.
- 36 S. S. van Berkel, J. Brem, A. M. Rydzik, R. Salimraj, R. Cain, A. Verma, R. J. Owens, C. W. G. Fishwick, J. Spencer and C. J. Schofield, *J. Med. Chem.*, 2013, **56**, 6945–6953.
- 37 A. Proschak, J. Kramer, E. Proschak and T. A. Wichelhaus, *J. Antimicrob. Chemother.*, 2017, **73**, 425–430.
- 38 S. T. Cahill, R. Cain, D. Y. Wang, C. T. Lohans, D. W. Wareham, H. P. Oswin, J. Mohammed, J. Spencer, C. W. G. Fishwick, M. A. McDonough, C. J. Schofield and J. Brem, *Antimicrob. Agents Chemother.*, 2017, **61**, e02260-16.
- 39 L. C. Ju, Z. Cheng, W. Fast, R. A. Bonomo and M. W. Crowder, *Trends Pharmacol. Sci.*, 2018, **39**, 635–647.
- 40 C. M. Rotondo and G. D. Wright, *Curr. Opin. Microbiol.*, 2017, **39**, 96–105.
- 41 A. Bergstrom, A. Katko, Z. Adkins, J. Hill, Z. Cheng, M. Burnett, H. Yang, M. Aitha, M. R. Mehaffey, J. S. Brodbelt, K. H. M. E. Tehrani, N. I. Martin, R. A. Bonomo, R. C. Page, D. L. Tierney, W. Fast, G. D. Wright and M. W. Crowder, *ACS Infect. Dis.*, 2018, **4**, 135–145.
- 42 L. Chung, K. S. Rajan, E. Merdinger and N. Grecz, *Biophys. J.*, 1971, **11**, 469–482.
- 43 H. A. Azab, Z. M. Anwar and M. Sokar, *J. Chem. Eng. Data*, 2004, **49**, 62–72.
- 44 C. R. Krishnamoorthy and R. Nakon, *J. Coord. Chem.*, 1991, **23**, 233–243.
- 45 D. Wyrzykowski, B. Pilarski, D. Jacewicz and L. Chmurzyński, *J. Therm. Anal. Calorim.*, 2013, **111**, 1829–1836.
- 46 D. Wyrzykowski, A. Tesmar, D. Jacewicz, J. Pranczk and L. Chmurzyński, *J. Mol. Recognit.*, 2014, **27**, 722–726.
- 47 A. Tesmar, D. Wyrzykowski, E. Muñoz, B. Pilarski, J. Pranczk, D. Jacewicz and L. Chmurzyński, *J. Mol. Recognit.*, 2017, **30**, e2589.
- 48 P. Lassaux, M. Hamel, M. Gulea, H. Delbrück, P. S. Mercuri, L. Horsfall, D. Dehareng,

- M. Kupper, J.-M. Frère, K. Hoffmann, M. Galleni and C. Bebrone, *J. Med. Chem.*, 2010, **53**, 4862–4876.
- 49 P. Hinchliffe, C. A. Tanner, A. P. Krismanich, G. Labbé, V. J. Goodfellow, L. Marrone, A. Y. Desoky, K. Calvopiña, E. E. Whittle, F. Zeng, M. B. Avison, N. C. Bols, S. Siemann, J. Spencer and G. I. Dmitrienko, *Biochemistry*, 2018, **57**, 1880–1892.
- 50 O. A. Pemberton, P. Jaishankar, A. Akhtar, J. L. Adams, L. N. Shaw, A. R. Renslo and Y. Chen, *J. Med. Chem.*, 2019, **62**, 8480–8496.



## Chapter 3

### Small-molecule aminocarboxylic acids as metallo- $\beta$ -lactamase inhibitors; Part II.

Parts of this chapter have been published in:

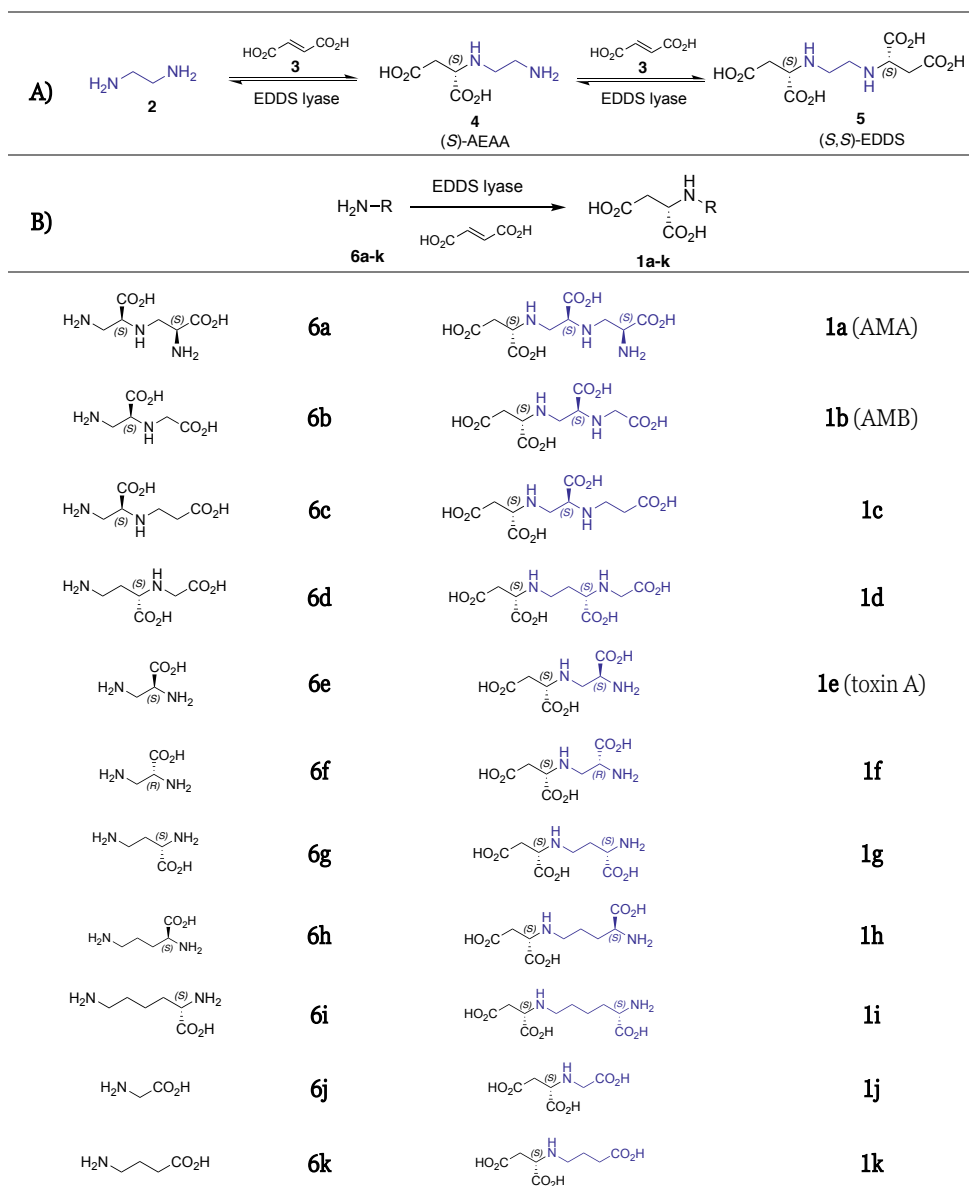
Tehrani, K. H. M. E.,\* Fu, H.,\* Bröchle, N. C., Mashayekhi, V., Prats Luján, A., van Haren, M. J., Poelarends, G. J., and Martin, N. I. (2020) Aminocarboxylic acids related to aspergillomarasmine A (AMA) and ethylenediamine-*N,N'*-disuccinic acid (EDDS) are strong zinc-binders and inhibitors of the metallo-beta-lactamase NDM-1. *Chem. Comm.* **56**, 3047–3049.

## 1. Introduction

Antibiotic resistance is a global public health concern with an increasing economic burden.<sup>1,2</sup> Among gram-negative pathogens,  $\beta$ -lactam resistance due to the production of  $\beta$ -lactamases is a major cause of antibiotic resistance.<sup>3</sup> Based on their mechanism of  $\beta$ -lactam hydrolysis,  $\beta$ -lactamases can be classified as serine- or metallo- $\beta$ -lactamases (SBLs and MBLs respectively). While SBLs hydrolyze  $\beta$ -lactams via an active site serine nucleophile, MBLs do so via a water molecule coordinated with active site zinc ion(s).<sup>4</sup> While there are clinically used SBL inhibitors available to counteract the infections caused by SBL-producing bacteria,<sup>5</sup> there are currently no approved MBL inhibitors available.

Recent screening efforts led to the identification of aspergillomarasmine A (AMA, entry **1a**, table 1) as a potent inhibitor of the clinically relevant NDM- and VIM-type MBLs.<sup>6</sup> This finding was followed by reports describing the chemical synthesis of AMA and its structural analogs.<sup>7-11</sup> Among them, synthetic routes using either a key *N*-nosyl protected aziridine intermediate<sup>10</sup> or a cyclic sufamidate<sup>9</sup> furnished AMA in relatively few steps and the highest reported yields (overall yields of 28% and 19% respectively).

Recently, our collaborators in the Poelarends group (Groningen) reported that ethylenediamine-*N,N'*-disuccinic acid (EDDS) lyase naturally catalyzes a reversible two-step sequential addition of ethylenediamine (**2**) to two molecules of fumaric acid (**3**), giving (*S*)-*N*-(2-aminoethyl)aspartic acid (AEAA, **4**) as an intermediate and (*S,S*)-EDDS (**5**) as the final product (table 1A).<sup>12</sup> EDDS lyase was subsequently found to have broad substrate promiscuity,<sup>13-15</sup> accepting a wide range of amino acids with terminal amino groups (**6a-k**) for regio- and stereoselective addition to fumarate, thus providing a straightforward biocatalytic method for the asymmetric synthesis of AMA (**1a**), AMB (**1b**), and related aminocarboxylic acids (**1c-k**, table 1B).<sup>13</sup> To further explore the substrate scope of EDDS lyase, as well as to prepare a small library of EDDS derivatives as potential NDM-1 inhibitors,<sup>16</sup> in this chapter we describe the MBL-inhibitory activity and zinc binding affinity of AMA and AMB analogs as well as a series of EDDS analogs prepared by the Poelarends group via the EDDS-lyase catalyzed reaction of fumaric acid with various diamines containing different aliphatic linkers between the two amino functional groups (**7a-i**) (table 2).

**Table 1.** Stereoselective C–N bond-formation reactions catalyzed by EDDS lyase

**(A)** Natural reaction catalyzed by EDDS lyase. **(B)** Previously reported<sup>12,13</sup> analogs of AMA, AMB, and toxin A prepared using the EDDS lyase methodology and here investigated as NDM-1 inhibitors.



**Table 2.** Enzymatic synthesis of EDDS analogs

$2 \text{ HO}_2\text{C}-\text{CH}=\text{CH}-\text{CO}_2\text{H} \quad \mathbf{3} + \text{H}_2\text{N}-\text{[Ring]}-\text{NH}_2 \quad \mathbf{7a-i} \xrightarrow[\text{Conditions}^a]{\text{EDDS lyase}}$		$\text{HO}_2\text{C}-\text{CH}(\text{CO}_2\text{H})-\text{CH}_2-\text{NH}-\text{[Ring]}-\text{NH}-\text{CH}_2-\text{CH}(\text{CO}_2\text{H})-\text{CO}_2\text{H} \quad \mathbf{8a-i}$	
Entry	Diamine	Product <sup>b</sup>	Conv. <sup>c</sup> (yield <sup>d</sup> )[%]
1	<b>7a</b>	<b>8a</b>	75 (31)
2	<b>7b</b>	<b>8b</b>	70 (21)
3	<b>7c</b>	<b>8c</b>	74 (33)
4	<b>7d</b>	<b>8d</b>	67 (31)
5	<b>7e</b>	<b>8e</b>	80 (60)
6	<b>7f</b>	<b>8f</b>	47 (26)
7	<b>7g</b>	<b>8g</b>	83 (32)
8	<b>7h</b>	<b>8h</b>	0
9	<b>7i</b>	<b>8i</b>	0

<sup>a</sup>Conditions and reagents: reaction mixture (15 mL) consisted of fumaric acid (**3**, 60 mM), a diamine substrate (**7a-i**, 10 mM) and purified EDDS lyase (0.05 mol% based on diamine) in 50 mM Na<sub>2</sub>HPO<sub>4</sub> buffer (pH 8.5). The reaction mixture was incubated at room temperature for 48 h (**7a-e** and **7g**) or 96 h (**7f** and **7h-i**). <sup>b</sup>Absolute stereochemistry of products not determined. <sup>c</sup>Conversion yields based on comparing <sup>1</sup>H-NMR signals of substrates and corresponding products. <sup>d</sup>Isolated yield after ion-exchange chromatography.

## 2. Results and discussion

Synthetic experiments revealed that diamine substrates with two to four atoms between the two amino groups (**7a–g**) were well accepted as substrates by EDDS lyase, giving good conversions (47–83%) and yielding the corresponding aminocarboxylic acid products (**8a–g**) in 21–60% isolated yield (table 2, entries 1–7). Hence, EDDS lyase has a broad diamine scope, allowing the two-step sequential addition of appropriate diamines to fumaric acid, providing a powerful synthetic tool for the preparation of valuable aminocarboxylic acids. However, the elongated diamines with five atoms between the two amino groups (**7h–i**) were not accepted as substrates by EDDS lyase (table 2, entries 8 and 9).

The ability of the AMA and EDDS analogs to inhibit NDM-1 was evaluated using a fluorescence-based assay previously described by Schofield and coworkers.<sup>17</sup> This assay makes use of a cephalosporin substrate (known as FC5) which upon hydrolysis releases 7-hydroxycoumarin. The well characterized NDM-1 inhibitors AMA, EDTA, and dipicolinic acid (DPA) were used as positive controls. In general, most of the AMA and EDDS analogs tested showed potent activity against NDM-1 with IC<sub>50</sub> values ranging from 1.3  $\mu$ M to 18.3  $\mu$ M (table 3).

Compared with its analogs **8a–g**, EDDS (**5**) proved to possess the highest activity (IC<sub>50</sub> = 2.21  $\mu$ M). Modifications to the central aliphatic spacer in length or steric bulk (or both) were generally tolerated. However, elongation of the linker to four methylene units (**8g**) led to a complete loss of activity. The inhibitory activity of the naturally occurring AMB (**1b**) was also promising (IC<sub>50</sub> = 2.63  $\mu$ M). Insertion of a methylene group (as in compounds **1c** and **1d**) maintained the activity leading to equipotent new AMB analogs.

Toxin A (**1e**) is believed to be the biosynthetic precursor of the related fungal aminocarboxylic acids AMA and AMB.<sup>18</sup> We found low IC<sub>50</sub> values for toxin A (**1e**) and its diastereomer **1f** (IC<sub>50</sub> = 2.33  $\mu$ M and 2.89  $\mu$ M respectively). Replacing the diaminopropionic acid moiety with the much simpler glycine unit as in **1j** led to a slight reduction of potency. Notably, elongation of the aliphatic spacers in both **1e** and **1j**, to generate compounds **1g–i** and **1k**, resulted in further or complete loss of NDM-1 inhibitory activity.

The majority of MBL inhibitors reported to date owe their activity to an ability to bind zinc. In general, MBL inhibitors either coordinate with zinc ions within the MBL active site or, if they are strong enough chelators, actively strip zinc from the MBL active site rendering the

**Table 3.** Activity of AMA and EDDS analogs against NDM-1 and an *E. coli* strain producing the same enzyme

Compound	IC <sub>50</sub> (μM) <sup>a</sup>	RC (μM) <sup>b,c</sup>	FICI <sup>e,d</sup>
<b>1a</b> (AMA)	0.94 ± 0.11	50	0.063
<b>1b</b> (AMB)	2.63 ± 0.10	50	0.063
<b>1c</b>	1.35 ± 0.12	200	0.156
<b>1d</b>	1.37 ± 0.04	100	0.094
<b>1e</b>	2.33 ± 0.18	>400	>0.281
<b>1f</b>	2.89 ± 0.24	>400	>0.281
<b>1g</b>	18.34 ± 3.67	>400	>0.281
<b>1h</b>	>400	>400	>0.281
<b>1i</b>	>400	>400	>0.281
<b>1j</b>	7.87 ± 0.29	>400	>0.281
<b>1k</b>	>400	>400	>0.281
<b>5</b> (EDDS.3Na)	2.21 ± 0.39	25	0.047
<b>8a</b>	4.33 ± 0.11	100	0.094
<b>8b</b>	9.65 ± 0.16	400	0.281
<b>8c</b>	3.11 ± 0.19	>400	>0.281
<b>8d</b>	2.85 ± 0.10	>400	>0.281
<b>8e</b>	3.50 ± 0.16	>400	>0.281
<b>8f</b>	2.85 ± 0.04	200	0.156
<b>8g</b>	>400	>400	>0.281
<b>EDTA.2Na</b>	1.25 ± 0.06	25	0.047
<b>DPA</b>	4.94 ± 0.22	100	0.094

<sup>a</sup>The half-maximal inhibitory concentration of the compounds tested against NDM-1 using FC5 as substrate. <sup>b</sup>RC (rescue concentration): the lowest concentration of the inhibitor that resensitizes the bacteria to meropenem. <sup>c</sup>The test microorganism was *E. coli* RC0089, an NDM-1 positive patient isolate with an MIC for meropenem of 32 mg/mL. <sup>d</sup>FICI: fractional inhibitory concentration index. FICI < 0.5 indicates synergy (see main text for formula used to calculate FICI).

enzyme inactive.<sup>19,20</sup> We have previously shown that the zinc-binding capacity of MBL inhibitors can be conveniently quantified using isothermal titration calorimetry (ITC).<sup>21</sup> To this end, we next measured the zinc-binding affinity of the aminocarboxylic acid analogs listed in table 3. These studies were conducted by titrating a zinc sulfate solution into the test compound with the heat of binding monitored using a microcalorimeter. The relevant thermodynamic parameters thus obtained ( $K_d$  and  $\Delta H$ ) are presented in table 4. For compounds **1e–f**, **1j**, and **8c** strong zinc binding was established with  $K_d$  values in the nM range. Notably, in the case of compounds **1b–d**, **5**, **8a**, **8b**, **8d**, **8e**, and **8f**, the zinc binding interactions were found to be so strong ( $K_d < 100$  nM) that only  $\Delta H$  values could be accurately determined. By comparison, for **1h**, **1i**, **1k**, and **8g** the zinc binding was too weak to allow for a reliable determination of any thermodynamic parameters. The data thus obtained reveals a clear correlation between zinc-binding affinity and

**Table 4.** The thermodynamic parameters of  $Zn^{2+}$  binding to the aminocarboxylic acid derivatives

Compound	$K_d$ ( $\mu M$ )	$\Delta H$ (kcal/mol)
<b>1b</b>	ND <sup>a</sup>	$-8.51 \pm 0.06$
<b>1c</b>	ND <sup>a</sup>	$-6.36 \pm 0.05$
<b>1d</b>	ND <sup>a</sup>	$-11.2 \pm 0.06$
<b>1e</b>	$0.181 \pm 0.013$	$-6.81 \pm 0.03$
<b>1f</b>	$0.240 \pm 0.017$	$-6.18 \pm 0.03$
<b>1g</b>	$2.810 \pm 0.088$	$-7.12 \pm 0.04$
<b>1h</b>	ND <sup>b</sup>	ND <sup>b</sup>
<b>1i</b>	ND <sup>b</sup>	ND <sup>b</sup>
<b>1j</b>	$0.828 \pm 0.035$	$-5.28 \pm 0.03$
<b>1k</b>	ND <sup>b</sup>	ND <sup>b</sup>
<b>5</b>	ND <sup>a</sup>	$-8.04 \pm 0.06$
<b>8a</b>	ND <sup>a</sup>	$-11.7 \pm 0.04$
<b>8b</b>	ND <sup>a</sup>	$-5.78 \pm 0.05$
<b>8c</b>	$0.334 \pm 0.031$	$-6.49 \pm 0.05$
<b>8d</b>	ND <sup>a</sup>	$-7.51 \pm 0.04$
<b>8e</b>	ND <sup>a</sup>	$-7.43 \pm 0.04$
<b>8f</b>	ND <sup>a</sup>	$-11.7 \pm 0.04$
<b>8g</b>	ND <sup>b</sup>	ND <sup>b</sup>

<sup>a</sup>Under the experimental conditions used,  $K_d$  values below 100 nM cannot be accurately determined. Only  $\Delta H$  could be reliably measured.

<sup>b</sup>ND: not determinable. No binding was observed or  $K_d$  was too high to allow an accurate determination of the thermodynamic parameters.

the IC<sub>50</sub> values measured against NDM-1. These findings indicate that the major mechanism of NDM-1 inhibition for the aminocarboxylic acids here studied can be attributed to their ability to bind zinc.

The compounds were also tested for their ability to resensitize an NDM-1 producing *E. coli* isolate to meropenem, a clinically important carbapenem antibiotic. This NDM-1 expressing strain of *E. coli* was found to be highly resistant to carbapenem antibiotics with a minimum inhibitory concentration (MIC) of 32 µg/mL for meropenem. As a measure of potency, we determined the “rescue concentration” of each test compound (table 3) which provides an indication of synergy.<sup>9</sup> Rescue concentration is defined as the lowest concentration of an MBL inhibitor that can resensitize a resistant strain to the antibiotic of interest when applied at its clinical breakpoint concentration (1 µg/mL for meropenem). In addition, the fractional inhibitory concentration index (FICI) values were determined for each compound and are provided in table 3. FICI values were established by applying the following formula where an FICI < 0.5 indicates synergy:

$$\text{FICI} = \frac{\text{MIC}_{\text{Meropenem in combination}}}{\text{MIC}_{\text{Meropenem alone}}} + \frac{\text{MIC}_{\text{Inhibitor in combination}}}{\text{MIC}_{\text{Inhibitor alone}}}$$

Among the EDDS analogs examined, **5** followed by **8a** were among the most potent synergizers. AMB (**1b**) and its related analogs **1c** and **1d** also showed potent to moderate activity. Interestingly, neither toxin A or its analogs (**1e–k**) demonstrated potent synergistic activity suggesting they may not be able to effectively access the enzyme target in the microorganism.

### 3. Conclusion

We here describe the application of a robust chemoenzymatic synthesis route in the preparation of a series of novel aminocarboxylic acids. A number of these compounds were found to be potent inhibitors of NDM-1, with inhibitory activities well correlated to their zinc binding ability. In addition, a number of the most active compounds demonstrated promising synergistic activity against an NDM-1 producing *E. coli* isolate when combined with meropenem. In the search for new agents to combat antibiotic resistance, chemoenzymatic methodologies such as those here described have the potential to provide access to novel inhibitors of metallo-β-lactamases of clinical relevance.

## **Acknowledgements**

We would like to thank professor Gerry Wright for generously providing an authentic sample of aspergillomarasmine A, and Professor Gerrit Poelarends' team for preparing the aminocarboxylic acid molecules. The enzyme experiments were made possible thanks to the contributions of Vida Mashayekhi to express and purify NDM-1, and Matthijs van Haren to synthesize the FC5 substrate.

## Experimental section

### Enzyme inhibition assays

NDM-1 plasmid was a generous gift from Prof. Christopher Schofield (Oxford University). The overexpression and purification of NDM-1 has been described in chapter 2, and FC5 substrate (figure 1) was prepared according to a previously reported procedure.<sup>17</sup> In order to determine half-maximal inhibitory concentration ( $IC_{50}$ ), the serially diluted aminocarboxylic derivatives were incubated with NDM-1 (50 pM) at 25 °C for 15 min. FC5 (0.5  $\mu$ M) was then added to the wells and fluorescence was monitored immediately over 30-40 cycles ( $\lambda_{ex}$  380 nm,  $\lambda_{em}$  460 nm) on a Tecan Spark plate reader. The initial velocity data were used for  $IC_{50}$  curve-fitting using GraphPad prism 7 software (figure 2). Aspergillomarasmine A, EDTA and dipicolinic acid were used as positive controls. The buffer was 50 mM HEPES pH 7.2 supplemented with 0.01% Triton X-100 and 1  $\mu$ M zinc sulfate. The assay microplate was  $\mu$ Clear®, black half-area 96-well plate (Greiner Bio-one).

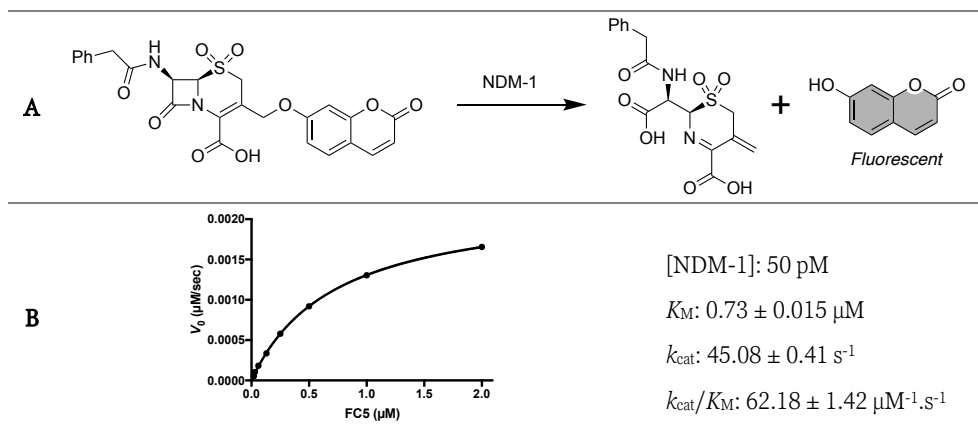


**Figure 1. A.** Hydrolysis mechanism of cephalosporin substrate known as FC5; **B.** Michaelis-Menten parameters of NDM-1 mediated hydrolysis of FC5.

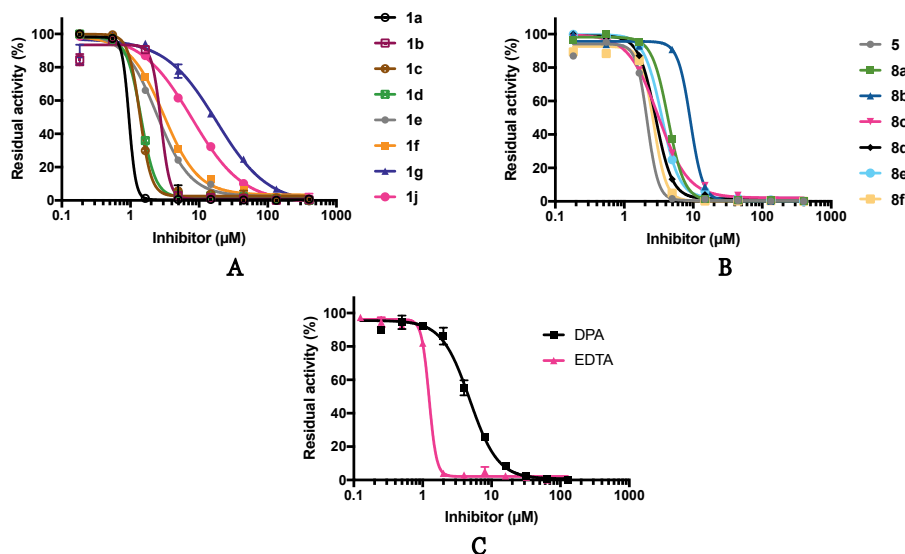


**Figure 2.** IC<sub>50</sub> curves of **1a-j** (A), EDDS analogs (B), and control compounds (C) tested against NDM-1 (50 pM) using FC5 (0.5  $\mu\text{M}$ ) as substrate.

### *Isothermal titration calorimetry*

The titrations were performed on an automated PEAQ-ITC calorimeter (Malvern). Test compounds were dissolved in 20 mM tris pH 7.0. Zinc sulfate (1 mM) was titrated in the 0.1 mM solutions of the aminocarboxylic acids over  $19 \times 2 \mu\text{L}$  aliquots (first aliquot was  $0.4 \mu\text{L}$ ). Reference power was set at  $10 \mu\text{cal}/\text{sec}$  and the assay temperature was  $25 \text{ }^\circ\text{C}$ . The blank titrations included the titration of buffer into the test compounds and zinc sulfate into buffer all of which showed negligible heat of dilution signals (see figure 3 for the thermograms). The signals were integrated and the thermodynamic parameters were calculated using the PEAQ-ITC analysis software.



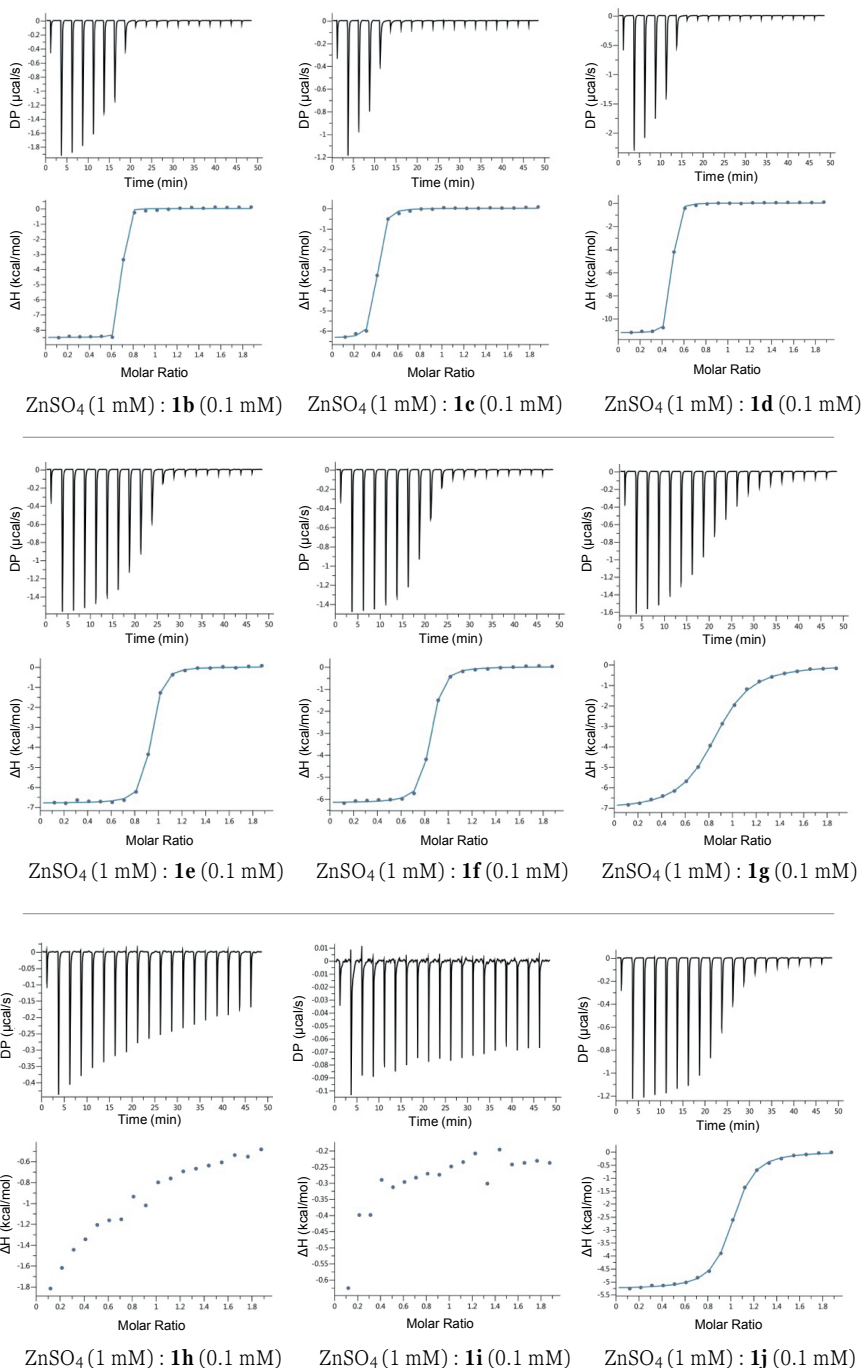


**Figure 3.** ITC thermograms of zinc sulfate titrated in the solutions of animocarboxylic acids.

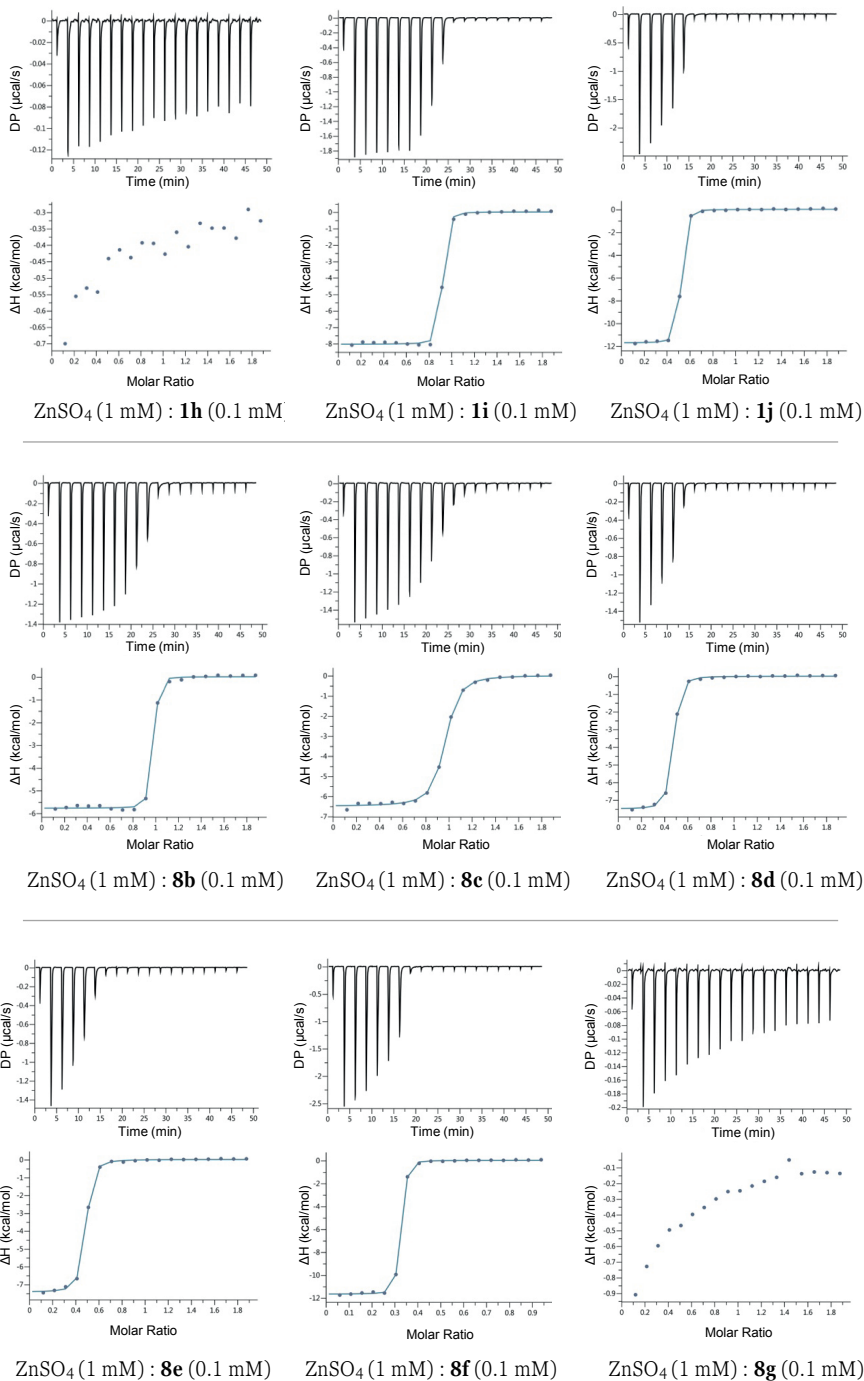


Figure 3. Continued

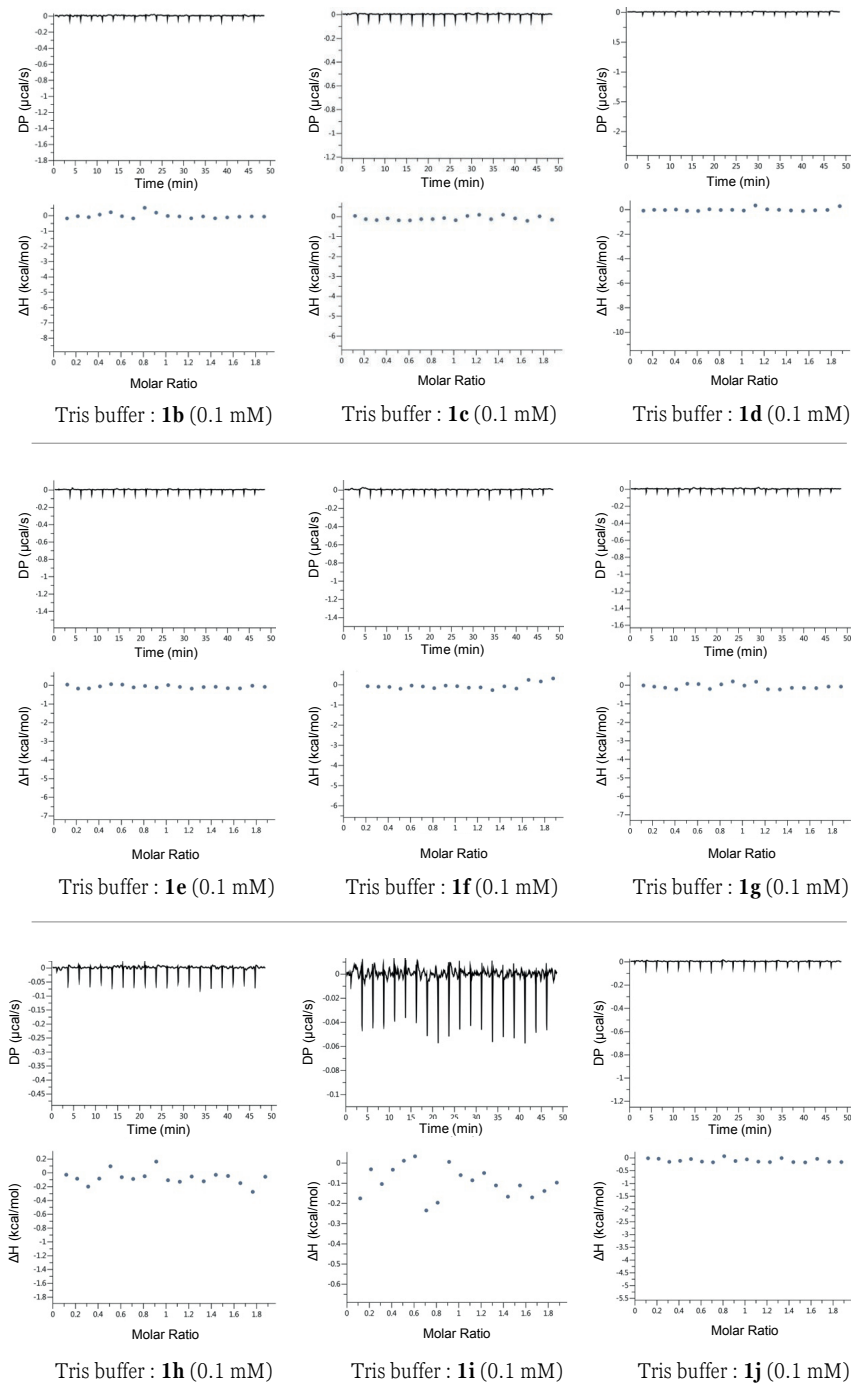


Figure 3. Continued

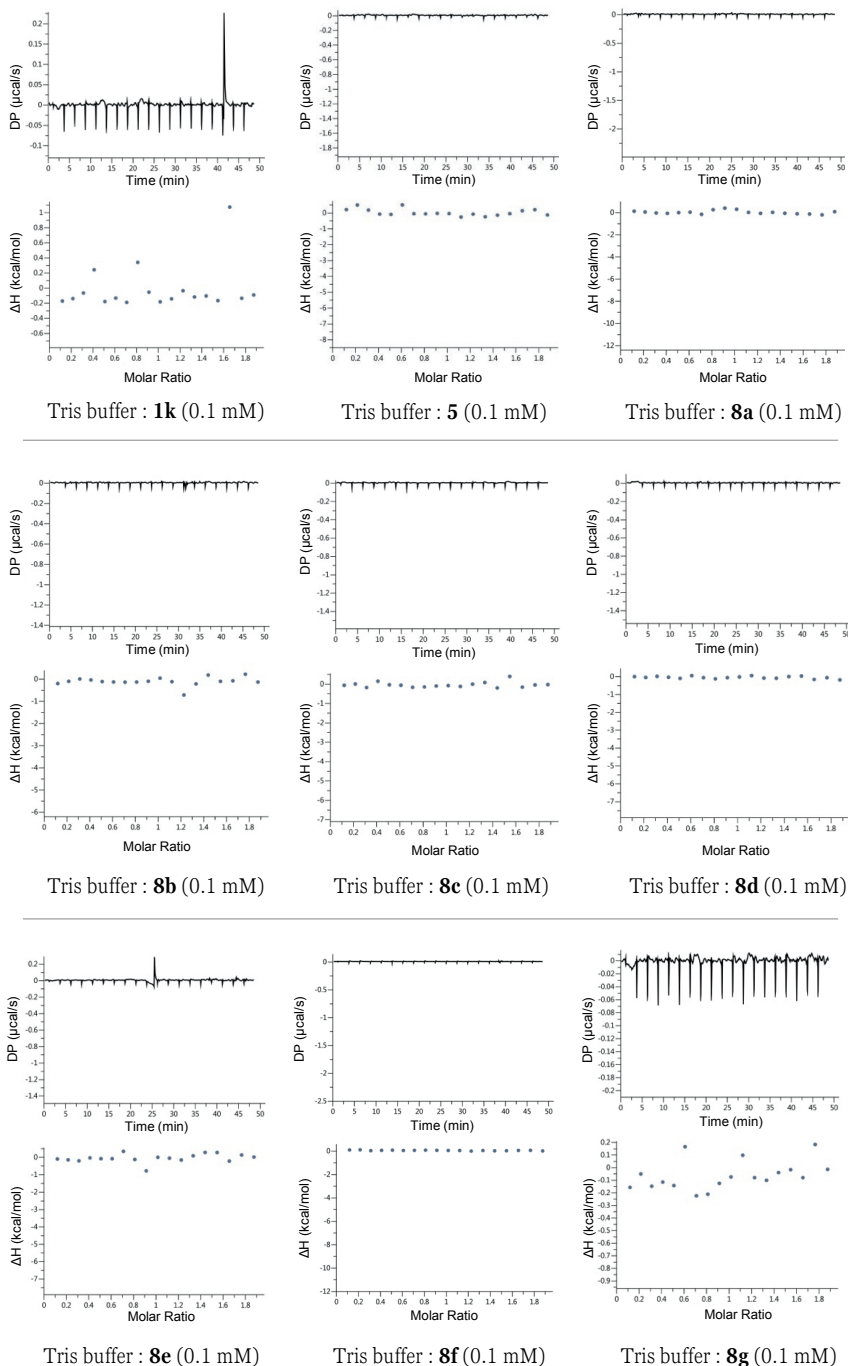


Figure 3. Continued

### ***Antibacterial activity***

*A. MIC assay.* The antibacterial assays were performed according to the guidelines published by the clinical and laboratory standards institute (CLSI). On a polypropylene 96-well plate, the aminocarboxylic acid derivatives as well as the control compounds were serially diluted in Mueller-Hinton broth (MHB). In the same day, a few colonies of *E. coli* RC0089 (NDM-1) were suspended in tryptic soy broth (TSB) and incubated with shaking at 37 °C. When the bacteria grew to the exponential phase ( $OD_{600} = 0.5$ ), the suspension was diluted in MHB to reach  $10^6$  CFU/mL and then added to the microplate containing the test compounds. After incubation at 37 °C for 15-20 h, the microplates were inspected for growth inhibition. MIC is defined as the lowest concentration of the compound that prevented the visible growth of the bacteria.

*B. Determination of rescue concentration (RC).* The test compounds were serially diluted starting from 400  $\mu$ M. Meropenem was then added to the wells with the final concentration of 1  $\mu$ g/mL. The bacteria were cultured and added to the microplates as described above. Rescue concentration was defined as the lowest concentration of the inhibitor that prevented the visible growth of the bacteria when combined with 1  $\mu$ g/mL of meropenem.

## References

- 1 M. Ferri, E. Ranucci, P. Romagnoli and V. Giaccone, *Crit. Rev. Food Sci. Nutr.*, 2017, **57**, 2857–2876.
- 2 B. Aslam, W. Wang, M. I. Arshad, M. Khurshid, S. Muzammil, M. H. Rasool, M. A. Nisar, R. F. Alvi, M. A. Aslam, M. U. Qamar, M. K. F. Salamat and Z. Baloch, *Infect. Drug Resist.*, 2018, **2018**, 1645–1658.
- 3 A. K. Thabit, J. L. Crandon and D. P. Nicolau, *Expert Opin. Pharmacother.*, 2015, **16**, 159–177.
- 4 S. M. Drawz and R. A. Bonomo, *Clin. Microbiol. Rev.*, 2010, **23**, 160–201.
- 5 K. H. M. E. Tehrani and N. I. Martin, *Medchemcomm*, 2018, **9**, 1439–1456.
- 6 A. M. King, S. A. Reid-Yu, W. Wang, D. T. King, G. De Pascale, N. C. Strynadka, T. R. Walsh, B. K. Coombes and G. D. Wright, *Nature*, 2014, **510**, 503–506.
- 7 D. Liao, S. Yang, J. Wang, J. Zhang, B. Hong, F. Wu and X. Lei, *Angew. Chemie - Int. Ed.*, 2016, **55**, 4291–4295.
- 8 K. Koteva, A. M. King, A. Capretta and G. D. Wright, *Angew. Chemie - Int. Ed.*, 2016, **55**, 2210–2212.
- 9 S. A. Albu, K. Koteva, A. M. King, S. Al-Karmi, G. D. Wright and A. Capretta, *Angew. Chemie - Int. Ed.*, 2016, **55**, 13259–13262.
- 10 J. Zhang, S. Wang, Y. Bai, Q. Guo, J. Zhou and X. Lei, *J. Org. Chem.*, 2017, **82**, 13643–13648.
- 11 J. Zhang, S. Wang, Q. Wei, Q. Guo, Y. Bai, S. Yang, F. Song, L. Zhang and X. Lei, *Bioorganic Med. Chem.*, 2017, **25**, 5133–5141.
- 12 H. Poddar, J. de Villiers, J. Zhang, V. Puthan Veetil, H. Raj, A.-M. W. H. Thunnissen and G. J. Poelarends, *Biochemistry*, 2018, **57**, 3752–3763.
- 13 H. Fu, J. Zhang, M. Saifuddin, G. Cruiming, P. G. Tepper and G. J. Poelarends, *Nat. Catal.*, 2018, **1**, 186–191.
- 14 H. Fu, A. Prats Luján, L. Bothof, J. Zhang, P. G. Tepper and G. J. Poelarends, *ACS Catal.*, 2019, **9**, 7292–7299.
- 15 J. Zhang, H. Fu, P. G. Tepper and G. J. Poelarends, *Adv. Synth. Catal.*, 2019, **361**, 2433–2437.
- 16 A. Proschak, J. Kramer, E. Proschak and T. A. Wichelhaus, *J. Antimicrob. Chemother.*, 2017, **73**, 425–430.
- 17 S. S. van Berkel, J. Brem, A. M. Rydzik, R. Salimraj, R. Cain, A. Verma, R. J. Owens, C.

- W. G. Fishwick, J. Spencer and C. J. Schofield, *J. Med. Chem.*, 2013, **56**, 6945–6953.
- 18 P. Friis, C. E. Olsen and B. L. Møller, *J. Biol. Chem.*, 1991, **266**, 13329–13335.
- 19 L. C. Ju, Z. Cheng, W. Fast, R. A. Bonomo and M. W. Crowder, *Trends Pharmacol. Sci.*, 2018, **39**, 635–647.
- 20 C. M. Rotondo and G. D. Wright, *Curr. Opin. Microbiol.*, 2017, **39**, 96–105.
- 21 K. H. M. E. Tehrani and N. I. Martin, *ACS Infect. Dis.*, 2017, **3**, 711–717.

## Chapter 4

# Thiol-containing metallo- $\beta$ -lactamase inhibitors: synergy, zinc-binding affinity and stability evaluation.

Parts of this chapter have been published in:

Tehrani, K. H. M. E., and Martin, N. I. (2017) Thiol-Containing Metallo- $\beta$ -Lactamase Inhibitors Resensitize Resistant Gram-Negative Bacteria to Meropenem. *ACS Infect. Dis.* **3**, 711–717.



## 1. Introduction

Resistance to  $\beta$ -lactam antibiotics poses a serious threat to human health. The enzymes responsible for such resistance are the  $\beta$ -lactamases and are especially prevalent among gram-negative bacteria.<sup>1,2</sup> These enzymes are divided in two classes: the serine  $\beta$ -lactamases (SBLs) which hydrolyze  $\beta$ -lactam ring by a serine nucleophile in their active site; and the metallo- $\beta$ -lactamases (MBLs) whose mechanism relies upon the presence of one or two active site zinc ions.<sup>3</sup> These zinc ions stabilize a nucleophilic hydroxide species that is believed to be the active agent in the hydrolysis the  $\beta$ -lactam ring leading to antibiotic inactivation. The best-studied MBLs include the NDM (New Delhi metallo- $\beta$ -lactamase), VIM (Verona integron-encoded metallo- $\beta$ -lactamase) and IMP (imipenemase) enzymes which collectively exhibit a broad substrate specificity and hydrolyze antibiotics from all known  $\beta$ -lactam classes with the exception of monobactams.<sup>4</sup>

The global concern relating to antibiotic resistance has led to a number of different strategies aimed at addressing the problem. One such approach involves the co-administration of antibiotic adjuvants capable of maintaining the activity of existing antibiotics.<sup>5</sup> This strategy is widely effective in treating infections due to bacteria that express SBLs. Clinically relevant SBL inhibitors include clavulanic acid, sulbactam, tazobactam, avibactam, and vaborbactam which effectively protect  $\beta$ -lactam antibiotics from inactivation when administered as combination therapies. By comparison, there are no clinically used MBL inhibitors available for use in addressing the growing threat posed to the  $\beta$ -lactam arsenal by these enzymes.

Attempts to identify inhibitors of the MBLs have revealed a number of compound classes that display promising activities when tested using *in vitro* enzyme inhibition assays.<sup>6</sup> Such compounds include small molecules that contain functionalities often associated with zinc binding such as thiols, dicarboxylates, hydroxamates, aryl sulfonamides, *N*-arylsulfonyl hydrazones and tetrazole-based compounds.<sup>3,7,8</sup> Among the known MBL inhibitors, sulfur-containing small molecules containing either a free thiol or a sulfur atom masked as a heterocycle<sup>9,10</sup> are among the best characterized.<sup>3,7,11–15</sup> Structures as simple as mercaptoacetic acid and mercaptopropionic acid have been shown to be effective inhibitors of the IMP-1 enzyme ( $K_i = 0.23 \mu\text{M}$  and  $0.19 \mu\text{M}$  respectively).<sup>16</sup> Follow-up studies identified higher analogs of mercapto-carboxylic acids including 2-arylmethyl-2-mercaptoacetic acids and their thioesters as potent MBL inhibitors with  $\text{IC}_{50}$  values in the low-nanomolar range.<sup>17</sup> Similarly, thiomandelic acid was found to be a broad-spectrum inhibitor of different MBLs including BCII ( $K_i = 0.34 \mu\text{M}$ ),

IMP-1 ( $K_i = 0.029 \mu\text{M}$ ), IMP-2 ( $K_i = 0.059 \mu\text{M}$ ) and VIM-1 ( $K_i = 0.230 \mu\text{M}$ )<sup>18</sup>, and 2- $\omega$ -phenylpropyl-3-mercaptopropionic acid has been reported as potent inhibitor of VIM-2 ( $K_i = 0.220 \mu\text{M}$ ).<sup>19,20</sup> Other examples of structurally similar MBL inhibitors include compounds containing a free thiol with a neighboring carbonyl functionality such as  $\alpha$ -mercaptoacetophenone,<sup>21</sup> thiosalicylic acid,<sup>18</sup> and interestingly, the dipeptide drug captopril which is used in the treatment of hypertension.<sup>22</sup> The inhibitory activity of these molecules is attributed to the ability of the thiol group to bind the zinc ion present in the MBL active site as supported by several X-ray crystallography studies.<sup>21,23–26</sup>

The inhibitory activity of thiol-containing small molecules against clinically relevant MBLs *in vitro* prompted us to conduct a series of antibacterial assays to evaluate the synergistic activity of such compounds with the representative  $\beta$ -lactams meropenem and cefoperazone. To do so, the sensitizing effects of thiols **1–5** (figure 1) on the activity of meropenem and cefoperazone were assessed against a panel of gram-negative bacteria expressing various  $\beta$ -lactamases. The stability of the thiols was also assessed under the assay condition employed and isothermal titration calorimetry (ITC) was used to measure the zinc-binding affinity of the most synergistically-active compounds.

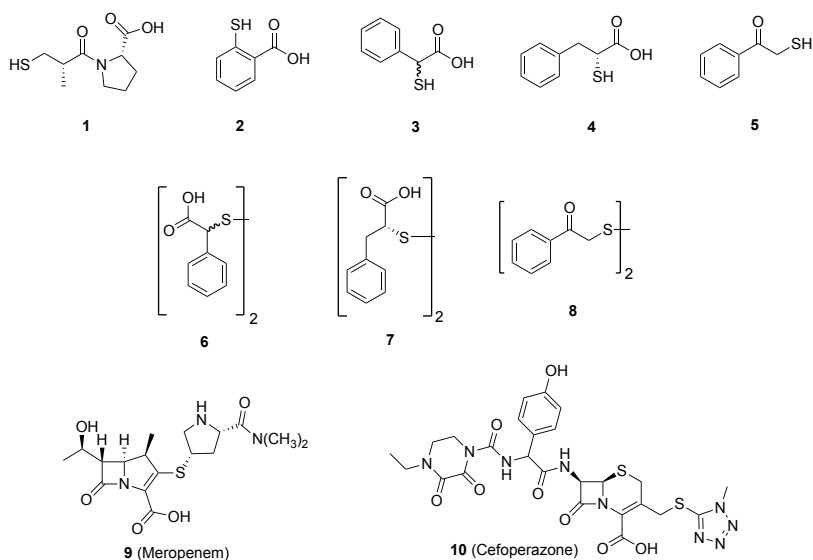


**Figure 1.** Thiol-based MBL inhibitors and disulfides evaluated for synergy with meropenem and cefoperazone in the current study.

## 2. Results and discussion

Thiols **1-5** were initially tested alone for antibacterial activity against a panel of carbapenem-resistant gram-negative pathogens expressing MBLs including NDM, VIM and IMP enzymes or SBLs such as KPC-2 and OXA-48. These studies revealed that none of the thiols inhibited bacterial growth at the highest concentration tested (64  $\mu\text{g}/\text{mL}$ ). All of the MBL-expressing strains used in our study exhibited resistance to both meropenem and cefoperazone with MIC values ranging from 8 to  $>256$   $\mu\text{g}/\text{mL}$ . For use as a reference MBL inhibitor known to synergize with  $\beta$ -lactam antibiotics, we turned to the work of Migliavacca and coworkers who reported a zinc chelating mixture of EDTA and 1,10-phenanthroline as being synergistic with imipenem in preventing growth of MBL-expressing strains of *Pseudomonas aeruginosa*.<sup>27</sup> We found that the EDTA/1,10-phenanthroline mixture was similarly effective in lowering the MIC of meropenem and cefoperazone against the MBL-expressing strains used in our study (table 1). Also, and as expected, the EDTA/1,10-phenanthroline mixture showed no synergistic effect with meropenem against the two SBL-expressing strains also evaluated.

With a reliable reference system in hand, the capacity for thiols **1-5** to synergize with meropenem was next investigated. Table 1 shows the synergy data of thiols **1-5**. Captopril **1** exhibited moderate to weak synergy at a concentration of 64  $\mu\text{g}/\text{mL}$  while thiosalicylic acid **2** displayed no appreciable synergy when tested at the same concentration. By comparison, when administered at 64  $\mu\text{g}/\text{mL}$  thiols **3** and **4** significantly lowered the MIC of meropenem against all the MBL-producing isolates tested. The activity of compound **5** was also promising but interestingly limited to only the two *Klebsiella* strains tested. Thiols **3-5** have previously been shown to be more potent MBL inhibitors than compounds **1** and **2** in biochemical enzyme inhibition assays<sup>17,18,21,23</sup> and our MIC synergy results follow the same trend. Notably, for compounds **3** and **4** we observed broad-spectrum, and in some cases, potent synergistic activity with meropenem against the MBL-producing isolates evaluated.

**Table 1.** MIC of meropenem (Mer) and Cefazone (Cef) tested alone or in combination with thiol MBI-inhibitors **1-5**

Isolates	Mer	Cef	Mer + 1 <sup>a</sup>	Mer + 2	Mer + 3	Cef + 3	Mer + 4	Cef + 4	Mer + 5	EPM <sup>b</sup>	EPCh
<i>K. pneumoniae</i> (KPC-2)	>128	>256	>128	>128	128	>256	>128	>256	128	>128 <sup>e</sup>	>256 <sup>e</sup>
<i>K. pneumoniae</i> (OXA-48)	64	>256	64	64	64	>256	64	>256	64	16 <sup>d</sup>	>256 <sup>d</sup>
<i>K. pneumoniae</i> (VIM-1)	64/32	>256	8 (4) <sup>e</sup>	16 (2)	0.5 (≥128)	256	1 (32)	>256	8 (8)	≤0.5 <sup>e</sup>	8 <sup>e</sup>
<i>K. pneumoniae</i> (IMP-28)	16/8	256	1 (8)	8	0.125 (128)	≤2 (≥128)	0.125 (64)	≤2 (≥128)	0.5 (32)	≤0.125 <sup>f</sup>	≤2 <sup>f</sup>
<i>E. coli</i> (NDM-1)	128/64	>256	16 (4)	128	16 (8)	>256	16 (8)	>256	64 (2)	≤1 <sup>e</sup>	>256 <sup>e</sup>
<i>P. aeruginosa</i> (VIM-2)	32	128	32	32	4 (8)	16 (8)	16 (4)	16 (8)	32	0.5 <sup>e</sup>	8 <sup>e</sup>
<i>P. aeruginosa</i> (IMP-13, IMP-37)	64	256	64	64	8 (8)	8 (32)	8 (8)	16 (16)	64	4 <sup>f</sup>	4 <sup>f</sup>
<i>K. pneumoniae</i> (VIM-1)	64/32	>256	n.d.	n.d.	0.5 (64)	>256	1 (32)	>256	n.d.	≤0.5 <sup>f</sup>	≤2 <sup>f</sup>
<i>E. aerogenes</i> (VIM-1)	32/16	>256	n.d.	n.d.	0.5 (64)	>256	1 (16)	>256	n.d.	≤0.25 <sup>f</sup>	64 <sup>f</sup>
<i>K. pneumoniae</i> (VIM-1)	>128/128	>256	n.d.	n.d.	4 (>32)	>256	8 (16)	>256	n.d.	≤1 <sup>f</sup>	≤2 <sup>f</sup>
<i>K. pneumoniae</i> (NDM-1)	32/16	>256	n.d.	n.d.	8 (4)	>256	2 (16)	>256	n.d.	≤0.5 <sup>f</sup>	>256 <sup>f</sup>
<i>K. pneumoniae</i> (NDM-1)	16/8	>256	n.d.	n.d.	4 (4)	>256	1 (8)	>256	n.d.	≤0.25 <sup>f</sup>	>256 <sup>f</sup>
<i>K. pneumoniae</i> (NDM-1)	64/32	>256	n.d.	n.d.	16 (4)	>256	16 (4)	>256	n.d.	≤1 <sup>f</sup>	>256 <sup>f</sup>

<sup>a</sup>Thiols **1-5** added at 64 µg/mL<sup>b</sup>EPM: EDTA/phenanthroline/meropenem; EPC: EDTA/phenanthroline/cefoperazone<sup>c</sup>EP mixture used at 16 and 1 µg/mL respectively<sup>d</sup>EP mixture used at 64 and 4 µg/mL respectively<sup>e</sup>Fold reduction of MIC shown in parentheses<sup>f</sup>EP mixture used at 32 µg/mL and 2 µg/mL respectively

Building on the encouraging results of the preliminary synergy assays (carried out at fixed thiol concentration of 64  $\mu\text{g}/\text{mL}$ ) we next performed a series of checkerboard synergy assays in which the MIC of meropenem was determined at varying concentrations of inhibitors **1-5**. Such an approach provides for a better picture of the synergistic relationship between the two combined agents and allows for determination of the fractional inhibitory concentration (FIC) index. Briefly, FIC values are calculated by adding the following two fractional values: (MIC of compound A in combination/MIC of compound A alone) + (MIC of compound B in combination/MIC of compound B alone). In general, an FIC index value  $<0.5$  is regarded as an indication of synergy.<sup>28</sup> Among the MBL-expressing strains used, the two *Klebsiella* isolates were most effectively resensitized to meropenem when administered in combination with thiols **3-5**. Of particular note, compounds **3** and **4** were both found to significantly potentiate meropenem against the IMP-28 producing *Klebsiella* strain tested with FIC values  $\leq 0.07$  and  $\leq 0.13$  respectively.

Thiols are well known for their tendency to form homo- or heterodisulfides in biological systems. Such reactivity is of special importance in the case of thiol-based MBL inhibitors such as compounds **1-5** as it has been reported that in their disulfide form their activity is significantly reduced.<sup>18</sup> In this regard we selected compounds **3-5** as the three most active thiols from our synergy assays and monitored their conversion to the corresponding disulfides under the assay conditions used. Thiols **3-5** were thus incubated in Mueller-Hinton broth at 37 °C and sample aliquots analyzed at time points ranging from 0 to 8 hours. As shown in figure 2, thiols **3** and **4** were found to form their corresponding disulfides (**6** and **7** respectively) with half-lives of *ca.* 5 hours. By comparison, thiol **5** was oxidized to **8** more rapidly with a half-life in the range of minutes which may also explain its lower level of synergy relative to **3** and **4**. Disulfides **6-8** were synthesized for use as reference compounds in the stability assays and were evaluated for their synergy with meropenem against the two most susceptible *Klebsiella* isolates identified (table 2). The three disulfides exhibited very low levels of synergy relative to that of the corresponding free thiols. The slight synergy observed for these disulfides may in fact be attributable to a reductive process carried out by the bacteria themselves to release a small amount of the more active thiol. Many bacteria contain redox active enzymes capable of disulfide reduction both in cytoplasm and periplasmic space.<sup>29</sup>

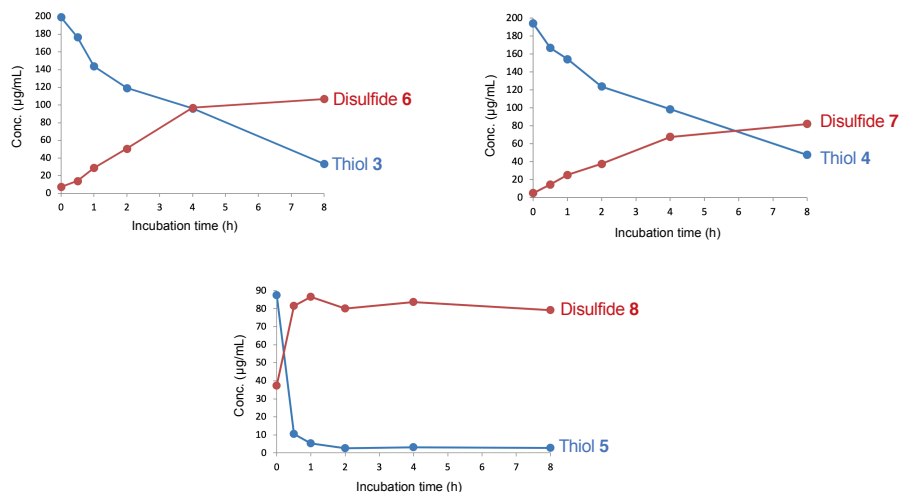


**Figure 2.** Time-dependent oxidation of thiols **3-5** to corresponding disulfides **6-8** by incubation in Mueller-Hinton broth at 37 °C.

The superior synergistic activity and relative stability of thiols **3** and **4** prompted us to further characterize their zinc binding abilities using isothermal titration calorimetry (ITC). To do so a solution of zinc chloride was titrated into the sample well containing either **3** or **4** (both found to be stable in the buffer conditions used for the ITC experiments) and the heat of binding monitored. In this way a number of thermodynamic binding parameters are revealed including  $K_d$  (dissociation constant),  $\Delta H$  (enthalpy),  $\Delta G$  (Gibbs free energy) and  $\Delta S$  (entropy). As shown in figure 3, compounds **3** and **4** exhibited high affinities for  $Zn^{2+}$  with  $K_d$  values of 9.8 and 20.0  $\mu M$  respectively. Also of note was the lack of any measurable binding interaction when zinc chloride was titrated into solutions of disulfides **6** and **7**. The zinc binding abilities of the reference compounds EDTA and 1,10-phenanthroline were also assessed using ITC showing strong

**Table 2.** MIC of meropenem (Mer) tested alone or in combination with disulfides **6-8**

Isolates	Mer	Mer + <b>6</b> <sup>a</sup>	Mer + <b>7</b>	Mer + <b>8</b>
<i>K. pneumoniae</i> (VIM-1)	64	64	64	32 (2) <sup>b</sup>
<i>K. pneumoniae</i> (IMP-28)	8	1 (8)	4 (2)	1 (8)

<sup>a</sup>Disulfides **6** and **7** were added at 64  $\mu g/mL$  and **8** added at 32  $\mu g/mL$ .

<sup>b</sup>Fold reduction of MIC has been shown in parentheses

interactions with  $K_d$  values of  $<100$  nM and  $2.3$   $\mu$ M respectively (see experimental section for thermograms). The results of these ITC studies correlate well with the synergy data obtained and suggest that zinc binding may be a useful predictor for a compound's ability to resensitize MBL-expressing organisms to  $\beta$ -lactam antibiotics. Furthermore, the relative ease with which ITC can be used to assess zinc binding by small molecules may make it a complimentary technique for identifying new lead compounds capable of effectively inhibiting MBLs.

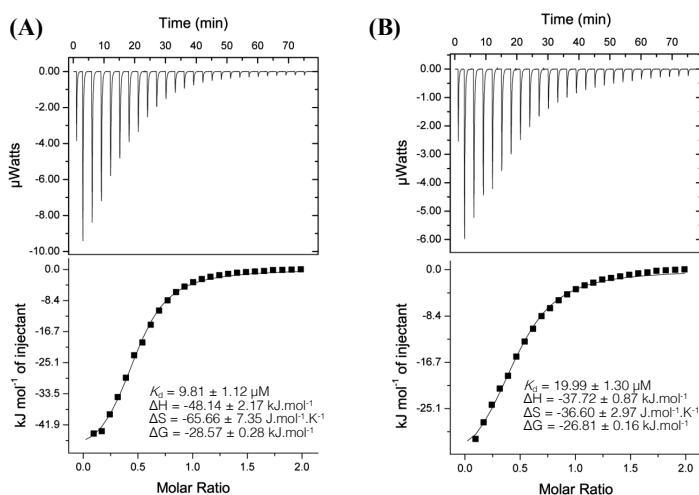


**Figure 3.** ITC Thermograms for binding of  $\text{Zn}^{2+}$  by thiols **3** (A) and **4** (B). A solution of zinc chloride ( $2.0$  mM) was titrated into the sample cell containing thiol **3** or **4** ( $0.2$  mM). Thermodynamic parameters shown based on triplicate binding assays and the reported as mean  $\pm$  SE.

### **3. Conclusion**

While small molecule thio-carbonyl compounds have previously been shown to inhibit various MBLs, their ability to synergize with  $\beta$ -lactam antibiotics in overcoming MBL-associated resistance has not been extensively studied. We here demonstrate a significant level of synergism between meropenem and a series of thiols, most notably thiomandelic acid **3** and 2-merpto-3-phenylpropionic acid **4**. Combinations of meropenem with **3** or **4** exhibit antibacterial activity against a number of gram-negative bacteria expressing different MBLs including IMP, NDM and VIM. Given the high degree of active site heterogeneity among the different types of MBL enzymes,<sup>11</sup> designing an inhibitor with potent inhibitory activity towards several types of MBL is challenging. In this light, thiomandelic acid **3** is unique given its ability to inhibit a range of MBLs and, as shown in the present study, its capacity to resensitize MBL-expressing gram-negative isolates to meropenem, an important  $\beta$ -lactam antibiotic of last resort. In addition, ITC studies showed thiols **3** and **4** to be effective zinc chelators with low-micromolar  $K_d$  values supporting the proposed mechanism of action for these compounds. In this regard, ITC may provide a useful means of (pre)screening for zinc-binding MBL inhibitors. While compounds **3** and **4** exhibit potent synergy with meropenem, their propensity to oxidize and likely ability to interact with free zinc and other metallo-proteins precludes their use as clinical MBL inhibitors. In this regard, MBL inhibitors employing free thiols as zinc binding groups are more likely to be of value as tool compounds for biochemical studies involving MBLs. Optimized analogs or other classes of MBL inhibitors capable of overcoming such pharmacokinetic hurdles present a key objective in the continued fight against antibiotic resistance.



## 4. Experimental Section

### General

Potassium thioacetate was purchased from Combi-Blocks Inc. (San Diego, CA USA). Thiosalicylic acid was purchased from Fisher Scientific (Waltham, MA USA). Other reagents including captopril, 2-bromoacetophenone, *S*-mandelic acid, *L*-phenylalanine, were purchased from Sigma-Aldrich company. The reaction progress was monitored by thin-layer chromatography (normal SiO<sub>2</sub>, Merck 60 F254) and ethyl acetate/petroleum ether combination was used as developing phase. The plates were visualized using UV indicator and/or stained by ceric ammonium molybdate reagent. The NMR spectra were obtained on an Agilent 400 MHz spectrometer. DMSO(*d*<sub>6</sub>) or CDCl<sub>3</sub> were used to dissolve the samples and tetramethylsilane was used as internal standard. High-resolution mass spectrometry was performed using an ESI instrument. As the only exception, the molecular ion of thiol **5** could not be detected by the ESI technique.

### Synthesis

Among the thiols selected for investigation, captopril **1** and thiosalicylic acid **2** were commercially available while compounds **3-5** required preparation via previously reported synthetic routes.<sup>21,30-32</sup> Briefly, compound **3** was synthesized via esterification of *S*-mandelic acid which was followed by mesylation of the hydroxyl group. Substitution of the tosylate ester with thioacetate anion followed by acidic hydrolysis furnished **3**.<sup>30</sup> For the synthesis of compound **4**, *L*-phenylalanine was converted to its corresponding  $\alpha$ -bromocarboxylic acid through a sodium nitrite mediated halo-deamination reaction, which was subsequently reacted with potassium thioacetate to afford *S*-acetyl derivative of **4**. Basic hydrolysis of the latter intermediate led to the final product **4**.<sup>31,32</sup> Thioacetophenone **5** was prepared via a two-step procedure involving thiolation of  $\alpha$ -bromoacetophenone with potassium thioacetate followed by a basic hydrolysis.<sup>21</sup> In addition, disulfides **6-8**<sup>33-35</sup> were readily prepared by reacting the corresponding thiol with iodine in water/acetonitrile.<sup>36</sup>

**Spectral characterization of compounds 3-8.**

- 3**  $^1\text{H-NMR}$  (400 MHz,  $\text{CDCl}_3$ ):  $\delta$  7.47–7.42 (m, phenyl H, 2H), 7.38–7.29 (m, phenyl H, 3H), 4.69 (d,  $J = 7.6$  Hz, -CH-, 1H), 2.60 (d,  $J = 7.6$  Hz, -SH, 1H).  
 $^{13}\text{C-NMR}$  (100 MHz,  $\text{CDCl}_3$ ):  $\delta$  177.62, 137.13, 128.86, 128.49, 127.86, 45.45.  
HRMS (ESI): [M-H]<sup>-</sup> calculated: 167.0178, found: 167.0172.
- 4**  $^1\text{H-NMR}$  (400 MHz,  $\text{CDCl}_3$ ):  $\delta$  7.39–7.11 (m, phenyl H, 5H), 3.62 (m, aliphatic H, 1H), 3.25 (dd,  $J = 14.0$  Hz,  $J = 8.2$  Hz, aliphatic H, 1H), 3.01 (dd,  $J = 14.0$  Hz,  $J = 7.0$  Hz, aliphatic H, 1H), 2.15 (d,  $J = 8.9$  Hz, -SH, 1H).  
 $^{13}\text{C-NMR}$  (100 MHz,  $\text{CDCl}_3$ ):  $\delta$  179.03, 137.26, 129.06, 128.64, 127.15, 42.22, 41.11.  
HRMS (ESI): [M-H]<sup>-</sup> calculated: 181.0329, found: 181.0318.
- 5**  $^1\text{H-NMR}$  (400 MHz,  $\text{CDCl}_3$ ):  $\delta$  7.95 (m, phenyl H, 2H), 7.58 (m, phenyl H, 1H), 7.47 (t,  $J = 8.0$  Hz, phenyl H, 2H), 3.95 (d,  $J = 7.3$  Hz, -CH<sub>2</sub>-, 2H), 2.12 (t,  $J = 7.3$  Hz, -SH, 1H).  
 $^{13}\text{C-NMR}$  (100 MHz,  $\text{CDCl}_3$ ):  $\delta$  194.71, 135.01, 133.59, 128.79, 128.47, 31.11.
- 6**  $^1\text{H-NMR}$  (400 MHz, Acetone-*d*<sub>6</sub>): Isomeric mixture (7:1)  $\delta$  7.46–7.35 (m, phenyl H, 10H), 4.79 and 4.71 (each s, -CH, isomeric ratio 1:7 respectively).  
 $^{13}\text{C-NMR}$  (100 MHz, DMSO-*d*<sub>6</sub>):  $\delta$  171.40, 171.34, 136.10, 136.05, 129.12, 129.10, 129.01, 128.84, 128.79, 57.77, 57.59.  
HRMS (ESI): [M-H]<sup>-</sup> calculated: 333.0261, found: 333.0259.
- 7**  $^1\text{H-NMR}$  (400 MHz,  $\text{CDCl}_3$ ):  $\delta$  7.29–7.14 (m, 10H, phenyl H), 3.65 (t,  $J = 7.7$  Hz, aliphatic H, 2H), 3.22 (dd,  $J = 14.3$  Hz,  $J = 8.2$  Hz, aliphatic H, 2H), 3.01 (dd,  $J = 14.3$  Hz,  $J = 7.2$  Hz, aliphatic H, 2H).  
 $^{13}\text{C-NMR}$  (100 MHz,  $\text{CDCl}_3$ ):  $\delta$  177.57, 136.70, 129.03, 128.62, 127.07, 53.03, 36.75.  
HRMS (ESI): [M-H]<sup>-</sup> calculated: 361.0574, found: 361.0569.
- 8**  $^1\text{H-NMR}$  (400 MHz,  $\text{CDCl}_3$ ):  $\delta$  7.92 (m, phenyl H, 4H), 7.56 (m, phenyl H, 2H), 7.45 (m, phenyl H, 4H), 4.18 (s, CH<sub>2</sub>, 4H).  
 $^{13}\text{C-NMR}$  (100 MHz,  $\text{CDCl}_3$ ):  $\delta$  194.27, 135.35, 133.64, 128.73, 128.69, 45.38.  
HRMS (ESI): [M+Na]<sup>+</sup> calculated: 325.0333, found: 325.0338.

### **MIC determinations and synergy assays**

The antibacterial activity of compounds **1-5** was evaluated alone and in combination with meropenem against a panel of  $\beta$ -lactamase producing gram-negative bacteria including *K. pneumoniae* RC10 (KPC-2), *K. pneumoniae* RC 45 (OXA-48), *K. pneumoniae* RC51 (VIM-1), *K. pneumoniae* JS265 (IMP-28), *E. coli* RC89 (NDM-1), *P. aeruginosa* RC60 (VIM-2), *P. aeruginosa* JS80 (IMP13, IMP-37), *K. pneumoniae* RC21 (VIM-1), *E. aerogenes* RC22 (VIM-1), *K. pneumoniae* RC48 (VIM-1), *K. pneumoniae* JS22 (NDM-1), *K. pneumoniae* JS177 (NDM-1), and *K. pneumoniae* JS37 (NDM-1). The CLSI guidelines were used to determine minimum inhibitory concentrations (MICs). Starting from glycerol stocks, bacterial strains were cultured on blood agar plates and incubated at 37 °C. A single colony was then transferred to tryptic soy broth (TSB) and incubated with shaking at 37 °C until the optical density of the bacterial suspension reached a level equivalent to the 0.5 McFarland standard. The suspension was then diluted to 10<sup>6</sup> CFU/mL in Mueller-Hinton broth (MHB). Using polypropylene microtiter plates, the wells of the first row received 50  $\mu$ L of the test compounds dissolved in MHB and were subjected to serial dilution. Finally, 50  $\mu$ L of the bacterial suspension was added and the plates were sealed and incubated at 37 °C with constant shaking (at 600 RPM). The next morning, the plates were inspected for visible bacterial growth (see table 3 for antibiotic susceptibility data).

Synergy between meropenem (or cefoperazone) and thiols **1-5** was evaluated as follows: To the top row of a 96-well plate, 100  $\mu$ L of a solution of meropenem at 4 $\times$ MIC was added. 50  $\mu$ L aliquots of this solution was serially diluted down each row to achieve a range of decreasing meropenem concentrations. Next, thiols **1-5** (50  $\mu$ L aliquots) were added to the wells to provide a concentration range of 128 to 16  $\mu$ g/mL. The relevant bacterial suspension (100  $\mu$ L/well) was finally added to each well to give a final concentration of thiols **1-5** ranging from 64 to 8  $\mu$ g/mL. The plates were sealed and incubated overnight at 37 °C. MICs were determined the next morning by visual inspection and used in calculating fractional inhibitory concentration index (FICI) values. As a standard MBL inhibitor cocktail, a 16:1 (w/w) mixture of ethylenediaminetetraacetic acid disodium salt-phenanthroline (EP) was also used. The MIC of the EP mixture was first determined against each strain so that a sub-MIC concentrations could be used for synergy assays. All the assays were performed in duplicates. Figure 4 provides a graphical representation of the checkerboard assays.

**Table 3.** Antibiotic susceptibility of the MBL-producing isolates

Isolates	MIC ( $\mu\text{g/mL}$ )					
	Meropenem	Cefoperazone	Ciprofloxacin	Gentamicin	Tobramycin	Colistin
<i>K. pneumoniae</i> (KPC-2)	>128 (R) <sup>a</sup>	>256 (R)	$\geq 4$ (R) <sup>b</sup>	4 (S) <sup>b</sup>	$\geq 16$ (R) <sup>b</sup>	1 (S) <sup>b</sup>
<i>K. pneumoniae</i> (OXA-48)	64 (R)	>256 (R)	>32 (R)	>32 (R)	32 (R)	$\leq 0.25$ (S)
<i>K. pneumoniae</i> (VIM-1)	64/32 (R)	>256 (R)	>32 (R)	>32 (R)	32 (R)	32 (R) <sup>b</sup>
<i>K. pneumoniae</i> (IMP-28)	16/8 (R)	256 (R)	1 (R)	0.5 (S)	1 (S)	$\leq 0.25$ (S)
<i>E. coli</i> (NDM-1)	128/64 (R)	>256 (R)	>32 (R)	>32 (R)	>32 (R)	$\leq 0.25$ (S)
<i>P. aeruginosa</i> (VIM-2)	32 (R)	128 (R)	$\geq 4$ (R) <sup>b</sup>	$\geq 16$ (R) <sup>b</sup>	$\geq 16$ (R) <sup>b</sup>	1 (S) <sup>b</sup>
<i>P. aeruginosa</i> (IMP-13, IMP-37)	64 (R)	256 (R)	32 (R)	>32 (R)	32 (R)	1 (S)
<i>K. pneumoniae</i> (VIM-1)	64/32 (R)	>256 (R)	$\geq 4$ (R) <sup>b</sup>	$\geq 16$ (R) <sup>b</sup>	$\geq 16$ (R) <sup>b</sup>	$\leq 0.5$ (S) <sup>b</sup>
<i>E. aerogenes</i> (VIM-1)	32/16 (R)	>256 (R)	1 (R) <sup>b</sup>	$\leq 1$ (S) <sup>b</sup>	$\geq 16$ (R) <sup>b</sup>	$\leq 0.05$ (S) <sup>b</sup>
<i>K. pneumoniae</i> (VIM-1)	>128/128 (R)	>256 (R)	$\geq 4$ (R) <sup>b</sup>	2 (S) <sup>b</sup>	16 (R)	$\leq 0.5$ (S) <sup>b</sup>
<i>K. pneumoniae</i> (NDM-1)	32/16 (R)	>256 (R)	$\geq 8$ (R) <sup>b</sup>	$\geq 16$ (R) <sup>b</sup>	$\geq 4$ (R) <sup>b</sup>	$\leq 1$ (S) <sup>b</sup>
<i>K. pneumoniae</i> (NDM-1)	16/8 (R)	>256 (R)	>32 (R)	>32 (R)	16 (R)	8 (R)
<i>K. pneumoniae</i> (NDM-1)	64/32 (R)	>256 (R)	$\geq 8$ (R) <sup>b</sup>	$\geq 16$ (R) <sup>b</sup>	$\geq 4$ (R) <sup>b</sup>	$\leq 1$ (S) <sup>b</sup>

<sup>a</sup>R: resistant; S: sensitive. Sensitivity to the tested antibiotics (except for cefoperazone) according to the clinical MIC breakpoints issued by the European Committee on Antimicrobial Susceptibility Testing (EUCAST).<sup>37</sup> For cefoperazone, the MIC breakpoint based on that published by the United States food and drug administration (FDA).<sup>38</sup>

<sup>b</sup>MIC data provided by Utrecht University medical center.

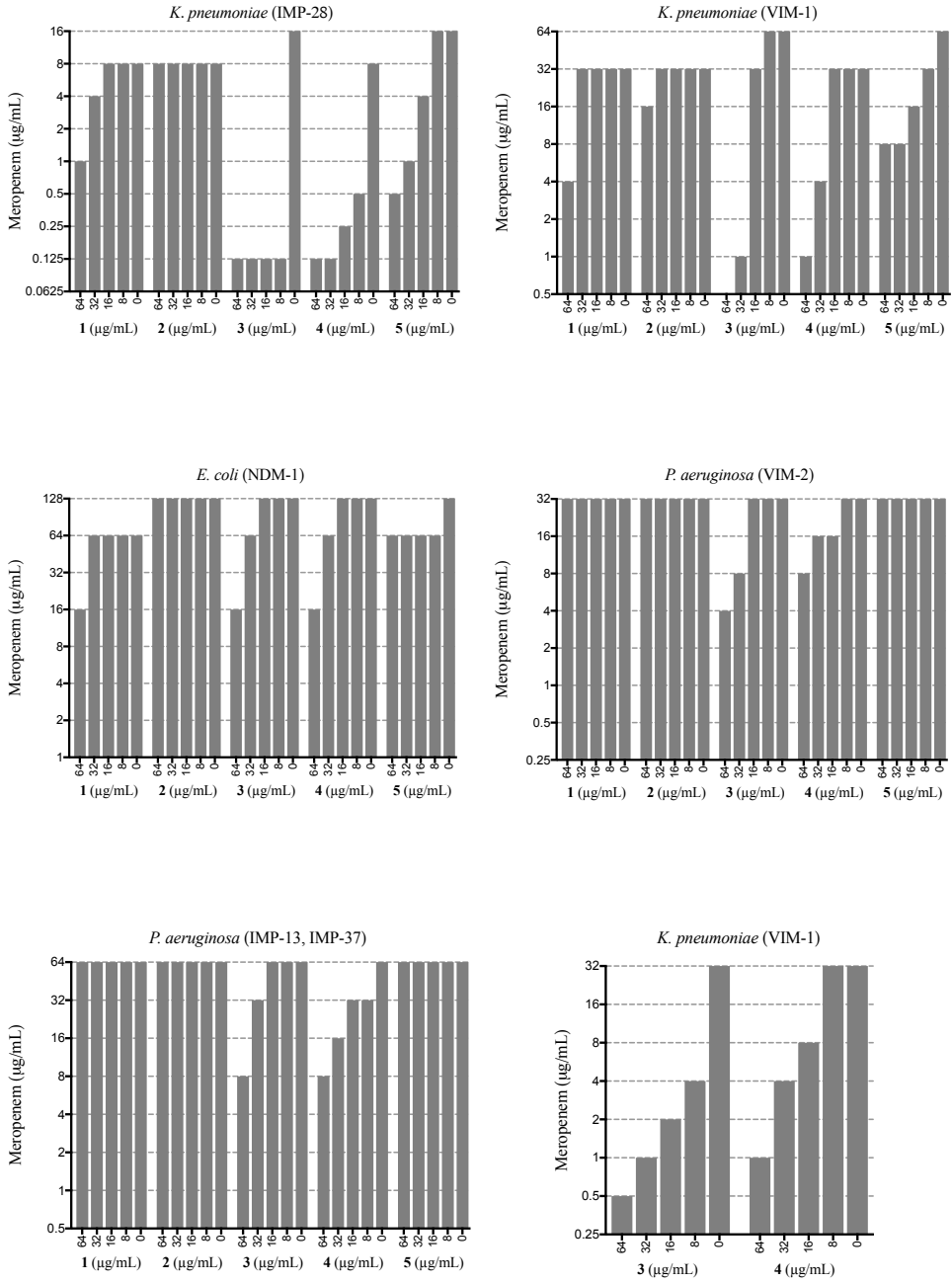


**Figure 4.** The MIC values of meropenem/cefoperazone in combination with thiols 1-5.

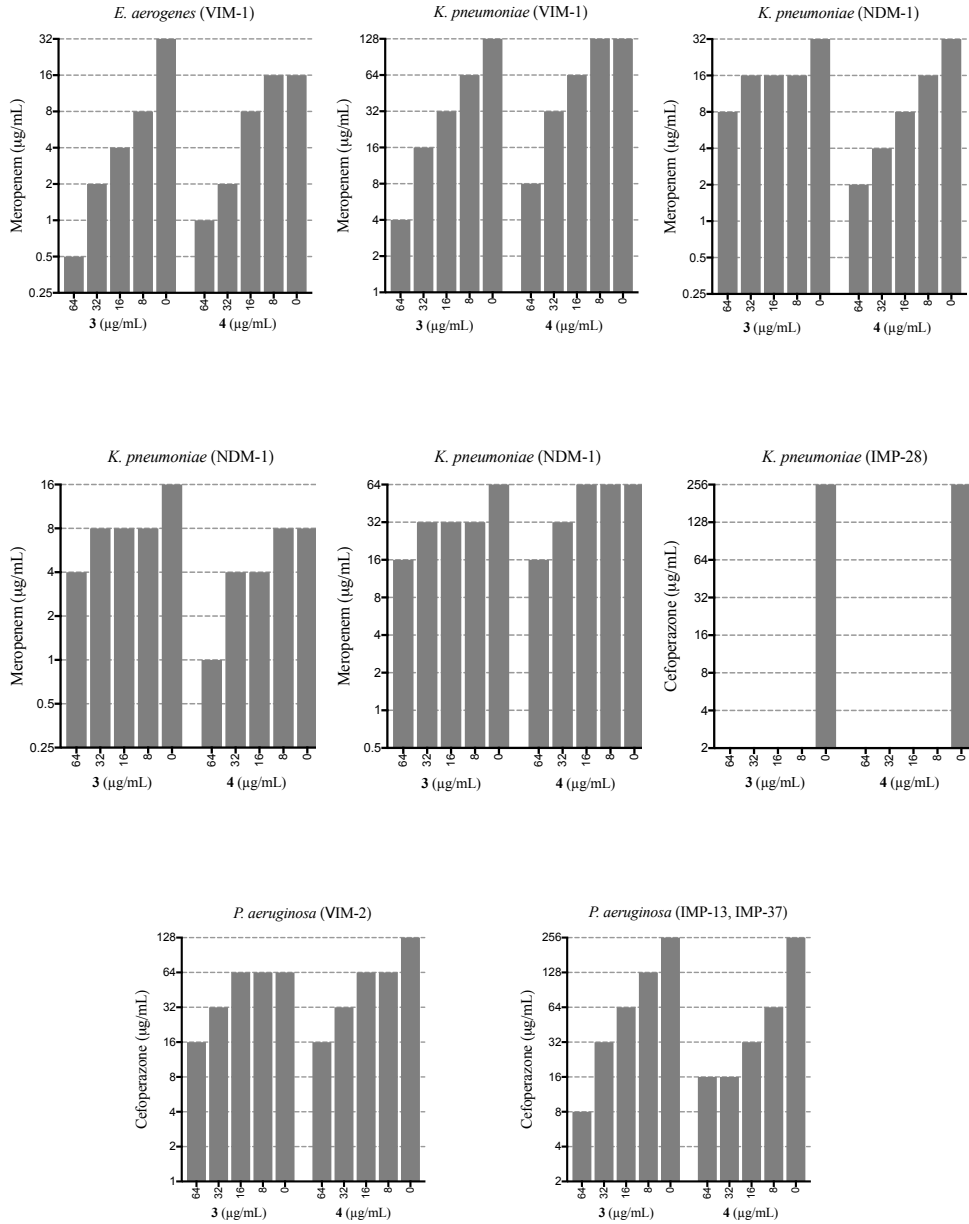


Figure 4. Continued.

### ***Stability analysis***

To prepare calibration curves for thiols **3-5** and the corresponding disulfides **6-8** each compound was dissolved in DMSO to prepare a stock solution (10 mg/mL) that was then immediately diluted in Mueller-Hinton broth (MHB) to reach concentrations ranging from 1 µg/mL to 256 µg/mL. The samples were then processed as follows: To precipitate undesired media components, the sample solutions were diluted with acetonitrile (1:3 v/v), vortexed for 10 seconds, and centrifuged at 10000 rpm for 10 min. The supernatant was retained and stored at -20 °C until HPLC analysis. Samples were analyzed by analytical RP-HPLC using a Phenomenex Gemini C-18 110A column (250×4.60 mm, 5 micron) at a flow rate of 1 mL/min and their UV absorbance were detected at 214 nm. For the analysis of compounds **4, 5, 7, and 8**, the gradient started with 0% of buffer B (5% H<sub>2</sub>O, 95% acetonitrile, 0.1% TFA) and 100% buffer A (95% H<sub>2</sub>O, 5% acetonitrile, 0.1% TFA) increasing to 50% buffer B over 5 min followed by an increase to 100% buffer B over 10 min and maintenance at 100% buffer B for 3 min. The buffer gradient was then returned to 0% buffer B in 2 min and maintained at 0% for an additional 5 min to re-equilibrate the system. For the analysis of compounds **3** and **6** the gradient started with 0% of buffer B, increased to 50% buffer B over 5 min, then to 90% buffer B over 8 min followed by a final increase to 100% buffer B over 1 min. After 1 min at 100% buffer B the gradient returned to 0% buffer B over 2 min and was maintained at 0% for 3 min to re-equilibrate the system. The calibration curves were linear from 2-256 µg/mL for compounds **3-6** and from 1.6-200 µg/mL for compounds **7** and **8** with  $r^2 > 0.990$  in all the cases. Due to the relatively short half-life of compound **5** in MHB, the medium needed to be supplemented with 5.0 mM TCEP to obtain a suitable calibration curve. To assess the half-lives of thiols **3-5** in MHB, each compound was dissolved in MHB (200 µg/mL) and incubated at 37 °C. At time points of 0, 0.5, 1, 2, 4 and 8 hours, 100 µL aliquots of each samples were taken and subjected to the same processing described above for the standards prior to HPLC analysis.

### ***Isothermal titration calorimetry***

ITC experiments were performed using a MicroCal Auto-ITC200 instrument (Malvern). The test compounds and zinc chloride were dissolved in Tris-HCl buffer (20 mM, pH 7.0) and degassed using a sonication bath (10 min) before running the experiments. The zinc chloride solution was titrated into a solution of **3**, **4**, **6**, **7**, EDTA, or 1,10-phenanthroline (see table 4 for specific concentrations used) over 26 aliquots of 1.5  $\mu$ L (except the first injection which was 0.5  $\mu$ L) with 120 seconds spacing between injections. All the experiments were performed at 25 °C in triplicate with reference power set at 2.0  $\mu$ cal/sec. The generated peaks were integrated using Origin 7.0 software (see figure 5 for thermograms). The error for all the reported thermodynamic parameters was estimated through Monte Carlo simulation the standard errors of three experiments.

**Table 4.** Concentrations of the metal/ligands used for the ITC experiments

Experiment (metal/ligand)	Zn <sup>2+</sup> concentration (mM)	Ligand concentration (mM)
ZnCl <sub>2</sub> / compound <b>3,4,6,7</b>	2.0	2.0
ZnCl <sub>2</sub> / EDTA	0.4	0.04
ZnCl <sub>2</sub> / phenanthroline	1.0	0.1



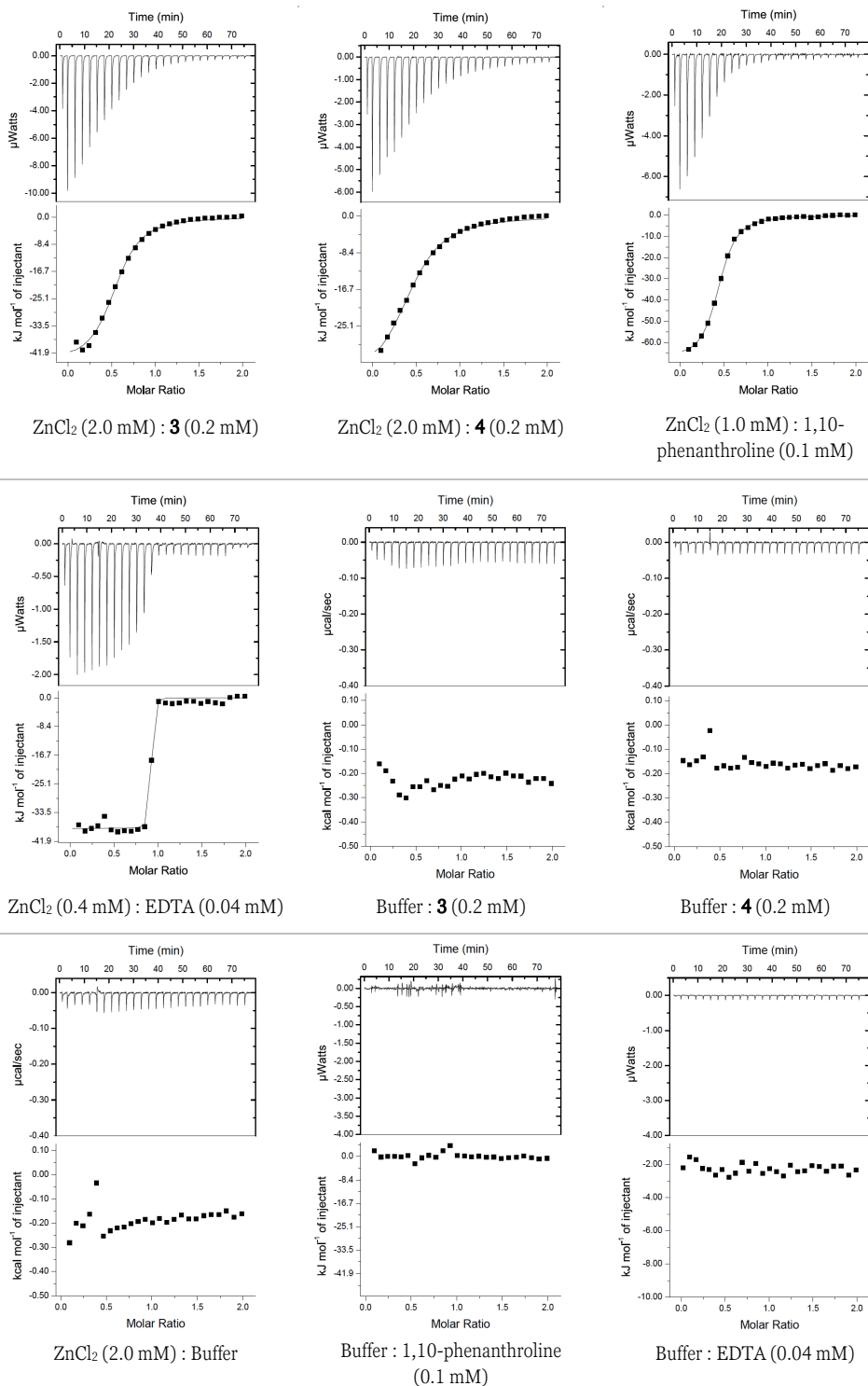


**Figure 5.** The ITC thermograms

## References

- 1 R. J. Worthington and C. Melander, *J. Org. Chem.*, 2013, **78**, 4207–4213.
- 2 K. Bush, *ACS Infect. Dis.*, 2015, **1**, 509–511.
- 3 J. D. Buynak, *Expert Opin. Ther. Pat.*, 2013, **23**, 1469–1481.
- 4 T. Palzkill, *Ann. N. Y. Acad. Sci.*, 2013, **1277**, 91–104.
- 5 G. D. Wright, *Trends Microbiol.*, 2016, **24**, 862–871.
- 6 R. P. McGeary, D. T. Tan and G. Schenk, *Future Med. Chem.*, 2017, **9**, 673–691.
- 7 Faridoon and N. Ul Islam, *Sci. Pharm.*, 2013, **81**, 309–327.
- 8 G.-B. Li, M. I. Abboud, J. Brem, H. Someya, C. T. Lohans, S.-Y. Yang, J. Spencer, D. W. Wareham, M. A. McDonough and C. J. Schofield, *Chem. Sci.*, 2017, **8**, 928–937.
- 9 S. B. Falconer, S. A. Reid-Yu, A. M. King, S. S. Gehrke, W. Wang, J. F. Britten, B. K. Coombes, G. D. Wright and E. D. Brown, *ACS Infect. Dis.*, 2015, **1**, 533–543.
- 10 A. N. Chan, A. L. Shiver, W. J. Wever, S. Z. A. Razvi, M. F. Traxler and B. Li, *Proc. Natl. Acad. Sci.*, 2017, **114**, 2717–2722.
- 11 W. Fast and L. D. Sutton, *Biochim. Biophys. Acta - Proteins Proteomics*, 2013, **1834**, 1648–1659.
- 12 Y.-N. Chang, Y. Xiang, Y.-J. Zhang, W.-M. Wang, C. Chen, P. Oelschlaeger and K.-W. Yang, *ACS Med. Chem. Lett.*, 2017, **8**, 527–532.
- 13 W. S. Shin, A. Bergstrom, R. A. Bonomo, M. W. Crowder, R. Muthyala and Y. Y. Sham, *ChemMedChem*, 2017, **12**, 845–849.
- 14 S. Skagseth, S. Akhter, M. H. Paulsen, Z. Muhammad, S. Lauksund, Ø. Samuelsen, H.-K. S. Leiros and A. Bayer, *Eur. J. Med. Chem.*, 2017, **135**, 159–173.
- 15 L. Seville, L. Gavara, C. Bebrone, F. De Luca, L. Nauton, M. Achard, P. Mercuri, S. Tanfoni, L. Borgianni, C. Guyon, P. Lonjon, G. Turan-Zitouni, J. Dzieciolowski, K. Becker, L. Bénard, C. Condon, L. Maillard, J. Martinez, J.-M. Frère, O. Dideberg, M. Galleni, J.-D. Docquier and J.-F. Hernandez, *ChemMedChem*, 2017, **12**, 972–985.
- 16 Y. Arakawa, N. Shibata, K. Shibayama, H. Kurokawa, T. Yagi, H. Fujiwara and M. Goto, *J. Clin. Microbiol.*, 2000, **38**, 40.
- 17 G. G. Hammond, J. L. Huber, M. L. Greenlee, J. B. Laub, K. Young, L. L. Silver, J. M. Balkovec, K. A. D. Pryor, J. K. Wu, B. Leiting, D. L. Pompliano and J. H. Toney, *FEMS Microbiol. Lett.*, 1999, **179**, 289–296.
- 18 C. Mollard, C. Moali, C. Papamicael, C. Damblon, S. Vessilier, G. Amicosante, C. J.

- Schofield, M. Galleni, J. M. Frère and G. C. K. Roberts, *J. Biol. Chem.*, 2001, **276**, 45015–45023.
- 19 W. Jin, Y. Arakawa, H. Yasuzawa, T. Taki, R. Hashiguchi, K. Mitsutani, A. Shoga, Y. Yamaguchi, H. Kurosaki, N. Shibata, M. Ohta and M. Goto, *Biol. Pharm. Bull.*, 2004, **27**, 851–856.
- 20 Y. Yamaguchi, W. Jin, K. Matsunaga, S. Ikemizu, Y. Yamagata, J. I. Wachino, N. Shibata, Y. Arakawa and H. Kurosaki, *J. Med. Chem.*, 2007, **50**, 6647–6653.
- 21 B. M. R. Liénard, G. Garau, L. Horsfall, A. I. Karsisiotis, C. Damblon, P. Lassaux, C. Papamicael, G. C. K. Roberts, M. Galleni, O. Dideberg, J.-M. Frère and C. J. Schofield, *Org. Biomol. Chem.*, 2008, **6**, 2282–2294.
- 22 F. M. Klingler, T. A. Wichelhaus, D. Frank, J. Cuesta-Bernal, J. El-Delik, H. F. Müller, H. Sjuts, S. Göttig, A. Koenigs, K. M. Pos, D. Pogoryelov and E. Proschak, *J. Med. Chem.*, 2015, **58**, 3626–3630.
- 23 J. Brem, S. S. Van Berkel, D. Zollman, S. Y. Lee, O. Gileadi, P. J. McHugh, T. R. Walsh, M. A. McDonough and C. J. Schofield, *Antimicrob. Agents Chemother.*, 2016, **60**, 142–150.
- 24 P. Hinchliffe, M. M. González, M. F. Mojica, J. M. González, V. Castillo and C. Saiz, *Proc. Natl. Acad. Sci. U. S. A.*, 2016, E3745–E3754.
- 25 A. I. Karsisiotis, C. F. Damblon and G. C. K. Roberts, *Biochem. J.*, 2013, **456**, 397–407.
- 26 J. Brem, S. S. van Berkel, W. Aik, A. M. Rydzik, M. B. Avison, I. Pettinati, K.-D. Umland, A. Kawamura, J. Spencer, T. D. W. Claridge, M. A. McDonough and C. J. Schofield, *Nat. Chem.*, 2014, **6**, 1084–1090.
- 27 R. Migliavacca, J.-D. Docquier, C. Mugnaioli, G. Amicosante, R. Daturi, K. Lee, G. M. Rossolini and L. Pagani, *J. Clin. Microbiol.*, 2002, **40**, 4388–90.
- 28 F. C. Odds, *J. Antimicrob. Chemother.*, 2003, **52**, 1.
- 29 D. Ritz and J. Beckwith, *Annu. Rev. Microbiol.*, 2001, **55**, 21–48.
- 30 B. Strijtveen and R. M. Kellogg, *J. Org. Chem.*, 1986, **51**, 3664–3671.
- 31 P. Coric, S. Turcaud, H. Meudal, B. P. Roques and M.-C. Fournie-Zaluski, *J. Med. Chem.*, 1996, **39**, 1210–1219.
- 32 J. G. Chen, J. Zhu, P. M. Skonezny, V. Rosso and J. J. Venit, *Org. Lett.*, 2004, **6**, 3233–3235.
- 33 W. A. Bonner, *J. Org. Chem.*, 1968, **33**, 1831–1836.

- 34 J. Z. Chandanshive, B. F. Bonini, D. Gentili, M. Fochi, L. Bernardi and M. C. Franchini, *European J. Org. Chem.*, 2010, 6440–6447.
- 35 E. Biilmann and E. H. Madsen, *Justus Liebig's Ann. der Chemie*, 1914, **402**, 331–342.
- 36 B. Zeynizadeh, *J. Chem. Res.*, 2002, 564–566.
- 37 The European Committee on Antimicrobial Susceptibility Testing. Breakpoint tables for interpretation of MICs and zone diameters. Version 7.1, 2017.  
<http://www.eucast.org>
- 38 The document is available online at:  
[https://www.accessdata.fda.gov/drugsatfda\\_docs/label/2015/050551s043lbl.pdf](https://www.accessdata.fda.gov/drugsatfda_docs/label/2015/050551s043lbl.pdf)



## Chapter 5

# Cephalosporin conjugates of the thiol inhibitors of metallo- $\beta$ -lactamases are potent inhibitors of IMP enzymes

Parts of this chapter have been published in:

- (1) 2019 Dutch Patent application filing; Title: “Prodrug metallo-beta-lactamase inhibitors”; Inventors: Martin, N. I., van Haren, M. J., Tehrani, K. H. M. E. Priority date: April 1, 2019.
- (2) Tehrani, K. H. M. E., Wade, N., Mashayekhi, V., Bröchle, N. C., Voskuil, K., Jaspers, W., Pesce, D., van Haren, M. J., van Westen, G. J. P., and Martin, N. I. (2020) Novel cephalosporins selectively inhibit the IMP type metallo- $\beta$ -lactamases. *Manuscript in preparation*

## 1. Introduction

Despite the growing threat of  $\beta$ -lactam resistance caused by metallo- $\beta$ -lactamases (MBLs), there are no approved drugs in the market that target this class of enzymes. Unlike serine- $\beta$ -lactamases, MBLs (figure 1) are metalloenzymes containing one or two zinc ions in their active site and an activated water molecule coordinated by the zinc ions hydrolyzes all classes of  $\beta$ -lactams (except monobactams).<sup>1</sup> The MBLs of particular clinical significance are the New Delhi metallo- $\beta$ -lactamase (NDM), Verona integron-encoded metallo- $\beta$ -lactamase (VIM) and imipenemase (IMP) families all of which possess broad  $\beta$ -lactamase activity.<sup>2</sup> The previously reported inhibitors of MBLs have been the subject of several comprehensive review articles.<sup>3-6</sup> Indeed, a wide range of compounds have been reported as MBL inhibitors with the majority acting by either sequestering zinc and/or by forming a ternary complex with the metalloenzyme.<sup>7,8</sup> In chapter 4, we described the *in vitro* ability of a selected group of thiols (**1-3**, figure 2A) to inhibit MBLs and in doing so resensitize a panel of MBL-producing clinical isolates to meropenem, a potent carbapenem antibiotic.<sup>9</sup> The binding experiments described in chapter 4 employed isothermal titration calorimetry (ITC) to demonstrate that thiols **1** and **2** bind zinc with  $K_d$  values of 10  $\mu$ M and 20  $\mu$ M respectively. However, as we also demonstrated, these thiol-containing compounds are prone to rapid oxidation to the corresponding disulfides, leading to the loss of zinc-binding affinity, MBL inhibition, and synergistic activity.<sup>9</sup> As a means of limiting this unwanted oxidation, we were drawn to consider the hydrolysis mechanism of the cephalosporin class of  $\beta$ -lactam antibiotics (figure 2B). Specifically, we hypothesized that if conjugated to the 3-position of the cephalosporin core, these thiols could be delivered as MBL-inhibitor prodrugs which would enhance their selectivity and stability. Only upon MBL-mediated hydrolysis of the cephalosporin moiety would the active thiol-based inhibitor be released, providing both spacial and temporal control of inhibitor delivery and activation. This chapter describes the preparation of cephalosporin-thiol conjugates based on thiols **1-3** and evaluation of

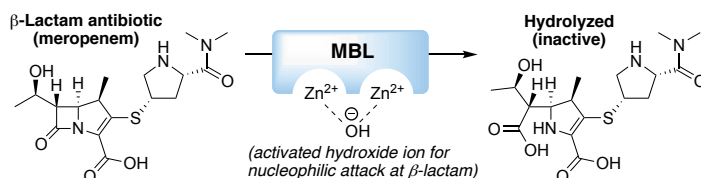


**Figure 1.** Metallo- $\beta$ -lactamases as zinc metallo-enzymes

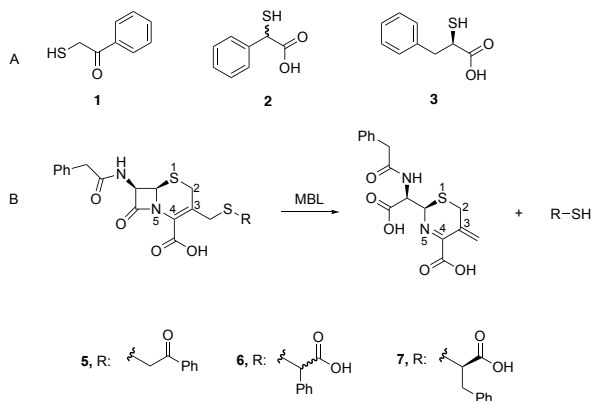


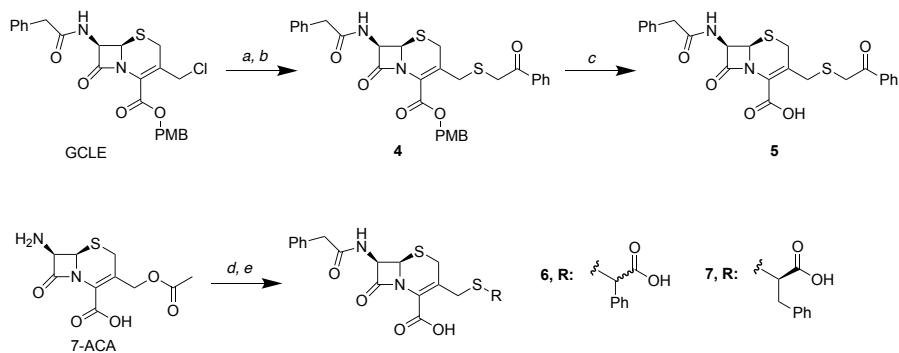
**Figure 2. A.** The previously reported thiols as MBL-inhibitors. **B.** Cephalosporin prodrugs of the thiols **1-3**.

their performance as MBL-inhibitor prodrugs capable of resensitizing MBL-expressing strains to  $\beta$ -lactam antibiotics.

## 2. Results and discussion

The cephalosporin-thiol conjugates were synthesized using two different routes (scheme 1). Thioalkylation of mercaptoacetophenone with the chloromethyl cephalosporin "GCLE", a common intermediate used in the industrial synthesis of cephalosporin antibiotics, yielded intermediate **4** followed by deprotection with TFA to yield compound **5**. Alternatively, compounds **6** and **7** were prepared via the  $\text{BF}_3$ -promoted substitution of 7-aminocephalosporanic acid (7-ACA) with thiomandelic acid or 2-mercapto-3-phenylpropionic acid, followed by acylation of the 7-amino group (see experimental section for detailed procedures). To assess the zinc-binding properties of the MBL-inhibitor prodrugs **5-7**, ITC binding studies were performed which revealed no binding interaction with zinc. This was in contrast with the starting thiols which were found to be relatively strong zinc-binders with low- $\mu\text{M}$   $K_d$  values<sup>9</sup>. In addition, stability analyses were performed to test whether inhibitor release occurred spontaneously. Following overnight incubation in Mueller-Hinton broth, HPLC analysis of the conjugates **5-7** showed very good stability (>95% after 15 h, table 1).





**Scheme 1.** Chemical route to the cephalosporin conjugates. Reagents and conditions: a. NaI, DMF, r.t., 30 min.; b. NaHCO<sub>3</sub>, 1, r.t., 20 h; c. TFA, anisole, 0 °C, 1 h; d. BF<sub>3</sub>·OEt<sub>2</sub>, **2/3**, ACN, 45 °C, 2 h; e. phenylacetyl chloride, saturated NaHCO<sub>3</sub> solution, acetone, r.t., 20 h.

**Table 1.** Stability of compounds **5-7** in Mueller-Hinton broth

Compound	(A <sub>T15</sub> /A <sub>T0</sub> )% <sup>a</sup>
<b>5</b>	95 ± 2
<b>6</b>	98 ± 1
<b>7</b>	98 ± 2

<sup>a</sup>A<sub>T15</sub>: peak area after 15 h incubation, A<sub>T0</sub>: peak area at time 0.

The compounds were next tested for their ability to restore the activity of meropenem against a panel of MBL-producing clinical isolates. The results showed that compound **6** and **7** were the most potent resensitizers, lowering the MIC of meropenem against IMP-producing isolates most effectively (figure 3).

Encouraged by the promising results against the MBL-producing clinical isolates, we tested the ability of the conjugates to inhibit purified IMP-1, IMP-28, VIM-2, and NDM-1 enzymes. The biochemical assay used for these studies employed the chromogenic cephalosporin nitrocefim as substrate. The IC<sub>50</sub> data obtained (table 2) are consistent with the trend observed in bacterial growth inhibition synergy assays with IMP enzymes most strongly inhibited by the conjugates with **6** and **7** demonstrating the most potent inhibitory activity.

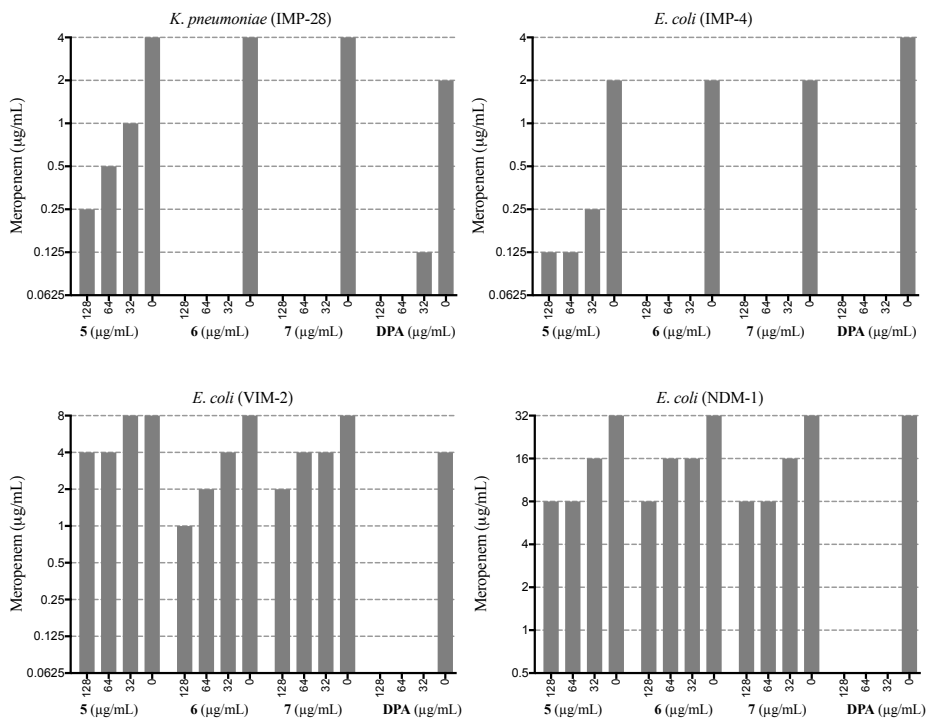


**Figure 3.** MIC of meropenem in combination with different concentrations of compounds **5-7** and dipicolinic acid (DPA).

**Table 2.** IC<sub>50</sub> (µM) of thiol conjugates reported as mean ± SD

Compound	IMP-1	IMP-28	NDM-1	VIM-2
<b>5</b>	3.3 ± 0.2	14 ± 1	77 ± 12	76 ± 11
<b>6</b>	0.47 ± 0.08	0.46 ± 0.04	123 ± 8	10 ± 0.5
<b>7</b>	4.7 ± 0.4	1.1 ± 0.2	94 ± 0.2	16 ± 1
DPA	29 ± 0.5	29 ± 5	10 ± 0.1	10 ± 0.8

To assess the release of the thiol inhibitors, the cephalosporin conjugates were incubated with IMP-28 and analyzed using <sup>1</sup>H-NMR and LC-MS techniques. It has been shown previously that the molecular mechanism of cephalosporin hydrolysis can be probed *in situ* using NMR techniques.<sup>10,11</sup> For our studies, we used the 7-phenylacetyl amide derivative of 7-ACA (compound **8**, figure 4) as a positive control. After incubating this compound with IMP-28, we detected the vinylic hydrogens of the corresponding elimination product as two singlets

resonating *ca.* 5.50 ppm (figure 4). Notably, however, when **6** and **7** were subjected to the same experiment, the vinylic hydrogens were not detected (figure 5 and 6). The results of these <sup>1</sup>H-NMR studies were further corroborated by LC-MS analyses of the hydrolysis products which revealed hydrolyzed β-lactam compounds **6H** and **7H** as the only detectable products (figure 7).

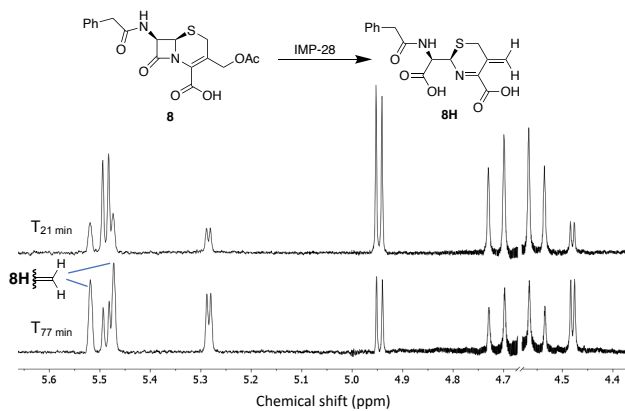


Figure 4. Hydrolysis of **8** monitored by  $^1\text{H-NMR}$

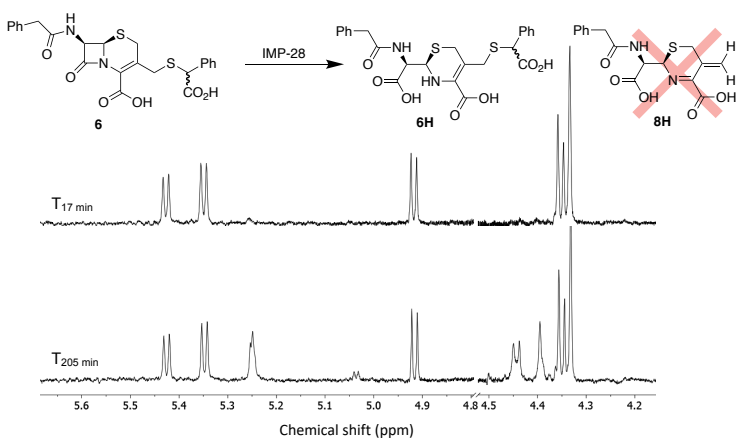


Figure 5. Hydrolysis of **6** monitored by  $^1\text{H-NMR}$

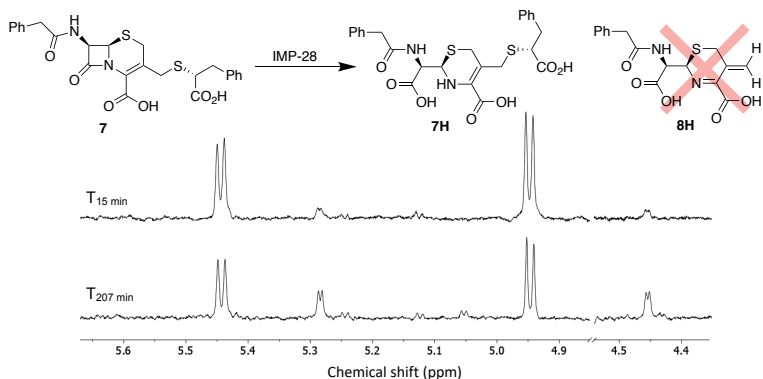
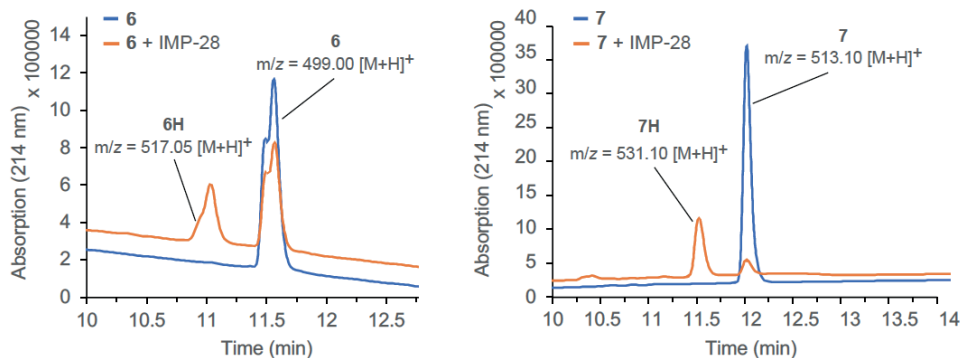
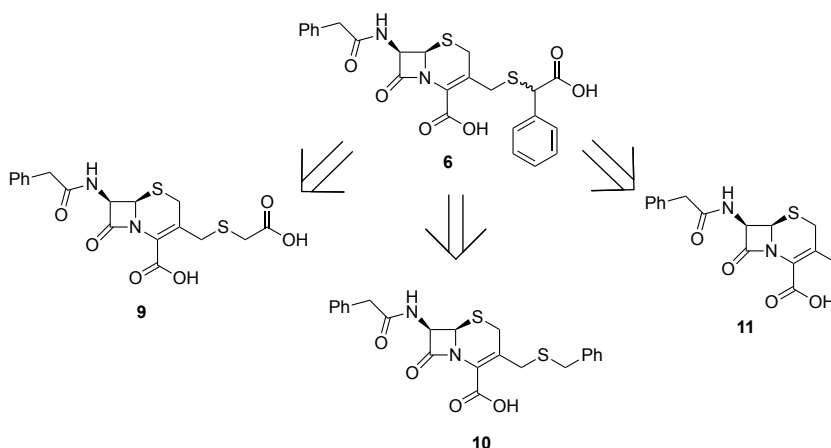


Figure 6. Hydrolysis of **7** monitored by  $^1\text{H-NMR}$



**Figure 7.** IMP-28-mediated hydrolysis of **6** and **7** monitored by HPLC-MS (procedure described in the experimental section).

The finding that compounds **6** and **7** demonstrate potent inhibition of IMP-28 despite not releasing the corresponding zinc-binding thiol inhibitors upon MBL-mediated  $\beta$ -lactam hydrolysis was surprising. To better understand the mechanism of inhibition of these cephalosporin conjugates, a series of structural variants of compound **6** were prepared to establish which structural features are most important for the inhibitory activity observed (figure 8, synthesis described in detail in the experimental section). Specifically, we designed compounds **9**, **10**, and **11** to systematically evaluate the contribution made by the aromatic group, the carboxylate moiety, or both.



**Figure 8.** New derivatives of **6** synthesized for structure-activity relationship (SAR) clarification.

The IC<sub>50</sub> data obtained (table 3) shows that upon the elimination of the phenyl group (**9**), carboxylic acid (**10**) or the entire thiomandelic acid fragment (**11**), the activity against IMP-1 and IMP-28 is decreased at least by ~100 times, suggesting that the thiomandelic acid fragment introduces productive binding interactions with the IMP active site.

The same trend was observed when the cephalosporin conjugates were tested for their synergy with meropenem against MBL-producing clinical isolates. To compare the potency of the cephalosporins, their ability to lower the MIC of meropenem by 4-fold were determined (table 4). The synergy data show the IMP selectivity of the cephalosporins among which **5** and **6** can reduce the MIC of meropenem by 4-fold when added at 1  $\mu$ g/mL or lower.

**Table 3.** IC<sub>50</sub> ( $\mu$ M) of cephalosporins **9-11** reported as mean  $\pm$  SD

Compound	IMP-1	IMP-28	NDM-1	VIM-2
<b>9</b>	>200	101 $\pm$ 4	72 $\pm$ 2	53 $\pm$ 12
<b>10</b>	43 $\pm$ 3	45 $\pm$ 5	131 $\pm$ 11	73 $\pm$ 0.1
<b>11</b>	>200	>200	>200	57 $\pm$ 9

**Table 4.** C<sub>MIC/4</sub> values defined as the lowest concentration of the inhibitors leading to 4-fold reduction in the MIC of meropenem

Isolate	MBL	C <sub>MIC/4</sub> ( $\mu$ g/mL)					
		<b>5</b>	<b>6</b>	<b>7</b>	<b>9</b>	<b>10</b>	<b>11</b>
<i>E. coli</i>	IMP-4	16	1	$\leq$ 0.5	4	4	32
<i>K. pneumoniae</i>	IMP-28	32	0.5	0.25	8	32	64
<i>E. coli</i>	VIM-2	>128	64	128	128	128	128
<i>E. coli</i>	NDM-1	64	128	64	128	>128	>128

The kinetic analysis of the hydrolysis of the cephalosporins by IMP-28, NDM-1 and VIM-2 provided additional insights on the observed IMP-28 selectivity for the inhibitors and the greater potency of **6** and **7**. These analyses showed that IMP-28 has the lowest catalytic efficiency for **6** and **7** among the tested cephalosporins (see table 5 for relative  $k_{\text{cat}}/K_M$  data). Comparison with the other major MBL families also revealed that **6** and **7** were hydrolyzed more efficiently by NDM-1 and VIM-2 than by IMP-28. These findings indicate that conjugates **6** and **7** inhibit IMP-28 either by acting as slowly turned-over substrates or that the hydrolyzed products **6H** and **7H** are more tightly bound within the IMP active site than either the NDM or VIM active sites.

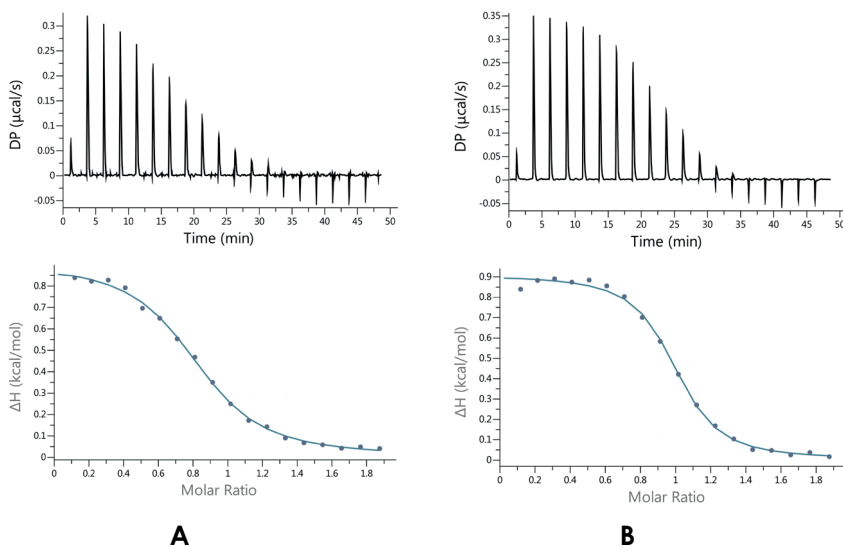
To evaluate the inhibitory activity of their corresponding hydrolysis products **6H** and **7H**, the intact conjugates **6** and **7** were fully hydrolyzed by incubation with NDM-1 as described in the experimental section. Following hydrolysis, the NDM-1 enzyme was completely removed via spin-filtration as confirmed by the lack of nitrocefin activity by the filtrate. The partially hydrolyzed **6H** and **7H** (see figure 5 and 6 for chemical structures) were then tested for their inhibition of MBLs. Interestingly both hydrolysis products were found to possess potent activity against IMP-1 and IMP-28 with sub- $\mu\text{M}$   $\text{IC}_{50}$  values (table 6). In addition, the hydrolysis products **6H** and **7H** were evaluated for their zinc-binding affinity using ITC. When zinc was titrated into the solution of **6** and **7** preincubated with NDM-1, a binding interaction with  $K_d$  values of 11.8  $\mu\text{M}$  and 2.9  $\mu\text{M}$  were observed respectively (figure 9), while the intact cephalosporins showed no zinc-binding affinity. This may suggest that the acquired affinity to zinc could play a partial role in the inhibitory activity of **6H** and **7H**.

**Table 5.** The Michaelis-Menten parameters determined for the cephalosporin conjugates as substrates of IMP-28, VIM-2 and NDM-1.

Enzyme	Substrate	$K_M$ ( $\mu\text{M}$ )	$k_{\text{cat}}$ ( $\text{s}^{-1}$ )	$k_{\text{cat}}/K_M$ ( $\mu\text{M}^{-1}\cdot\text{s}^{-1}$ )	Relative $k_{\text{cat}}/K_M$
IMP-28	<b>6</b>	$130 \pm 14$	0.386	0.003	0.3
	<b>7</b>	$250 \pm 8$	2.84	0.011	1.2
	<b>9</b>	$219 \pm 24$	37.1	0.169	18
	<b>10</b>	$21 \pm 4$	10.8	0.529	57
	<b>11</b>	$393 \pm 74$	23.3	0.059	6.3
VIM-2	<b>6</b>	$8.29 \pm 2.3$	4.06	0.490	52
	<b>7</b>	$4.31 \pm 1.2$	2.35	0.546	58
NDM-1	<b>6</b>	$14 \pm 3$	13.13	0.936	100
	<b>7</b>	$21 \pm 4$	17.5	0.821	88

**Table 6.** IC<sub>50</sub> ( $\mu$ M) of the hydrolysis products **6H** and **7H** reported as mean  $\pm$  SD

Compound	IMP-1	IMP-28	NDM-1	VIM-2
<b>6H</b>	0.54 $\pm$ 0.02	0.75 $\pm$ 0.06	135.8 $\pm$ 32.6	65.6 $\pm$ 8.9
<b>7H</b>	0.59 $\pm$ 0.06	0.64 $\pm$ 0.05	118.4 $\pm$ 24.5	69 $\pm$ 15

**Figure 9.** Thermograms of zinc sulphate (2 mM) titrated in a 0.2 mM solution of **6** (A) and **7** (B) incubated with NDM-1 (187 nM) for 2 h at room temperature.

### 3. Conclusion

We here describe a series of cephalosporin-based MBL inhibitor prodrugs designed to release zinc-chelating small molecule thiols upon MBL-mediated hydrolysis. Notably, these conjugates did not function as expected. While MBL-mediated hydrolysis was observed, the release of the small molecule thiol fragment did not spontaneously occur for the conjugates included in this study. This lack of release is presumably due to the pK<sub>a</sub> of the corresponding thiols not being low enough, *i. e.* they do not possess sufficient “leaving group character”. It was therefore surprising to find that the cephalosporin conjugates (**5-7**) selectively inhibit IMP enzymes despite the fact that  $\beta$ -lactam hydrolysis does not result in release of thiols **1-3**. Based



on kinetic analyses, the most potent conjugates **6** and **7** were shown to be slowly turned over substrates of IMP-28. In addition, the hydrolysis products **6H** and **7H** were found to be IMP-selective inhibitors. Taken together these findings suggest that the inhibitory activity observed for the conjugates is due to combination of effects. Future investigations will probe the interaction of these cephalosporin conjugates with the IMP active site as compared with the other MBLs as a means of better understanding the observed selectivity of inhibition.

## 4. Experimental Section

### General

The chlorocephalosporin GCLE, 7-ACA, and 7-ADCA were purchased from Combi-Blocks (US) and nitrocefin from Cayman chemical. The preparation of thiols **1-3** has been described in chapter 4. Compound **8** was synthesized via the acylation of 7-ACA following a previously reported procedure.<sup>12</sup> Proton and carbon nuclear magnetic resonance spectra were recorded on an AV400 NMR spectrometer (Bruker) and samples were dissolved in CDCl<sub>3</sub> or DMSO-*d*<sub>6</sub>. HRMS analyses were performed on a Thermo Scientific Dionex UltiMate 3000 HPLC system with a Phenomenex Kinetex C18 column (2.1 x 150 mm, 2.6 μm) at 35 °C and equipped with a diode array detector. The samples were eluted over a gradient of solution A (0.1 % formic acid in water) vs. solution B (0.1% formic acid in acetonitrile). This system was connected to a Bruker micrOTOF-Q II mass spectrometer (ESI ionization) calibrated internally with sodium formate.

### Synthesis

**Compound 5.** GCLE (1.0 g, 2.1 mmol) and NaI (314 mg, 2.1 mmol) were stirred in DMF (10 mL) for 30 min at room temperature. Then mercaptoacetophenone (479 mg, 3.15 mmol) and sodium bicarbonate (200 mg, 2.38 mmol) were added successively and the mixture was stirred overnight. The reaction mixture was then partitioned between water and DCM followed by washing the organic layer with brine (3×20 mL). Concentration of the organic layer and purification of the residue on silica using ethyl acetate and DCM mixture as eluent furnished the intermediate **4** as a pale yellow solid (854 mg, 68%). <sup>1</sup>H-NMR (400 MHz, CDCl<sub>3</sub>): δ 7.89 (d, *J* = 8.3 Hz, aromatic H, 1H), 7.58 (t, *J* = 8.0 Hz, aromatic H, 1H), 7.45 (t, *J* = 8.0 Hz, aromatic H, 2H), 7.37-7.25 (m, aromatic H, 7H), 6.85 (dd, *J* = 8.6 Hz, *J* = 1.8 Hz, aromatic H, 2H), 5.99 (d, *J* = 9.2 Hz, 1H), 5.77 (m, β-lactam C-H, 1H), 5.14 (s, benzyloxy CH<sub>2</sub>, 2H), 4.90 (d, *J* = 4.9 Hz, 1H), 3.99-3.45 (m, aliphatic H, 11H), <sup>13</sup>C-NMR (100 MHz, DMSO-*d*<sub>6</sub>): δ 194.41, 171.14, 164.50, 161.52, 159.83, 135.37, 133.72, 133.46, 130.67, 129.40, 129.10, 128.69, 128.53,

128.49, 127.64, 126.78, 124.58, 113.91, 67.93, 59.03, 57.74, 55.23, 43.26, 37.81, 33.81, 27.72. HRMS (ESI):  $[M+H]^+$  calculated: 603.1624, found: 603.1620. To **4** (600 mg, 1.0 mmol) was added TFA/anisole (15 mL/3 mL) and the mixture was stirred at 0 °C for 1 h. It was then concentration under vacuum and the residue was precipitated by 1:1 mixture of diethyl ether and petroleum ether. The solid was isolated by centrifugation and purified by reversed-phase prep-HPLC using C18 and an optimal gradient of buffer A (H<sub>2</sub>O 95%, ACN 5%, TFA 0.1%) vs. buffer B (ACN 95%, H<sub>2</sub>O 5%, TFA 0.1%) to afford **5** (51 mg, 35%, based on the purification of ~100 mg of the crude product by prep-HPLC). <sup>1</sup>H-NMR (400 MHz, CDCl<sub>3</sub>): δ 7.85 (d, *J* = 7.3 Hz, aromatic H, 1H), 7.53-7.22 (m, aromatic H, 8H), 6.50 (d, *J* = 8.8 Hz, 1H), 5.72 (dd, *J* = 8.9 Hz, *J* = 4.7 Hz, β-lactam C-H, 1H), 4.90 (d, *J* = 4.7 Hz, β-lactam C-H, 1H), 3.97-3.44 (m, aliphatic H, 8H), <sup>13</sup>C-NMR (100 MHz, DMSO-*d*<sub>6</sub>): δ 195.06, 171.36, 165.01, 163.45, 136.24, 135.91, 133.78, 129.44, 129.15, 128.79, 128.63, 127.36, 126.90, 125.49, 59.37, 58.22, 42.03, 38.20, 33.70, 27.45. HRMS (ESI):  $[M-H]^-$  calculated: 481.0897, found: 481.0863.

*General procedure for the synthesis of compounds 6, 7, 9, and 10.* To a solution of BF<sub>3</sub>·OEt<sub>2</sub> (2.6 mL, 21.3 mmol, 3.0 eq.) in acetonitrile (10 mL) were added the corresponding thiols (10.7 mmol, 1.5 eq.) and 7-ACA (1.9 g, 7.1 mmol, 1.0 eq.) successively. The mixture was stirred at 45-50 °C for 2 h after which it was diluted with water and pH was adjusted to 4 by adding 28% ammonium hydroxide solution. The precipitate was filtered off and washed with cold water and acetone respectively. The crude product (1.0 g) was added to a mixture of saturated bicarbonate solution (6 mL) and acetone (9 mL). Then phenylacetyl chloride (2.0 eq.) was added dropwise and the mixture was stirred overnight at room temperature. Diluting the mixture with water followed by acidification to pH 2.0 using 1.0 M HCl resulted in a white solid which was filtered off and washed with minimum water and ether respectively. The crude material was purified by reversed-phase prep-HPLC using C18 and an optimal gradient of buffer A (H<sub>2</sub>O 95%, ACN 5%, TFA 0.1%) vs. buffer B (ACN 95%, H<sub>2</sub>O 5%, TFA 0.1%). The quantities and yields below are reported based on the purification of ~100 mg of the crude product by prep-HPLC.

*Compound 6.* 40 mg (26%, over two steps). <sup>1</sup>H-NMR (400 MHz, DMSO-*d*<sub>6</sub>): diastereomeric mixture δ 9.07 (apparent t, 1.8 H), 7.44-7.21 (m, aromatic H, 9H), 5.61 (m, β-lactam C-H, 1.8H), 5.04 (d, *J* = 4.8 Hz, β-lactam C-H, 0.8H), 4.88 (d, *J* = 4.7 Hz, β-lactam C-H, 1H), 4.65 (apparent d, aliphatic C-H, 1.8H), 3.69-3.32 (m, aliphatic CH<sub>2</sub>, 10.8H), HRMS (ESI):  $[M-H]^-$  calculated: 497.0847, found: 497.0842.

**Compound 7.** 69 mg (47%, over two steps). <sup>1</sup>H-NMR (400 MHz, CDCl<sub>3</sub>): δ 7.41-7.14 (m, aromatic H, 10H), 6.16 (br s, 1H), 5.81 (dd, *J* = 8.9 Hz, *J* = 4.7 Hz, β-lactam C-H, 1H), 4.92 (d, *J* = 4.8 Hz, β-lactam C-H, 1H), 4.19 (d, *J* = 13.7 Hz, aliphatic C-H, 1H), 3.71-2.92 (m, aliphatic C-H, 8H), <sup>13</sup>C-NMR (100 MHz, DMSO-*d*<sub>6</sub>): δ 172.61, 170.99, 164.66, 163.08, 138.14, 135.84, 129.03, 129.01, 128.27, 128.23, 127.45, 126.55, 126.50, 124.95, 58.96, 57.75, 48.23, 41.58, 38.16, 33.38, 26.97, HRMS (ESI): [M-H]<sup>-</sup> calculated: 511.1003, found: 511.1000.

**Compound 9.** 88 mg (27%, over two steps). <sup>1</sup>H-NMR (400 MHz, DMSO-*d*<sub>6</sub>): δ 9.14 (d, *J* = 8.3 Hz, N-H, 1H), 7.34-7.21 (m, aromatic H, 5H), 5.65 (dd, *J* = 8.3 Hz, *J* = 4.7 Hz, β-lactam C-H, 1H), 5.11 (d, *J* = 4.8 Hz, β-lactam C-H, 1H), 3.73-3.20 (m, aliphatic H, 8H), <sup>13</sup>C-NMR (100 MHz, DMSO-*d*<sub>6</sub>): δ 170.55, 170.44, 164.10, 162.47, 135.31, 128.51, 127.72, 126.48, 125.99, 124.48, 58.43, 57.31, 41.10, 32.94, 32.74, 26.42. HRMS (ESI): [M+H]<sup>+</sup> calculated: 423.0685, found: 423.0702.

**Compound 10.** 82 mg (74%, over two steps). <sup>1</sup>H-NMR (400 MHz, DMSO-*d*<sub>6</sub>): δ 9.13 (d, *J* = 8.3 Hz, NH, 1H), 7.35-7.22 (m, aromatic H, 5H), 5.65 (dd, *J* = 8.3 Hz, *J* = 4.7 Hz, β-lactam C-H, 1H), 5.06 (d, *J* = 4.7 Hz, β-lactam C-H, 1H), 3.79-3.47 (m, aliphatic H, 8H), <sup>13</sup>C-NMR (100 MHz, DMSO-*d*<sub>6</sub>): δ 171.41, 165.11, 163.62, 138.81, 136.29, 129.49, 129.34, 128.89, 128.69, 128.22, 127.37, 126.96, 125.25, 59.40, 58.36, 42.06, 35.81, 33.78, 27.44. HRMS (ESI): [M+H]<sup>+</sup> calculated 455.1099, found: 455.1098.

**Compound 11.** 7-ADCA (2.14 g, 10 mmol) was dissolved in saturated bicarbonate solution (20 mL) to which phenylacetyl chloride (1.5 mL, 11.3 mmol) dissolved in acetone (10 mL) was added in several portions. The mixture was stirred overnight at room temperature, then acidified to pH 2.0 using 1 M HCl. The precipitate was filtered off and washed with minimum amount of cold water. The crude was purified by reversed-phase prep-HPLC using C18 and an optimal gradient of buffer A (H<sub>2</sub>O 95%, ACN 5%, TFA 0.1%) vs. buffer B (ACN 95%, H<sub>2</sub>O 5%, TFA 0.1%). (85 mg, 75%, based on the purification of ~100 mg of the crude product by prep-HPLC). <sup>1</sup>H-NMR (400 MHz, DMSO-*d*<sub>6</sub>): δ 9.09 (d, *J* = 8.2 Hz, NH, 1H), 7.33-7.21 (m, aromatic H, 5H), 5.60 (dd, *J* = 8.2 Hz, *J* = 4.6 Hz, β-lactam C-H, 1H), 5.03 (d, *J* = 4.7 Hz, β-lactam C-H, 1H), 3.61-3.35 (m, aliphatic H, 4H), 2.03 (s, methyl, 3H), <sup>13</sup>C-NMR (100 MHz, DMSO-*d*<sub>6</sub>): δ 171.44, 164.82, 163.98, 136.33, 130.21, 129.48, 128.68, 126.93, 123.21, 59.33, 57.56, 42.03, 29.40, 19.87. HRMS (ESI): [M+H]<sup>+</sup> calculated: 333.0909, found: 333.0917.

### Enzyme production and purification

NDM-1, VIM-2, and IMP-28 were expressed and purified as described in chapter 2. The procedure for the production of IMP-1 has been reported in previous literature.<sup>13</sup>

### Enzymatic preparation of 6H and 7H

Compound **6** or **7** (2.0 mM each) was incubated with NDM-1 (187 nM) at room temperature in 50 mM HEPES-NaOH, pH 7.2 supplemented with 1  $\mu$ M ZnSO<sub>4</sub> and 0.01% triton X-100. The progress of hydrolysis was monitored by LC-MS (figure 10). After 2 h the conversion was complete, and compounds **6H** and **7H** were separated from the enzyme by spin-filtration (3K filter cutoff, Amicon) at 12000 rpm for 5 min.

### Enzyme inhibition assay

The cephalosporin derivatives were tested for their inhibitory activity against NDM-1, VIM-2 and IMP-28 using the chromogenic substrate nitrocefim. The assay buffer was 50 mM HEPES pH 7.2, supplemented with 1  $\mu$ M ZnSO<sub>4</sub> and 0.01% triton X-100. Briefly, on a flat-bottom polystyrene 96-well microplate NDM-1 (6 nM), VIM-2 (8 nM) IMP-1 (2 nM) or IMP-28 (1 nM) were incubated with various concentrations of the test compounds for 15 min at 25 °C. Nitrocefim (10  $\mu$ M for NDM-1, VIM-2, and IMP-28, 13  $\mu$ M for IMP-1) was added to the wells and absorption at 492 nm was immediately monitored on a TECAN Spark microplate reader over 30 scan cycles. The initial velocity data were used for IC<sub>50</sub> curve-fitting using GraphPad Prism 7.

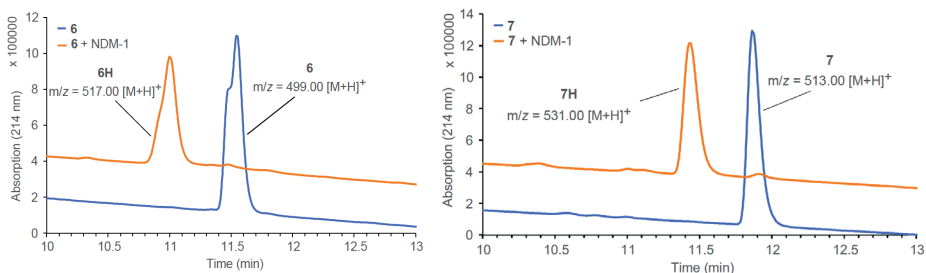


**Figure 10.** LCMS trace of the enzymatic preparation of **6H** and **7H**.

### ***Determination of the kinetic parameters of cephalosporin conjugates***

Hydrolysis of the cephalosporin conjugates was monitored on a Tecan Spark microplate reader using UV-transparent 96-well plates (UV-Star®, Greiner). Various concentrations of the test compounds were dissolved in 50 mM HEPES-NaOH, pH 7.2 supplemented with 1  $\mu$ M ZnSO<sub>4</sub> and 0.01% triton X-100. Followed by the addition of MBLs dissolved in the same buffer, absorption at 260 nm was measured immediately over 30-40 scan cycles at 25 °C. The obtained initial velocity data were plotted against substrate concentration, and  $K_M$  and  $V_{max}$  were determined using Michaelis-Menten fitting model on GraphPad Prism 7.

### ***MIC determination and synergy assays***

Minimum inhibitory concentration (MIC) of the test compounds were determined following the guidelines published by clinical and laboratory standards institute (CLSI) and as described earlier.<sup>9</sup> Synergy between the cephalosporin derivatives and  $\beta$ -lactam antibiotics were evaluated by the following protocol:  $\beta$ -lactam antibiotics dissolved in Mueller-Hinton broth (MHB) with the concentration corresponding to 4 $\times$ MIC was added to polypropylene 96-well microplates and serially diluted (25  $\mu$ L/well). Then each 3 columns received a fixed concentration of the test compounds dissolved in MHB (25  $\mu$ L/well). Multiple concentrations of the test compounds were evaluated this way. Finally, bacterial suspensions grown to the OD<sub>600</sub> of 0.5 were diluted 100x in MHB before adding to the plate (50  $\mu$ L/well). The microplates were then covered with breathable seals and incubated overnight with shaking at 37 °C for 15-20 h. Dipicolinic acid was used as positive control.

### ***Stability analysis in MHB***

The solutions of the test compounds (1.0 mM) in MHB were incubated at 37 °C for 15 h. Then, 100  $\mu$ L of the MHB solution was precipitated by adding to acetonitrile (200  $\mu$ L) supplemented with 2 mM benzocaine, vortexed and centrifuged (12000 rpm, 5 min). The supernatant was analyzed by reversed-phase analytical HPLC using a C<sub>18</sub> column and an optimal gradient of buffer A (H<sub>2</sub>O 95%, ACN 5%, TFA 0.1%) vs. buffer B (ACN 95%, H<sub>2</sub>O 5%, TFA 0.1%). The detector wavelength was set at 254 nm.

**Isothermal titration calorimetry**

The ITC titrations were performed on a PEAQ-ITC calorimeter (Malvern). All the test compounds and zinc sulfate were dissolved in 20 mM Tris-HCl buffer (pH 7.0). The experiments consisted of titrating 2 mM zinc sulfate through 19  $\times$  2.0  $\mu$ L aliquots (except the first aliquot which was 0.4  $\mu$ L) into 200  $\mu$ M solutions of the cephalosporin conjugates incubated with NDM-1 (187 nM) for 2 h at room temperature. Experiments were performed at 25  $^{\circ}$ C with 150 s interval between titrations and reference power was set at 10.0  $\mu$ cal/s. Data was analyzed using Microcal PEAQ-ITC analysis software. In separate experiments, upon the titration of zinc sulfate into the solutions of cephalosporin conjugates or NDM-1, no binding interaction was observed (figure 11).

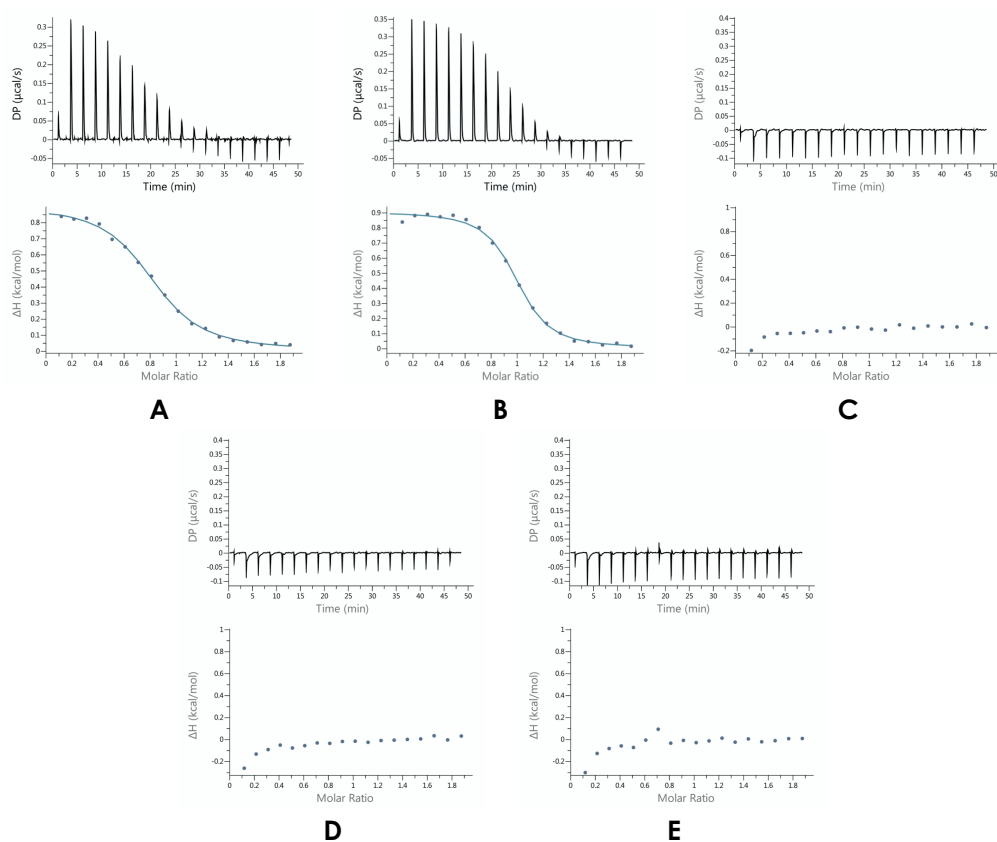


**Figure 11.** Thermograms of zinc sulphate (2 mM) titrated in a 0.2 mM solution of **6** (A) and **7** (B) incubated with NDM-1 (187 nM) for 2 h at room temperature. Control experiments include: **C.** zinc sulphate (2 mM) titrated to **6** (0.2 mM), **D.** zinc sulphate (2 mM) titrated to **7** (0.2 mM), and **E.** zinc sulphate (2 mM) titrated to NDM-1 (187 nM).

***NMR-based monitoring of the enzymatic hydrolysis***

The cephalosporin conjugates dissolved in DMSO- $d_6$  were diluted in deuterated PBS (pH 7.4) or deuterated 20 mM HEPES (pH 7.4) each supplemented with 1  $\mu$ M ZnSO<sub>4</sub>. IMP-28 was added to the solution and the final concentration of the enzyme, test compounds and DMSO were 320 nM, 1 mg/mL and 1% respectively. Following incubation at 25 °C, the <sup>1</sup>H-NMR spectra were measured on a Bruker 400 MHz spectrometer in various time points.

***LCMS-based monitoring of the enzymatic hydrolysis***

The cephalosporin conjugates were dissolved in 20 mM HEPES buffer (pH 7.2) supplemented with 1  $\mu$ M ZnSO<sub>4</sub> and 0.01% triton X-100. IMP-28 was added to the solution and the final concentration of the enzyme, test compounds and DMSO were 320 nM, 1 mg/mL and 1% respectively. Following incubation at 25 °C and in different time points, the solution was diluted in ACN (1:2 v/v) and centrifuged at 12000 rpm for 5 min. The supernatant was analyzed on an LCMS-8040 triple quadrupole liquid chromatograph mass spectrometer (LC-MS/MS, Shimadzu) using a C18 column (3  $\mu$ m, 3.0×150 mm, Shimadzu) and a gradient of 5-100% pure acetonitrile against 0.5% formic acid.

**Acknowledgements**

The enzyme experiments were made possible thanks to the contributions of Diego Pesce to design the plasmid construct of IMP-28, Vida Mashayekhi to express and purify NDM-1, VIM-2, and IMP-28, and Nicola Wade to express and purify IMP-1.

## References

- 1 S. M. Drawz and R. A. Bonomo, *Clin. Microbiol. Rev.*, 2010, **23**, 160–201.
- 2 R. A. Bonomo, E. M. Burd, J. Conly, B. M. Limbago, L. Poirel, J. A. Segre and L. F. Westblade, *Clin. Infect. Dis.*, 2017, **66**, 1290–1297.
- 3 R. P. McGeary, D. T. Tan and G. Schenk, *Future Med. Chem.*, 2017, **9**, 673–691.
- 4 P. W. Groundwater, S. Xu, F. Lai, L. Váradi, J. Tan, J. D. Perry and D. E. Hibbs, *Future Med. Chem.*, 2016, **8**, 993–1012.
- 5 K. H. M. E. Tehrani and N. I. Martin, *Medchemcomm*, 2018, **9**, 1439–1456.
- 6 W. Fast and L. D. Sutton, *Biochim. Biophys. Acta - Proteins Proteomics*, 2013, **1834**, 1648–1659.
- 7 L. C. Ju, Z. Cheng, W. Fast, R. A. Bonomo and M. W. Crowder, *Trends Pharmacol. Sci.*, 2018, **39**, 635–647.
- 8 C. M. Rotondo and G. D. Wright, *Curr. Opin. Microbiol.*, 2017, **39**, 96–105.
- 9 K. H. M. E. Tehrani and N. I. Martin, *ACS Infect. Dis.*, 2017, **3**, 711–717.
- 10 S. Hanessian and J. Wang, *Can. J. Chem.*, 1993, **71**, 896–906.
- 11 H. Feng, J. Ding, D. Zhu, X. Liu, X. Xu, Y. Zhang, S. Zang, D.-C. Wang and W. Liu, *J. Am. Chem. Soc.*, 2014, **136**, 14694–14697.
- 12 R. Keltjens, S. K. Vadiel, E. De Vroom, A. J. H. Klunder and B. Zwanenburg, *European J. Org. Chem.*, 2001, **2001**, 2529–2534.
- 13 S. S. van Berkel, J. Brem, A. M. Rydzik, R. Salimraj, R. Cain, A. Verma, R. J. Owens, C. W. G. Fishwick, J. Spencer and C. J. Schofield, *J. Med. Chem.*, 2013, **56**, 6945–6953.





## Chapter 6

# Biochemical evaluation of FLC-1, a novel carbapenemase encoded by an *Enterobacter cloacae* complex isolated from food products

Parts of this chapter have been published in:

Brouwer, M. S. M., Tehrani, K. H. M. E., Rapallini, M., Geurts, Y., Kant, A., Harders, F., Mashayekhi, V., Martin, N. I., Bossers, A., Mevius, D. J., Wit, B., and Veldman, K. T. (2019) Novel carbapenemases FLC-1 and IMI-2 encoded by an enterobacter cloacae complex isolated from food products. *Antimicrob. Agents Chemother.* **63**, e02338-18.

## 1. Introduction

To combat antimicrobial resistance (AMR) effectively, it is important to monitor reservoirs that may be sources of transmission to humans. Relevant reservoirs are those that may be attributed to the AMR genes found in the general population and patients. Seafood has been implicated as a potential source of AMR genes entering populations when several aquatic bacteria carrying carbapenemase genes were identified in seafood imported from Southeast Asia.<sup>1,2</sup> Often, these genes are chromosomally located in nonpathogenic aquatic bacterial species, limiting them as relevant threats for the general population.<sup>3</sup> However, more recent studies screening seafood imported from Southeast Asia have found carbapenemases encoded in human pathogens or on conjugative plasmids.<sup>4-6</sup> As such, seafood imported from countries with high carbapenemase prevalence may need to be included in monitoring programs.

Proteins with carbapenemase activity fall into the three major Ambler classes A, B, and D  $\beta$ -lactamases.<sup>7</sup> Genes of these classes have been described on mobile genetic elements, such as plasmids and chromosomally integrated elements, which adds to the concerns regarding these genes because they facilitate the spread of these genes among both commensal and pathogenic bacteria.<sup>6,8,9</sup> The family of *Enterobacteriaceae* consists of many commensal, opportunistic, and infectious species that can readily exchange genetic material. The organisms are collectively referred to as carbapenemase-producing *Enterobacteriaceae* when they have acquired and express one of these genes.

Recently, *Enterobacter cloacae* complex and *Vibrio cholerae* isolates have been described with a distinctive phenotype of hydrolyzing penicillins, aztreonam, and carbapenems but not extended-spectrum cephalosporins.<sup>10</sup>

In the present chapter, the biochemical evaluations on a newly identified class A carbapenemase named FRI-like carbapenemase-1 (FLC-1) will be discussed.

## 2. Results and discussion

In March 2017, our collaborators from Wageningen Bioveterinary Research isolated an *E. cloacae* complex isolate, designated 3442, from a sample of frozen vannamei white shrimp (*Litopenaeus vannamei*) originating in India. The isolate exhibited an unusual phenotype, *i. e.*, resistant to carbapenems (meropenem, ertapenem, and imipenem) and susceptible to extended-spectrum cephalosporins (cefotaxime, ceftazidime, and cefepime) (table 1).

Sequencing analyses confirmed the presence of a 93 kb plasmid later named p3442-FLC-1 which carries a novel carbapenemase with close sequence similarity to *bla*<sub>FRI-1</sub>.<sup>10</sup> It was hypothesized that the *bla*<sub>FRI-1</sub>-related gene may have carbapenemase activity. Because the plasmid carrying the gene could not be transformed or conjugated into *E. coli* cells, the gene was cloned into an arabinose-inducible expression vector, pBAD-FLC, and expressed in *E. coli* LMG194.<sup>11</sup> The MIC of *E. coli* LMG194 pBAD-FLC was determined by broth microdilution after an overnight culture in RPMI medium plus 0.2% glucose followed by dilution in Mueller-Hinton broth containing 0.2% arabinose and incubation at 37 °C for 1 h to enable expression to start. Standard protocols were followed thereafter and *E. coli* LMG194 and ATCC 25922 were used as negative controls. *E. coli* LMG194 pBAD-FLC showed resistance against carbapenems and extended-spectrum cephalosporins (table 1). This new FRI variant was concluded to be a carbapenemase and further referred to as FRI-like carbapenemase-1 (*bla*<sub>FLC-1</sub>).

Multiple sequence alignments were made comparing FLC-1 with several members of plasmid-encoded Ambler class A carbapenemases. All conserved residues among class A β-lactamases were present. The most related protein family was that of the French imipenemase (FRI), with 82% identity to FRI-1 and 87% to FRI-5.<sup>10,12,13</sup>

The soluble protein fractions of arabinose-induced *E. coli* LMG194 pBAD-FLC and *E. coli* LMG194 were prepared as described in the experimental section, and their biochemical properties were evaluated. Analysis of the periplasmic protein fractions by SDS-PAGE showed induction of a protein between 25 and 35 kDa as expected (FLC-1 molecular weight, ~33 kDa; see figure 1).

**Table 1.** Susceptibility data (MIC, µg/mL) of *E. cloacae* complex 3442, *E. coli* recipient, and transformant of pBAD-FLC.

Antibiotic	<i>E. cloacae</i> 3442	<i>E. coli</i> LMG194 pBAD-FLC	<i>E. coli</i> LMG194
Ampicillin	>64	>64	4
Cefepime	0.12	0.5	0.12
Cefotaxime	<=0.25	2	<=0.25
Cefotaxime/ clavulanic acid	0.25/4	0.12/4	<=0.06/4
Cefoxitin	64	8	8
Ceftazidime	<=0.5	1	0.5
Ceftazidime/ clavulanic acid	<=0.12/4	0.25/4	0.25/4
Ertapenem	>2	>2	<=0.015
Imipenem	>16	16	0.25
Meropenem	>16	4	<=0.03
Temocillin	4	16	8

The initial testing of the cytoplasmic fractions of *E. coli* containing the plasmid showed hydrolysis of nitrocefin, while cytoplasmic fractions of *E. coli* lacking the plasmid did not (figure 2a). Expanding these measurements to several  $\beta$ -lactam antibiotics over time allowed for the determination of kinetic parameters of the protein-expressing cells (table 2). The enzymatic activity of FLC-1 clearly showed greater efficiency of the enzyme toward carbapenems than toward cephalosporins (as evident by the relative  $k_{cat}/K_M$  values) (table 2), with activity against ceftazidime and cefepime below the threshold of detection. Using nitrocefin as the substrate, the inhibition of FLC-1 enzymatic activity by clavulanic acid was tested, and the 50% inhibitory concentration ( $IC_{50}$ ) was calculated ( $1.97 \pm 0.09 \mu M$ ) (figure 2b).

Class A carbapenemases include members of GES, KPC, SME, and IMI/NMC-A enzymes plus SFC-1 and SHV-38.<sup>14</sup> With the exception of GES-1, most class A carbapenemases demonstrate higher carbapenemase activity of various degrees relative to extended-spectrum  $\beta$ -lactamases.<sup>14–17</sup> FRI-1 is the closest member of the class A carbapenemases relative to FLC-1 and was found to be at least 15 times more efficient in degrading carbapenems than extended-spectrum cephalosporins.<sup>10</sup> Here, we report a similar substrate preference for the FLC-1 enzyme, which hydrolyzes imipenem, ertapenem, and meropenem with greater efficiency than the cephalosporins tested (table 2).



**Figure 1.** SDS-PAGE gel of *E. coli* LMG-194 pBAD-FLC. Periplasmic protein fractions were loaded before induction (lane A) and after 2 hr induction with 0.2% arabinose (lane B).

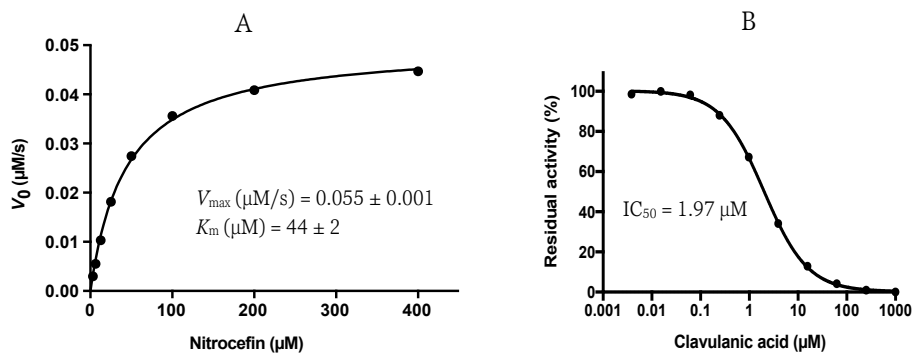


**Figure 2.** Inhibitory effect of clavulanic acid on FLC-1 enzymatic activity. **(A)** Michaelis-Menten plot of nitrocefin using 2 µg/mL of FLC-1 protein fraction. **(B)** Representative dose-response curve of FLC-1 inhibited by clavulanic acid.  $IC_{50} = 1.97 \mu\text{M}$  ( $\pm 0.09$ ). Nitrocefin was used as chromogenic substrate.

**Table 2.** Kinetic parameters determined for the cytoplasmic fraction of *E. coli* LMG-194 producing FLC-1.

Antibiotic	[Protein] (µg.mL) <sup>a,b</sup>	$K_M$ (µM)	$V_{\text{max}}/\mu\text{g protein}^c$	Relative $k_{\text{cat}}/K_M$
Ampicillin	5.53	$1649 \pm 174.2$	$(1490 \pm 70) \times 10^{-3}$	1.00
Meropenem	100	$32.4 \pm 9.3$	$(2.05 \pm 0.14) \times 10^{-3}$	0.07
Imipenem	17.68	$177.2 \pm 12.5$	$(48.61 \pm 1.40) \times 10^{-3}$	0.30
Ertapenem	44.21	$29.6 \pm 11.7$	$(6.34 \pm 0.67) \times 10^{-3}$	0.24
Cefotaxime	106.1	$377.1 \pm 110.6$	$(7.85 \pm 1.25) \times 10^{-3}$	0.02
Ceftazidime		ND <sup>d</sup>	ND <sup>d</sup>	
Cefepime		ND <sup>d</sup>	ND <sup>d</sup>	

<sup>a</sup>Protein concentration of the cytoplasmic fraction.

<sup>b</sup>The *E. coli* strain producing FLC-1 and the non-transformed strain were used to prepare cytoplasmic fractions. The highest tested concentration of both preparations was 176.83 µg/mL. None of the tested antibiotics were hydrolyzed by the non-transformed *E. coli* cytoplasmic fraction.

<sup>c</sup>Expressed as µM/s/µg of protein.

<sup>d</sup>Not determinable.

### 3. Conclusion

To control AMR and retain effective use of antimicrobials in human and veterinary medicine, a complete and correct overview of the impact that these human and animal reservoirs have on each other is essential. *bla<sub>FLC-1</sub>* was detected here in a sample of raw shrimp from India, but members of the FRI family, to which FLC is most closely related, and IMI, NMC-a, and SME have been described in a various global reservoirs.<sup>8,10,12,13,16,18</sup> Reliable databases of acquired resistance genes and point mutations leading to resistance are essential to determine the gene responsible for a particular resistant phenotype. The complete analysis presented here of the novel carbapenemase FLC-1 in its complete genetic carrier context will aid in the future for the recognition of its gene, *bla<sub>FLC-1</sub>*, and related carbapenemases.

### 4. Experimental section

#### *Preparation of bacterial cytoplasmic fractions*

Cells were grown in YT2x (0.1% glucose, 50 µg/mL kanamycin). Upon reaching OD<sub>600</sub> = 0.65, arabinose (0.2% final concentration) was added and after 2 h the cells were harvested by centrifugation at 6000 rpm (20 min, 4 °C). Pellets were resuspended in PBS (0.05% Triton X-100, 150 mM NaCl pH 7.4) and cells disrupted by two freeze-thaw cycles and three 30-second sonication cycles. Cell debris was removed by centrifugation at 12000 rpm (20 min, 4 °C). Protein content of the supernatant was determined by Pierce™ BCA protein assay kit following the manufacturer's protocol.

### Kinetic experiments

Hydrolysis of various  $\beta$ -lactam antibiotics was monitored with a Spark microplate reader (Tecan) at 23 °C using 96-well UV-Star microplates. Phosphate-buffered saline (0.01% Triton X-100, pH 7.4) was used as the assay buffer. The extinction coefficients for the  $\beta$ -lactam antibiotics studied were  $\Delta\epsilon_{235} = 900 \text{ M}^{-1}\text{cm}^{-1}$  for ampicillin,  $\Delta\epsilon_{297} = 10940 \text{ M}^{-1}\text{cm}^{-1}$  for meropenem,  $\Delta\epsilon_{295} = 11500 \text{ M}^{-1}\text{cm}^{-1}$  for imipenem,  $\Delta\epsilon_{300} = 6920 \text{ M}^{-1}\text{cm}^{-1}$  for ertapenem, and  $\Delta\epsilon_{264} = 7250 \text{ M}^{-1}\text{cm}^{-1}$  for cefotaxime. To calculate kinetic parameters, including  $K_M$  and  $V_{max}$ , the measured initial velocities of the hydrolysis of the substrates were fit into the Michaelis-Menten equation using GraphPad Prism 7 software (see figure 3 for Michaelis-Menten curves).

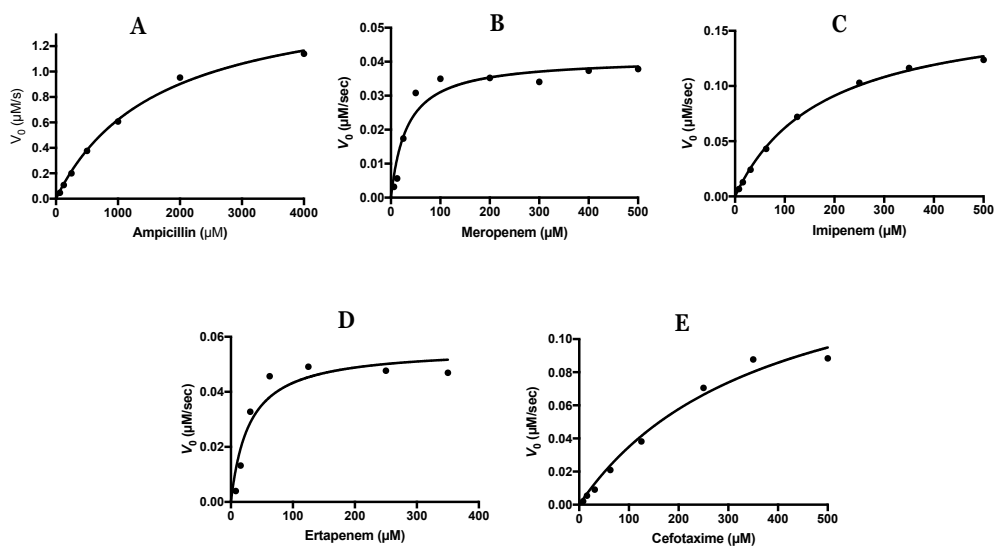


**Figure 3.** Michaelis-Menten plots of FLC-mediated hydrolysis of selected  $\beta$ -lactam antibiotics: (A) Ampicillin, (B) Meropenem, (C) Imipenem, (D) Ertapenem, (E) Cefotaxime.



### ***IC<sub>50</sub> determination***

The inhibitory activity of clavulanic acid against FLC-1 fraction was assessed using nitrocefin as substrate. On a polystyrene 96-well plate and using the assay buffer described above, FLC-1 fraction (2 µg/mL) was incubated with clavulanic acid ranging from 1000 to 0.004 µM for 15 min at 25 °C. Nitrocefin with the concentration corresponding to  $K_M$  value (44 µM) was added to all the wells and absorption at 492 nm was monitored over 30 scan cycles. The initial velocity data was normalized using nitrocefin with enzyme in the absence of inhibitor as 100% activity and nitrocefin in the absence of enzyme as 0% activity.  $IC_{50}$  curve-fitting was performed on Log(concentration) vs. Activity (%) data using GraphPad Prism 7 software.

### **Acknowledgements**

Isolation and characterization of FLC-1 gene was carried out by Dr Mike Brouwer and his colleagues. FLC-1 protein fraction was prepared by Vida Mashayekhi.

## References

- 1 J. E. Rubin, S. Ekanayake and C. Fernando, *Emerg. Infect. Dis.*, 2014, **20**, 1264–1265.
- 2 B. J. Morrison and J. E. Rubin, *PLoS One*, 2015, **10**, e0126717.
- 3 D. Ceccarelli, A. van Essen-Zandbergen, K. T. Veldman, N. Tafro, O. Haenen and D. J. Mevius, *Antimicrob. Agents Chemother.*, 2017, **61**, e01013-16.
- 4 C. S. Mangat, D. Boyd, N. Janecko, S.-L. Martz, A. Desruisseau, M. Carpenter, R. J. Reid-Smith and M. R. Mulvey, *Antimicrob. Agents Chemother.*, 2016, **60**, 1819–1825.
- 5 N. Roschanski, S. Guenther, T. T. T. Vu, J. Fischer, T. Semmler, S. Huehn, T. Alter and U. Roesler, *Euro Surveill.*, 2017, **22**, 17–00032.
- 6 M. S. M. Brouwer, M. Rapallini, Y. Geurts, F. Harders, A. Bossers, D. J. Mevius, B. Wit and K. T. Veldman, *Antimicrob. Agents Chemother.*, 2018, **62**, e00398-18.
- 7 P. Nordmann, T. Naas and L. Poirel, *Emerg. Infect. Dis.*, 2011, **17**, 1791–1798.
- 8 D. A. Boyd, L. F. Mataseje, R. Davidson, J. A. Delport, J. Fuller, L. Hoang, B. Lefebvre, P. N. Levett, D. L. Roscoe, B. M. Willey and M. R. Mulvey, *Antimicrob. Agents Chemother.*, 2017, **61**, e02578-16.
- 9 T. R. Walsh, M. A. Toleman, L. Poirel and P. Nordmann, *Clin. Microbiol. Rev.*, 2005, **18**, 306 LP – 325.
- 10 L. Dortet, L. Poirel, S. Abbas, S. Oueslati and P. Nordmann, *Antimicrob. Agents Chemother.*, 2015, **59**, 7420–7425.
- 11 L. M. Guzman, D. Belin, M. J. Carson and J. Beckwith, *J. Bacteriol.*, 1995, **177**, 4121–4130.
- 12 D. Meunier, J. Findlay, M. Doumith, D. Godoy, C. Perry, R. Pike, F. Gronthoud, T. Shryane, L. Poirel, W. Welfare, N. Woodford and K. L. Hopkins, *J. Antimicrob. Chemother.*, 2017, **72**, 2478–2482.
- 13 H. Kubota, Y. Uwamino, M. Matsui, T. Sekizuka, Y. Suzuki, R. Okuno, Y. Uchitani, T. Ariyoshi, W. Aoki, S. Suzuki, M. Kuroda, T. Shinkai, K. Yokoyama, K. Sadamasu, T. Funakoshi, M. Murata, N. Hasegawa and S. Iwata, *J. Antimicrob. Chemother.*, 2018, **73**, 2969–2972.
- 14 J. Walther-Rasmussen and N. Høiby, *J. Antimicrob. Chemother.*, 2007, **60**, 470–482.
- 15 A. M. Queenan and K. Bush, *Clin. Microbiol. Rev.*, 2007, **20**, 440–458.
- 16 B. A. Rasmussen, K. Bush, D. Keeney, Y. Yang, R. Hare, C. O’Gara and A. A. Medeiros, *Antimicrob. Agents Chemother.*, 1996, **40**, 2080–2086.
- 17 K. L. Hopkins, J. Findlay, M. Doumith, B. Mather, D. Meunier, S. D’Arcy, R. Pike, N.

- Mustafa, R. Howe, M. Wootton and N. Woodford, *J. Antimicrob. Chemother.*, 2017, **72**, 2129–2131.
- 18 T. Naas, L. Vandel, W. Sougakoff, D. M. Livermore and P. Nordmann, *Antimicrob. Agents Chemother.*, 1994, **38**, 1262–1270.

# Addendum

Summary

Samenvatting

*Curriculum vitae*

List of publications

Afterword

## Summary

If left unmitigated, antibiotic resistance will continue its path to become a global catastrophe in the 21<sup>st</sup> century.  $\beta$ -Lactams are the most prescribed group of antibiotics making modern medicine and many surgical interventions possible. However, infections, especially those caused by gram-negative pathogens are becoming increasingly difficult to treat largely due to the presence of  $\beta$ -lactamases. A number of innovative drugs have been developed over the past decades to rescue the efficacy of  $\beta$ -lactams while treating  $\beta$ -lactamase-producing bacterial infections. However, these agents only inhibit serine-type  $\beta$ -lactamases (SBLs, Ambler class A, C, and D). This renders  $\beta$ -lactams, including the last-resort carbapenems, clinically ineffective against the infections caused by the bacteria that express the rapidly emerging metallo- $\beta$ -lactamases (MBLs, Ambler class B). There is an unmet and urgent need to add inhibitors that target MBLs to our antibiotic arsenal.

The  $\beta$ -lactamase inhibitors approved by the FDA or being evaluated in clinical trials have been reviewed in **chapter 1**. While the earlier generations of SBL inhibitors such as clavulanic acid, sulbactam, and tazobactam were all  $\beta$ -lactam derivatives themselves, discovery of avibactam (a diazabicyclooctane) and vaborbactam (a cyclic boronate) broadened the chemical space available to develop potent and broad-spectrum  $\beta$ -lactamase inhibitors. Interestingly, multiple studies have shown that certain cyclic boronates can mimic the intermediates formed when  $\beta$ -lactams are attacked by both SBLs and MBLs. This provides a valuable opportunity in the pursuit of a “pan-spectrum”  $\beta$ -lactamase inhibitor. Taniborbactam, which is currently in a phase III clinical trial is a cyclic boronate optimized to inhibit the clinically important  $\beta$ -lactamases of all 4 Ambler classes (figure 1). MBLs are a diverse group of zinc metallo-enzymes capable of hydrolyzing penicillins, cephalosporins, and also carbapenems. The majority of the reported MBL-inhibitors either act by zinc-sequestration or binding the active site zinc thereby

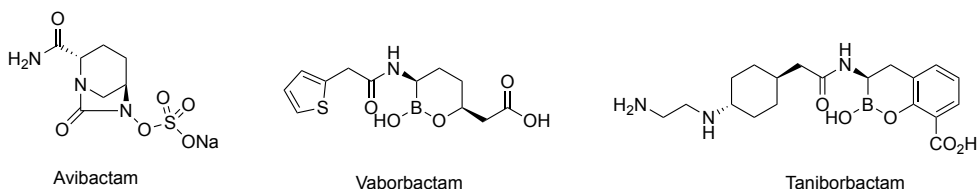


**Figure 1.** Structures of approved SBL inhibitors avibactam, and vaborbactam, and the SBL-MBL inhibitor taniborbactam.

forming a ternary complex. Since zinc is essential for the hydrolytic activity of MBLs, many chelating agents have been applied for the phenotypic screening and biochemical characterization of  $\beta$ -lactam resistant bacterial isolates. Other inhibitors containing a zinc-binding moiety include thiols, diacids, and picolinic acid derivatives (figure 2). The following 4 chapters describe our efforts to identify new compounds with ability to *a.* inhibit clinically relevant MBLs of the NDM, VIM, and IMP families, and *b.* restore the activity of  $\beta$ -lactams in cell-based phenotypic assays. This was followed up by our attempts to use a prodrug approach to improve the druggability of the MBL-inhibitors.

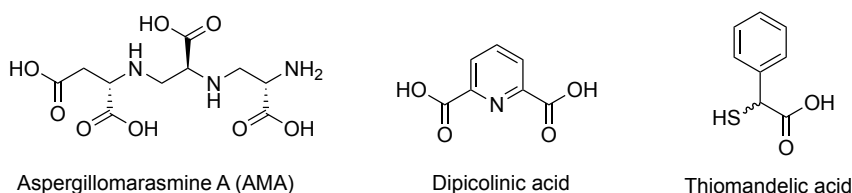


**Figure 2.** Zinc-chelators, picolinic acid derivatives, and thiols represented by AMA, dipicolinic acid, and thiomandelic acid respectively, all reported as MBL inhibitors.

In **chapter 2**, we describe our study leading to the identification of *N*-(phosphonomethyl)iminodiacetic acid (PMIDA) and nitrilotriacetic acid (NTA) as potent inhibitors of NDM-1 (figure 3). Building on literature reports in which commonly used buffering agents were reported to possess MBL inhibitory activity, we screened a larger group of buffering agents known to have metal-binding affinity. Among the tested compounds, PMIDA and NTA exhibited the highest potency against purified NDM-1 and VIM-2, with moderate to weak activity against IMP-28. The results of Zn-dependency studies and isothermal titration calorimetry (ITC) assays shed light on the inhibitory mechanism of the most potent compounds, showing that they act primarily by chelating the zinc ions crucial for the catalytic activity of the MBLs. Our data do not support the possibility of the inhibitors forming a complex with the metallo-enzyme itself. Phenotypic screenings revealed the strong synergistic relationship between PMIDA/NTA and meropenem when tested against a large panel of carbapenem-resistant gram-negative clinical isolates. We suggest that such readily available small molecules can serve as biochemical tool compounds for enzymatic and phenotypic studies of MBLs, as well as leads for further optimization on the path towards clinical development.

	PMIDA	NTA
$IC_{50}$ ( $\mu\text{M}$ ) against NDM-1	0.91	1.3
Zn dissociation constant ( $K_d$ , nM)	56	121

**Figure 3.** PMIDA and NTA are potent NDM-1 inhibitors and strong zinc-binders.

**Chapter 3**, describes additional efforts to identify MBL inhibitors by screening a series of small-molecule aminocarboxylic acids related to the secondary metabolites produced by *Aspergillus* spp. including aspergillomarasmine A (AMA) and aspergillomarasmine B (AMB), as well as the chelating agent ethylenediamine-*N,N'*-disuccinic acid (EDDS, figure 4). The various analogs synthesized in Prof. Gerrit Poelarends' group were first tested for their inhibition of the NDM-1 enzyme. The promising  $IC_{50}$  values of some of the analogs prompted us to evaluate their Zn-binding affinity using ITC. There was a clear correlation between Zn-binding affinity and inhibitory activity of the aminocarboxylic acids. Notably, the 2 methylene units between the aspartate fragments of EDDS were found to be the optimal length for maximum zinc-binding and NDM-1 inhibition. Interestingly, some of the potent inhibitors identified did not exhibit synergy with meropenem when tested against an NDM-1 producing *E. coli* isolate, most probably due to sub-optimal cellular accumulation. On the other hand, a methyl substituted EDDS, as well as a methylene homolog of AMB, were among the most potent synergizers rescuing meropenem at 100  $\mu\text{M}$ .

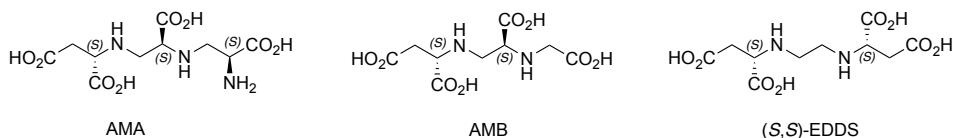


**Figure 4.** Previously reported aminocarboxylic acids as potent NDM-1 inhibitors.

In **chapter 4**, another group of small-molecule MBL inhibitors (*i.e.* thiols) were evaluated. Focusing on a series of previously reported thiol-containing MBL inhibitors, we reported the first checkerboard synergy assays and zinc-binding affinity studies, and assessed the chemical stability of these compounds. In the synergy experiments, thiomandelic acid and 2-mercapto-3-phenylpropionic acid (compounds **3** and **4** respectively in chapter 4, figure 5) largely reduced the MIC of meropenem and cefoperazone when tested against a panel of MBL-producing gram-negative clinical isolates. The lack of synergy against KPC- and OXA-producing isolate indicates that the activity of the thiols is MBL-specific. Despite their strong synergistic activity and zinc-binding affinity, we found that thiols **3** and **4** suffer from poor stability in the assay medium. With a half-life of *ca.* 5 hours, they oxidize to their corresponding disulfides which in turn exhibit moderate to no synergistic activity.

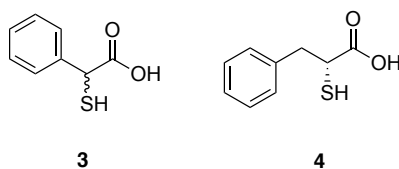


**Figure 5.** Thiomandelic acid (**3**) and 2-mercapto-3-phenylpropionic acid (**4**).

**Chapter 5**, describes the synthesis and bioactivity evaluation of a series of cephalosporin-thiol conjugates which were designed to act as prodrugs of the thiols described in chapter 4. Following our findings on the poor stability and specificity of these thiols and given the well-known hydrolysis mechanism of cephalosporins, we designed and synthesized a small group of cephalosporin thiol conjugates (compounds **5-7** in chapter 5, figure 6). The IC<sub>50</sub> assays against IMP-1, IMP-28, NDM-1 and VIM-2 revealed the potent activity of compounds **6** and **7** with selectivity towards IMP enzymes. The same trend was observed in synergy assays against MBL-producing gram-negative bacterial isolates where **6** and **7** largely reduced the MIC of meropenem against the IMP-producing bacteria. Despite the promising activity data, mechanistic studies using <sup>1</sup>H-NMR and LC-MS indicated that exposure of the cephalosporin conjugates to IMP-28 does not lead to the expected release of the small-molecule thiols. This observation prompted us to determine the mode of action of the cephalosporin conjugates. In doing so, a structure-activity relationship analysis of compound **6** was performed by synthesizing and testing a series of structural variants. The bioactivity data obtained pointed towards the contribution of both phenyl and carboxylate residues of compound **6** to its potency. Secondly, we



determined the kinetic parameters of the MBL-mediated hydrolysis of the synthesized cephalosporins. The calculated catalytic efficiency values suggest slow substrate turn-over as the inhibitory mechanism of compounds **6** and **7**. Finally, the bioactivity evaluation of the partially hydrolyzed products of **6** and **7** (i.e. **6H** and **7H**) revealed that IMP enzymes can be inhibited by both substrates **6** and **7** as well as their hydrolysis products **6H** and **7H**.

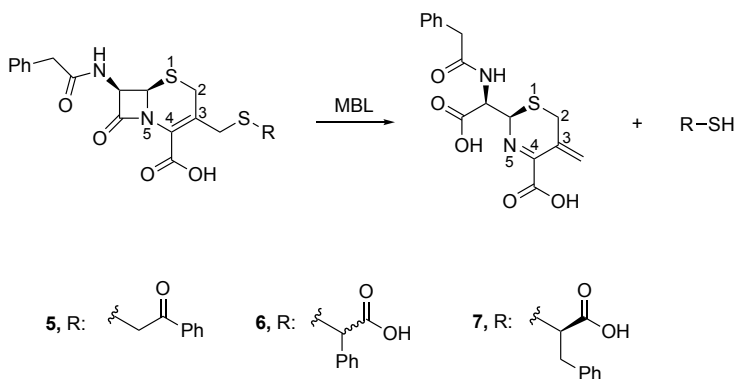


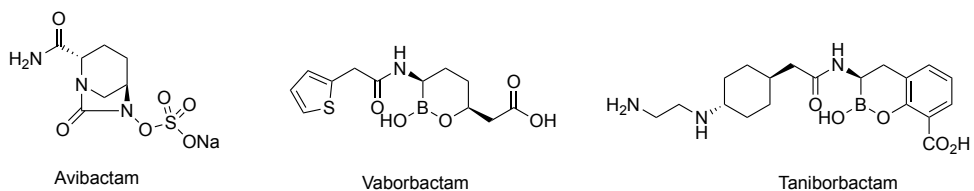
**Figure 6.** The cephalosporin conjugates hypothesized to release the thiol MBL-inhibitors after MBL-mediated hydrolysis.

**Chapter 6** was the result of a collaborative project with Dr. Mike Brouwers from Wageningen Bioveterinary Research to evaluate the enzymatic activity of a newly discovered class A carbapenemase. The enzyme, named FLC-1 (FRI-like carbapenemase-1), was originally identified in *E. cloacae* isolated through the screening of food products imported to The Netherlands. After transformation of *E. coli* with the FLC-1 plasmid and arabinose-induced over-expression, the protein fraction of the bacterial culture was prepared and used for the determination of kinetic parameters. The FLC-1 fraction demonstrated preference for hydrolyzing the tested carbapenems over third-generation cephalosporins as indicated by higher catalytic efficiency values. This preference was mirrored by the MIC data previously determined where the transformed *E. coli* showed higher resistance to carbapenems vs. third generation cephalosporins. We also found that FLC-1 is inhibited by clavulanic acid with an  $\text{IC}_{50}$  value of  $1.97 \mu\text{M}$ .

## Samenvatting

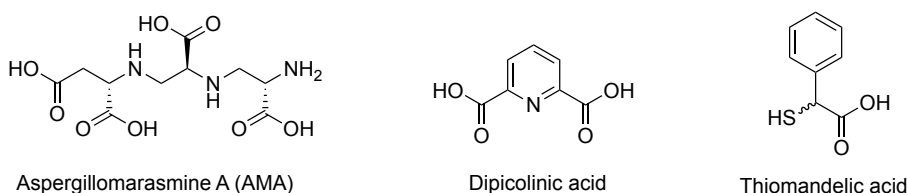
Als de antibioticaresistentie niet wordt aangepakt zal dat in de 21e eeuw een wereldwijde catastrofe tot gevolg hebben.  $\beta$ -Lactammen zijn de meest voorgeschreven groep antibiotic.  $\beta$ -Lactammantibiotika maken de moderne geneeskunde en vele chirurgische ingrepen mogelijk. Echter, infecties, vooral die veroorzaakt door gram-negatieve ziekteverwekkers, worden steeds moeilijker te behandelen, vooral door de aanwezigheid van  $\beta$ -lactamasen. In de afgelopen decennia is een aantal innovatieve geneesmiddelen ontwikkeld om de werkzaamheid van  $\beta$ -lactammen te herstellen bij de behandeling van  $\beta$ -lactamase-producerende bacteriële infecties. Deze middelen blokkeren echter alleen serine-type  $\beta$ -lactamasen (SBL's, Ambler klasse A, C en D). Dit maakt  $\beta$ -lactammen, inclusief de last-resort carbapenems, klinisch ineffectief tegen de infecties die worden veroorzaakt door de bacteriën die de snel opkomende metallo- $\beta$ -lactamasen aanmaken (MBL's, Ambler klasse B). Er is een on vervulde en dringende behoefte naar remmers die gericht zijn op MBL's toe te voegen aan ons antibiotica-arsenaal.

De  $\beta$ -lactamase-remmers die zijn goedgekeurd door de FDA of die worden geëvalueerd in klinische trials, worden beschreven in **hoofdstuk 1**. Eerdere generaties SBL-remmers zoals clavulaanzuur, sulbactam en tazobactam waren allemaal  $\beta$ -lactamderivaten. De ontdekking van avibactam (een diazabicyclooctaan) en vaborbactam (een cyclisch boronaat) hebben de beschikbare chemische ruimte voor de ontwikkeling van krachtige en breed-spectrum  $\beta$ -lactamaseremmers verruimd. Interessant is dat meerdere studies hebben aangetoond dat bepaalde cyclische boronaten de tussenproducten kunnen nabootsen die gevormd worden wanneer  $\beta$ -lactammen worden aangevallen door zowel SBL's als MBL's. Dit biedt een waardevolle kans in het streven naar een 'pan-spectrum'  $\beta$ -lactamaseremmer. Taniborbactam dat zich momenteel in een fase III klinische studie bevindt, is een cyclisch boronaat dat geoptimaliseerd is om klinisch relevante  $\beta$ -lactamasen te remmen van alle 4 Ambler klassen (figuur 1). MBL's zijn een diverse groep van zinkafhankelijke enzymen die in staat zijn om



**Figuur 1.** Structuur van de goedgekeurde SBL-remmers avibactam, en vaborbactam, en de SBL-MBL-remmer taniborbactam.

penicillines, cefalosporines en ook carbapenems te hydrolyseren. De meerderheid van de gerapporteerde MBL-remmers werken door zink-sequestratie of door het binden van zink in de active site waarbij een ternair complex vormt. Aangezien zink essentieel is voor de hydrolytische activiteit van MBL's, worden voor fenotypische screening en biochemische karakterisering van  $\beta$ -lactamresistente bacteriële isolaten vaak chelatoren gebruikt. Andere remmers die een zinkbindend motief bevatten zijn onder andere thiolen, dizuren en picolinezuurderivaten (figuur 2). De volgende 4 hoofdstukken beschrijven onze inspanningen om nieuwe verbindingen te identificeren met het vermogen om *a.* klinisch relevante MBL's van de NDM, VIM en IMP-families te remmen, en *b.* de activiteit van  $\beta$ -lactamantibiotica in fenotypische cel assays te herstellen. Dit werd opgevolgd door onze pogingen om een prodrugsbenadering te gebruiken om de medicijneigenschappen van de MBL-remmers te verbeteren.



**Figuur 2.** Zink-chelatoren, picolinezuurderivaten en thiolen vertegenwoordigd door respectievelijk AMA, dipicolinezuur en thiomandelzuur.

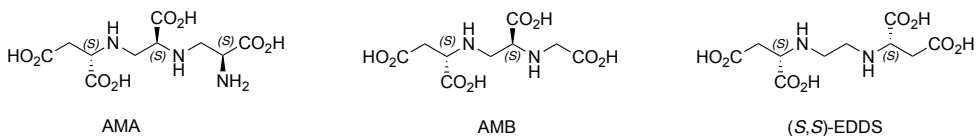
In **hoofdstuk 2** beschrijven we onze studie die heeft geleid tot de identificatie van *N*-(fosfonomethyl)iminodiazijnzuur (PMIDA) en nitrilotriazijnzuur (NTA) als krachtige remmers van NDM-1 (figuur 3). We hebben een grotere groep buffers gescreend waarvan bekend is dat ze metaalbindende eigenschappen hebben. Van de geteste verbindingen waren PMIDA en NTA het meest actief tegen gezuiverde NDM-1 en VIM-2, met een matige tot zwakke activiteit tegen IMP-28. De resultaten van Zn-afhankelijkheid studies en isothermische titratie calorimetrie (ITC) analyses werpen licht op het remmende mechanisme van de meest krachtige verbindingen, waaruit blijkt dat ze vooral werken door de zinkionen te cheleren die cruciaal zijn voor de katalytische activiteit van de MBLs. Ons onderzoek wijst er niet op dat de remmers een complex vormen met het metallo-enzym zelf. Fenotypische screenings onthulden de sterke synergetische relatie tussen PMIDA/NTA en meropenem wanneer ze werden getest tegen een groot aantal van carbapenem-resistente gram-negatieve klinische isolaten. Wij stellen voor dat dergelijke direct beschikbare kleine moleculen kunnen dienen als hulpmiddelen voor enzymatische en

	PMIDA	NTA
IC <sub>50</sub> (μM) tegen NDM-1	0.91	1.3
Zn dissociatie constante (K <sub>d</sub> , nM)	56	121

**Figuur 3.** PMIDA en NTA zijn krachtige NDM-1-remmers en sterke zinkbinders.

fenotypische studies van MBL's en dat ze ook kunnen dienen als startpunt voor verdere optimalisatie op weg naar klinische ontwikkeling.

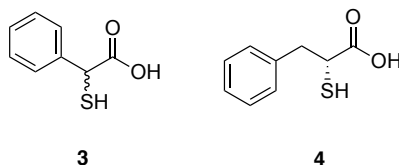
In **hoofdstuk 3** wordt beschreven hoe om MBL-remmers geïdentificeerd kunnen worden door middel van het screenen van kleine molecuul aminocarbonsuren. Deze aminocarbonsuren zijn verwant aan secundaire metabolieten die door *Aspergillus* spp. worden geproduceerd, waaronder aspergillomarasmine A (AMA), aspergillomarasmine B (AMB), en de chelaatvormer ethyleendiamine-*N,N'*-disuccinezuur (EDDS, figuur 4). De verschillende in de groep van Prof. Gerrit Poelarends gesynthetiseerde, analogen werden eerst getest op inhibitie van het NDM-1 enzym. De veelbelovende IC<sub>50</sub>-waarden van sommige van de analogen hebben ons ertoe aangezet hun Zn-bindende eigenschappen te evalueren met behulp van ITC. Er was een duidelijke correlatie tussen de Zn-binding en de remmende activiteit van de aminocarbonsuren. Met name de 2 methyleen eenheden tussen de asparaatfragmenten van EDDS bleken de optimale lengte te zijn voor maximale zinkbinding en NDM-1 remming. Interessant is dat sommige van de geïdentificeerde krachtige remmers geen synergie met meropenem vertoonden toen ze getest werden tegen een NDM-1 producerend *E. coli* isolaat, hoogstwaarschijnlijk als gevolg van onvoldoende cellulaire accumulatie. Desalniettemin behoorden een methyl gesubstitueerde



**Figuur 4.** Eerder gerapporteerde aminocarbonsuren als krachtige NDM-1-remmers.

EDDS en een methyleenhomoloog van AMB tot de meest krachtige synergisten voor het herstellen van de activiteit van meropenem.

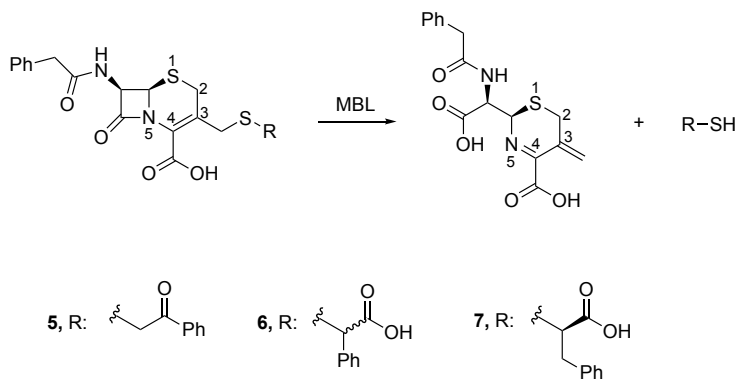
In **hoofdstuk 4** werd een andere groep van kleine moleculaire MBL-remmers (d.w.z. thiolen) geëvalueerd. De focus lag op een reeks eerder gerapporteerde thiol-bevattende MBL-remmers. Hier hebben we de eerste checkerboard-synergieanalyses met betrekking tot zinkbinding uitgevoerd en de chemische stabiliteit van deze verbindingen getest. Thio-amandelzuur en 2-mercapto-3-fenylpropionzuur (respectievelijk genummerd **3** en **4** in hoofdstuk 4, figuur 5) verlaagden de MIC van meropenem en cefoperazone wanneer ze werden getest tegen een panel van MBL-producerende gram-negatieve klinische isolaten. Het gebrek aan synergie met KPC- en OXA-producerende isolaten geeft aan dat de activiteit van de thiolen MBL-specifiek is. Ondanks de sterk synergistische activiteit en zinkbindende eigenschappen, waren de thiolen **3** en **4** slechts beperkt stabiel in het testmedium. Met een halfwaardetijd van *ca.* 5 uur oxideren ze tot de overeenkomstige disulfiden, die geen of matige synergetische activiteit vertonen.



**Figuur 5.** Thio-amandelzuur (**3**) en 2-mercapto-3-fenylpropionzuur (**4**).

In **hoofdstuk 5** wordt de synthese en bioactiviteitsevaluatie beschreven van een reeks cefalosporine-thiolconjugaten die zijn ontworpen als prodrugs van de in hoofdstuk 4 beschreven thiolen. Naar aanleiding van onze bevindingen over de slechte stabiliteit en specificiteit van de thiolen beschreven in hoofdstuk 4 en gezien het bekende hydrolysemechanisme van cefalosporinen, hebben we een kleine groep cefalosporine-thiolconjugaten ontworpen en gesynthetiseerd (genummerd **5-7** in hoofdstuk 5, figuur 6). De  $IC_{50}$ -testen tegen IMP-1, IMP-28, NDM-1 en VIM-2 onthulden sterke activiteit van verbindingen **6** en **7** met selectiviteit voor IMP-enzymen. Dezelfde trend werd waargenomen in de synergetests tegen MBL-producerende gram-negatieve bacteriële isolaten, waarbij **6** en **7** de MIC van meropenem tegen de IMP-producerende bacteriën grotendeels verminderden. Ondanks de veelbelovende activiteitsresultaten van deze stoffen duiden mechanistische studies met behulp van  $^1H$ -NMR en LC-MS erop dat blootstelling van de cefalosporineconjugaten aan IMP-28 niet leidt tot het verwachte vrijkomen van de kleine-molecuul thiolen. Dit heeft ons ertoe aangezet de werkingswijze van de

cefalosporineconjugaten te bepalen. Er werd een structuur-activiteitsanalyse van verbinding **6** uitgevoerd door een reeks structurele varianten te synthetiseren en te testen. De verkregen activiteitsresultaten wezen op de bijdrage van zowel fenyl- als carboxylgroepen van verbinding **6** aan de potentie. Ten tweede hebben we de kinetische parameters van de MBL-gemedieerde hydrolyse van de gesynthetiseerde cefalosporines bepaald. De berekende katalytische efficiëntie suggereerde een trage omzetting van het substraat als het remmende mechanisme van de verbindingen **6** en **7**. Ten slotte heeft de activiteitsevaluatie van de gedeeltelijk gehydrolyseerde producten van **6** en **7** aangetoond dat deze verbindingen de IMP-enzymen kunnen blokkeren als substraten en als hydrolyseproducten.



**Figuur 6.** De cefalosporine conjugaten verondersteld om de thiol MBL-remmers vrij te geven na MBL-gemedieerde hydrolyse.

**Hoofdstuk 6** is het resultaat van een samenwerkingsproject met dr. Mike Brouwers van Wageningen Bioveterinary Research naar de enzymatische activiteit van een nieuw ontdekte klasse A carbapenemase. Het enzym, genaamd FLC-1 (FRI-achtige carbapenemase-1), werd oorspronkelijk geïdentificeerd in *E. Cloacae* geïsoleerd uit naar Nederland geïmporteerde voedingsmiddelen. Na transformatie van *E. coli* met het FLC-1 plasmide en arabinose-geïnduceerde over-expressie werd de eiwitfractie van de bacteriecultuur gebruikt voor de bepaling van kinetische parameters. De FLC-1 veroorzaakte selectieve hydrolyse van de geteste carbapenems. De voorkeur voor carbapenems komt overeen met de resultaten van de eerder uitgevoerde MIC-assays. De getransformeerde *E. coli* was in hogere mate resistent tegen carbapenems dan tegen derde generatie cefalosporines. We vonden ook dat FLC-1 wordt geremd door clavulaanzuur ( $\text{IC}_{50} = 1.97 \mu\text{M}$ ).

## List of publications

## Publications from doctoral research period

- (1) Tehrani, K. H. M. E., and Martin, N. I. (2018)  $\beta$ -lactam/ $\beta$ -lactamase inhibitor combinations: an update. *MedChemComm* **9**, 1439–1456.
- (2) Tehrani, K. H. M. E., Bröchle, N. C., Wade, N., Mashayekhi, V., Pesce, D., van Haren, M., and I. Martin, N. (2020) Small molecule carboxylates inhibit metallo- $\beta$ -lactamases and resensitize carbapenem-resistant bacteria to meropenem. *ACS Infectious Diseases*, **6**, 1366–1371.
- (3) Tehrani, K. H. M. E., Fu, H., Bröchle, N. C., Mashayekhi, V., Prats Luján, A., van Haren, M. J., Poelarends, G. J., and Martin, N. I. (2020) Aminocarboxylic acids related to aspergillomarasmine A (AMA) and ethylenediamine-*N,N'*-disuccinic acid (EDDS) are strong zinc-binders and inhibitors of the metallo-beta-lactamase NDM-1. *Chemical Communications* **56**, 3047–3049.
- (4) Tehrani, K. H. M. E., and Martin, N. I. (2017) Thiol-Containing Metallo- $\beta$ -Lactamase Inhibitors Resensitize Resistant Gram-Negative Bacteria to Meropenem. *ACS Infectious Diseases* **3**, 711–717.
- (5) Brouwer, M. S. M., Tehrani, K. H. M. E., Rapallini, M., Geurts, Y., Kant, A., Harders, F., Mashayekhi, V., Martin, N. I., Bossers, A., Mevius, D. J., Wit, B., and Veldman, K. T. (2019) Novel carbapenemases FLC-1 and IMI-2 encoded by an *Enterobacter cloacae* complex isolated from food products. *Antimicrobial Agents and Chemotherapy* **63**, e02338-18.
- (6) t'Hart, P., Wood, T. M., Tehrani, K. H. M. E., Van Harten, R. M., Śleszyńska, M., Rentero Rebollo, I., Hendrickx, A. P. A., Willems, R. J. L., Breukink, E., and Martin, N. I. (2017) *De novo* identification of lipid II binding lipopeptides with antibacterial activity against vancomycin-resistant bacteria. *Chemical Science* **8**, 7991–7997.
- (7) Bergstrom, A., Katko, A., Adkins, Z., Hill, J., Cheng, Z., Burnett, M., Yang, H., Aitha, M., Mehaffey, M. R., Brodbelt, J. S., Tehrani, K. H. M. E., Martin, N. I., Bonomo, R. A., Page, R. C., Tierney, D. L., Fast, W., Wright, G. D., and Crowder, M. W. (2018) Probing the Interaction of Aspergillomarasmine A with Metallo- $\beta$ -lactamases NDM-1, VIM-2, and

IMP-7. *ACS Infectious Diseases* **4**, 135–145.

- (8) Potel, C. M., Tehrani, K. H. M. E., Lemeer, S., Martin, N. I., Heck, A. J. R., and Lin, M.-H. (2018) A New Tool to Reveal Bacterial Signaling Mechanisms in Antibiotic Treatment and Resistance. *Molecular and Cellular Proteomics* **17**, 2496–2507.
- (9) Tehrani, K. H. M. E., Wade, N., Mashayekhi, V., Brüchle, N. C., Voskuil, K., Jespers, W., Pesce, D., van Haren, M. J., van Westen, G. J. P., and Martin, N. I. (2020) Novel cephalosporins selectively inhibit the IMP type metallo- $\beta$ -lactamases. *Manuscript in preparation*

#### Patents from doctoral research period

- (1) 2019 Dutch Patent application filing; Title: “Prodrug metallo-beta-lactamase inhibitors”; Inventors: Martin, N. I., van Haren, M. J., Tehrani, K. H. M. E. Priority date: April 1, 2019.
- (2) 2019 Dutch Patent application filing; Title: “A novel class of lipidated glycopeptide antibiotics with potent antibacterial activity”; Inventors: Martin, N. I., van Groesen, E., Tehrani, K. H. M. E., Wade, N. Priority date: September 24, 2019.

#### Publications from previous research works

- (1) Tehrani, K. H. M. E., Mashayekhi, V., Azerang, P., Sardari, S., Kobarfard, F., and Rostamizadeh, K. (2014) Synthesis and antimycobacterial activity of novel thiadiazolylhydrazones of 1-substituted indole-3-carboxaldehydes. *Chemical Biology and Drug Design* **83**, 224–236.
- (2) Tehrani, K. H. M. E., Azerang, P., Esfahani Zadeh, M., Mashayekhi, V., Kobarfard, F., and Sardari, S. (2013) One Pot Synthesis and Biological Activity Evaluation of Novel Schiff Bases Derived from 2-Hydrazinyl-1,3,4-thiadiazole. *Chemical and Pharmaceutical Bulletin* **61**, 160–166.
- (3) Mashayekhi, V., Tehrani, K. H. M. E., Amidi, S., and Kobarfard, F. (2013) Synthesis of Novel Indole Hydrazone Derivatives and Evaluation of Their Antiplatelet Aggregation Activity. *Chemical and Pharmaceutical Bulletin* **61**, 144–150.



## *Curriculum Vitae*

Kamaleddin H.M.E. Tehrani was born in 30 July 1987 in Tehran, Iran. He studied pharmacy in Shahid Beheshti university of medical sciences and graduated with Pharm.D. degree in 2011. The subject of his thesis was synthesis of novel hydrazone derivatives with antimycobacterial activity. He continued his research activities in collaboration with Professor Farzad Kobarfard and Dr. Shohreh Mohebbi until he joined Professor Nathaniel Martin's group in September 2014 as a PhD student. The primary focus of his research since then has been development of novel inhibitors of bacterial metallo- $\beta$ -lactamases. As a PhD researcher he acquired a range of practical skills including organic synthesis, spectral characterization of organic compounds using NMR and LCMS, HPLC analysis (analytical and preparative), thermodynamic profiling of binding interactions using isothermal titration calorimetry, biochemical enzyme kinetics and inhibition assays, and antimicrobial activity assays. During this time, he supervised 4 bachelor and master projects leading to a number of publications and manuscripts under preparation. His research efforts to date have resulted in 2 patents, 21 papers (8 from PhD, 13 from previous research positions), and 6 manuscripts currently submitted or under preparation.

## Afterword

No clouds, no full moon, not much light pollution. Sky is full of stars. It is the summer of 2006 and I am about to sleep on the rooftop of my childhood house in Shiraz. My father comes upstairs unexpectedly and sits down in front of me. “You wanted to talk to me earlier today. Here I am. What is it about?” I tell him how I picture my future, and what my goals and ambitions are. I tell him that I like to study abroad to become more scientifically capable and competent to serve my country the best I can. Then he starts. Like life in Shiraz, his talking is slow, with long pauses between his words. “Whatever your plan is, you should look at your life with a global perspective. Even better with a cosmic perspective. And wherever you go to live and study, be a curious student of their culture. Try their food, learn their social norms, their history and their way of life”. Now I’m in Utrecht lying in bed in my apartment, watching the old George Carlin on Youtube. He reminds me of my father, not only because he is unapologetically honest and doesn’t try to protect anyone’s feelings, but also because of what he says about national and ethnic pride: “... pride should be reserved for what you achieve or attain on your own, not because of something that happened by the accident of birth”. For someone who chose to make his world as big as the world allows him to, someone who feels he belongs to everywhere and nowhere, someone who lives between two fears of the unknown, someone who leaves a lot behind to travel light, moments of hesitation and self-doubt are frequent. In such moments I think about Carlin’s words and that slow conversation with my father under a sky full of stars.

